University of Alberta

Conjugated Cyclotetraynes: Synthesis and Characterization

by

Andreea Spantulescu 

A thesis submitted to the Faculty of Graduate Studies and Research in partial fulfillment of the requirements of the degree of Master of Science

Department of Chemistry

Edmonton, Alberta

Fall, 2006

Your file Votre référence
ISBN: 978-0-494-22376-5
Our file Notre référence
ISBN: 978-0-494-22376-5

UNIVERSITY OF ALBERTA

LIBRARY RELEASE FORM

NAME OF AUTHOR:	ANDREEA SPANTULESCU
TITLE OF THESIS:	Conjugated Cyclotetraynes: Synthesis and Characterization
DEGREE:	Master of Science
YEAR GRANTED:	2006

DATED: _____ _____

UNIVERSITY OF ALBERTA

FACULTY OF GRADUATE STUDIES AND RESEARCH

The undersigned certify that they have read, and recommend to the Faculty of Graduate Studies and Research for acceptance, a thesis entitled "Conjugated Cyclotetraynes: Synthesis and Characterization" submitted by Andreea Spantulescu in partial fulfillment of the requirements for the degree of Master of Science.

_____

Dr. Rik R. Tykwinski (Supervisor)

_____

Dr.

_____

Dr.

DATED:_____

Abstract

Cyclotetraynes presented in this thesis feature four conjugated triple bonds and an alkyl tether that completes the cyclic structure. This series of strained cyclotetraynes have been synthesized due to their synthetically challenging structures and to explore their unique physical properties as a function of ring strain. The Hay acetylenic homocoupling method and the Fritsch-Buttenberg-Wiechell rearrangement represent the key steps in obtaining these molecules. ^{13}C NMR and UV–vis spectroscopies have been used to establish trends as function of ring strain and show, for example, that the more the strained the cycle is, the more deshielded the chemical shifts of the sp-hybridized carbon atoms. Herein, the synthesis and characterization of cyclic tetracycloalkynes **202–204** and one linear analogue **205** are discussed.

Acknowledgements

I would like to acknowledge my supervisor, Professor Dr. Rik Tykwinski, for his support and guidance through the entire period spent at University of Alberta. I would like to thank to all past and present group members for their support. Special thanks to my good friend and *coffee partner*, Thanh Luu for his support, friendship and humor, his laughter is unmistakable and contagious. I would also like to thank Jamie Kendall for making the life in the lab very enjoyable with his crazy music and comments. I would like to acknowledge Amber Sadowy for all her patience in the enormous amount of time and work that she put into proof-reading this thesis. I am indebted to Dan Lehnherr for a careful examination of the experimental chapter. I would like to thank the staff in spectral and analytical services for their assistance in characterizing my compounds. Finally I would like to acknowledge my husband, Dan, for his understanding and support. I would like to acknowledge the University of Alberta for the financial support.

TABLE OF CONTENTS

List of Figures

List of Schemes

1. Introduction

The discovery of fullerenes has raised a series of questions to be answered. First, why can fullerenes form at temperatures of over 3000 °C, since those conditions should favor the existence of structures with little or even no organization, and yet a highly symmetrical and organized molecule is formed? Second, why is C_{60} formed to the detriment of C_{70}, which is thermodynamically more stable?[1] These questions still need to be answered and understanding the mechanism of the formation of fullerenes may bring insight to these ongoing scientific puzzles.

On the other side of this problem stands the question why someone would want to spend time and resources to find solutions to the above-mentioned questions when the starting material for fullerene is graphite, a compound so cheap and convenient to use. The answer comes very easily, because there is a need for synthetic methodology to obtain carbon rich materials.[2]

The discovery of C_{60} as a very stable polycyclic-cluster (hollow closed-cage) has drawn attention towards exploring the possibility of other carbon clusters. For example monocyclic carbon clusters are believed to play a key role in the formation of fullerene because the nucleation is thought to take place through aggregation of medium sized carbon clusters, rather then addition of small carbon pieces, which in the end collapse to form caged structures. The small carbon clusters, such as C_9 are thought to be linear, medium sized clusters such as C_{10} – C_{24} monocyclic, and higher numbered carbon clusters bi-, tri-, and polycyclic in structure.[3]

Strained cycloalkynes are predicted to be suitable candidates for transformation into more thermodynamically stable fullerenes. Therefore studies towards the formation and characterization of dehydrobenzoannulenes and alkyne based cyclophynes, enynes and cyclo[*n*]carbons and alkyne rich-conjugated π-systems have been conducted.[4-6]

A common name for cycloalkynes is just simply cyclynes, and according to a more precise definition,[7] a cyclyne is defined as any ring of atoms that contains at least one alkyne unit. In this chapter I focus mainly on an introduction to strained cyclynes that are formed of carbon and hydrogen. Although in the literature there exist some examples of heterocyclynes,[7] which incorporate in the cycle a heteroatom (usually Si, Ge, P, Pt or even Ti), these were left out due to space considerations. Therefore, a brief history of strained cyclynes will be presented, followed by the discussion which contains more extraordinary examples of strained cyclynes (pericyclynes, benzocyclynes and cyclo[*n*]carbons).

1.1. Short history of strained cyclynes

Long before the discovery of fullerenes, strained conjugated cyclyne synthesis proved to be a challenge to scientists due to the kinetic instability of these products. These targets were nevertheless pursued due to their interesting properties.

The first two examples of strained cycloalkynes were synthesized by Blomquist: cyclononyne in 1952 and cyclooctayne in 1953, where he reported the naming of these compounds as "many-membered carbon rings".[8] The earliest examples of conjugated strained cyclynes were synthesized by Sondheimer in 1957,[9] where the coupling of terminal dialkynes gave as a final result the dimers (**101a–c**), among many other linear compounds (Scheme 1.1). The longest (six methylene units) and the shortest (two

methylene units) dialkynes did not yield the dimer, and the latter compound was thought to polymerize during the reaction. Although NMR spectroscopy was not employed for the characterization of these compounds, carefully done melting points, elemental analysis, IR and UV–vis spectroscopys were used.

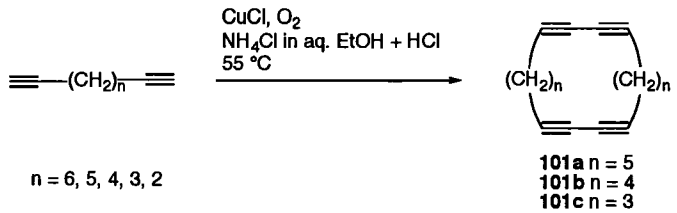

Scheme 1.1 Synthesis of compounds **101a–c**

The unique motif of compound **102**, an octamethyl analogue of compound **101** (with n = 2) was synthesized by Scott in 1976,[10] (Scheme 1.2). X-ray analysis of compound **102** showed that acetylenic carbon atoms have bond angles of 166° and UV–vis spectroscopic analysis of **102** showed a pronounced bathochromic shift in comparison with a linear tetrayne homologue.

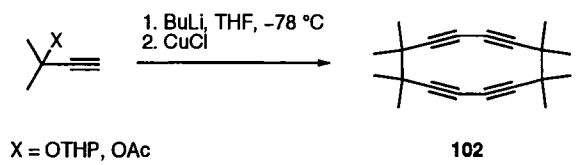

Scheme 1.2 Synthesis of compound **102**

In 1961, Sondheimer published the synthesis of a new class of compounds, conjugated macrocyclic polyene-polyynes and in this work he introduced the terms annulene and dehydroannulene (annulus meaning ring in Latin).[11] Starting from 1,5-hexadiyne, compounds **103, 104, 105** and **106** were synthesized as precursors of

annulenes in approximately 6, 6, 6 and 2% yields, respectively. Total separation was not possible due to the fact these compounds eluted together on chromatographic supports. Careful chromatography did, however, provide enough sample necessary for characterization. It should be noted that these compounds decomposed violently during attempts to conduct melting points.

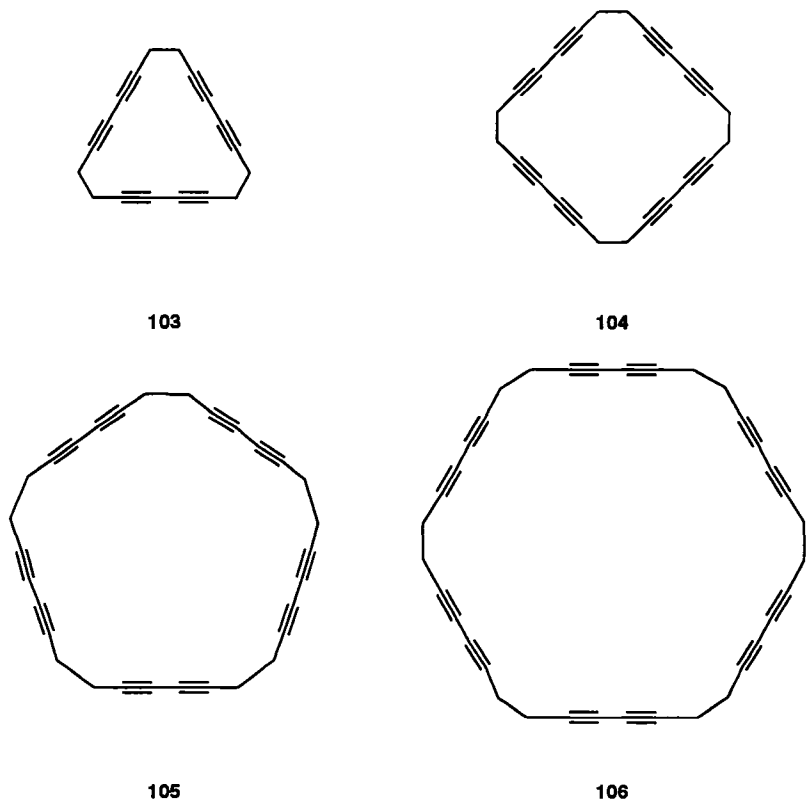

Figure 1.1 Compounds **103–106** (Sondheimer series)

In 1972 Matsuoka's group[12] reported the synthesis and properties of [5.5], [4.4], [3.4], [3.3] and [2.4]paracyclophadiynes (compounds **107a–e**, Scheme 1.3) in conjunction with the synthesis of cyclic diacetylenes **108a**, **b** (Scheme 1.4). A succinct synthesis is presented in Scheme 1.3 where compounds **107a–e** represent the target

species and compounds **109a,b** are the cyclic dimers formed in the homocoupling reaction (only symmetrical ones reported). Analyzing the electronic spectra of the strained compounds **107a–e** resulted in an interesting trend, a bathochromic shift of the longest wavelength absorption band was observed. The appearance of a new peak, not accounted in for the reference model **109b** was also observed. These trends were explained by two possibilities: distortion of the chromophores and transannular interaction between them.

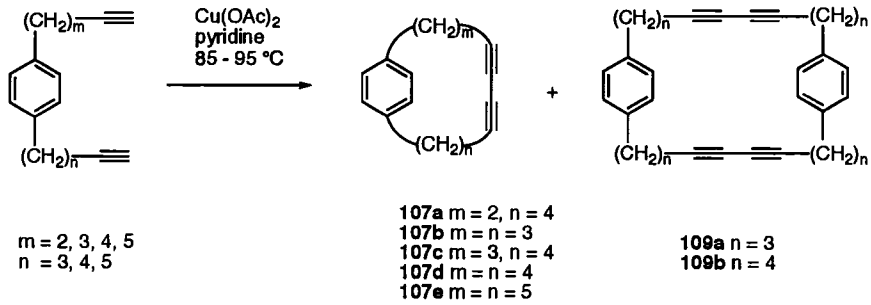

Scheme 1.3 Synthesis of compounds **107a–e** and **109a–b**

In the same study, the synthesis of a cyclodiyne, compound **108a** was reported, which at that time was the record holder for the smallest monocyclic conjugated diacetylenes (Scheme 1.4). As expected, compound **108a** was not stable, but could be stored in solution at –20 °C.

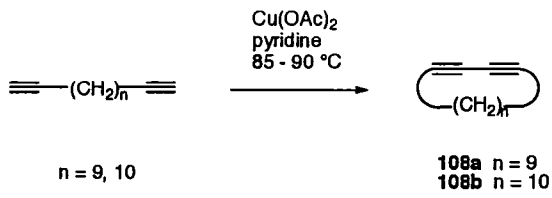

Scheme 1.4 Synthesis of compounds **108a** and **108b**

In the early 1980s, Sondheimer continued his breakthrough research through the synthesis of dehydrobenzoannulenes **110** and **111** (Figure 1.2).[13] It is interesting to note that compound **110** is too reactive to be isolated, while compound **111,** on the other hand is isolated as an unstable yellow solid.

110 **111**

Figure 1.2 Structure of compounds **110** and **111**

In 2000 Tykwinski reported the synthesis and characterization of cyclic expanded dendralenes **112** (Figure 1.3). The effects of ring strain were explored with the aid of ^{13}C NMR, Raman and UV–vis spectroscopies and X–ray crystallography.[14]

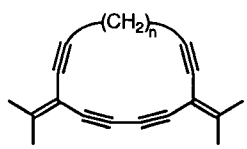

112

n = 2, 3, 4, 5, 7

Figure 1.3 Structure of dendralenes **112**

1.2. Pericyclynes

Cyclynes with a single carbon atom spacer are referred to as pericyclynes.[15] Pericyclynes are neither precursors of fullerene nor are they belived to be involved in the mechanism of fullerene formation, but they were thought to be one example of homoconjugated macrocycle due to the electronic interaction between the acetylenic units,[16] although this fact was disproved later.[17] Since pericyclynes are cyclic

polyacetylenes, they have attracted a considerable interest from both synthetic and theoretical point of view.[17,18] This class of compounds was expected to have a series of interesting properties. Indeed they have shown special electronic properties due to orbital interactions and various conformations structures that were somehow unusual mainly due to the lack of torsional strain and transannular van der Waals repulsions.[19] The higher members (**116–118**) of this particular class of compounds were not planar and were calculated to have different conformational possibilities. For example compound **116** can exhibit three different conformational possibilities analogous to cyclohexane: chair **I**, boat **II**, and twist **III** conformation (Figure 1.5). Therefore these pericyclynes can be viewed as exploded cycloalkanes obtained from the parent cyclic hydrocarbon by insertion of a triple bond between every pair of original sp^3 hybridized carbons.

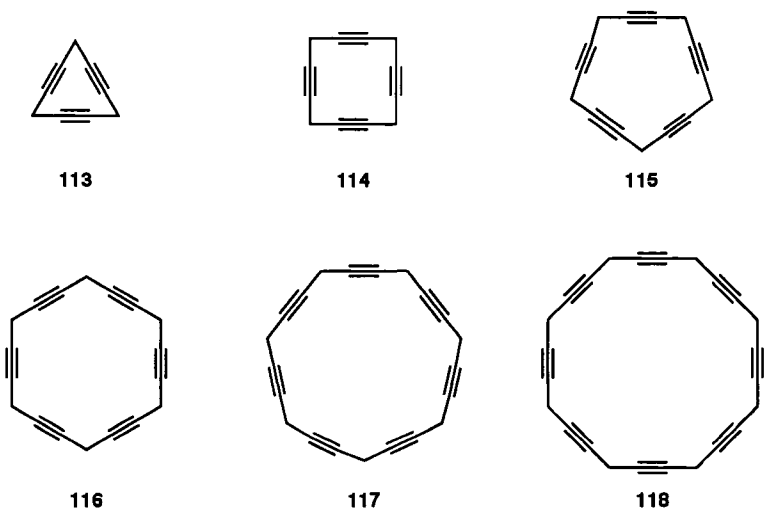

Figure 1.4 Pericyclcynes (**116–118**)

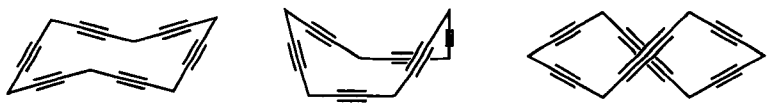

I II III

Figure 1.5 Conformers of pericyclyne **116**

1.3. Benzocyclynes

Benzocyclynes are macrocycles in which aryl rings connected by carbon-carbon triple bonds. Strained benzocyclynes are known to undergo the transformation to carbon rich materials or fullerenoid-like compounds when heated.[20] The energy content of such strained molecules, based on the phenyl-alkynyl moieties, is crucial to this purpose. It has been noted that very strained benzocyclynes fail to produce fullerenes when heated, but afford rather a polymer-like material. In 1997, Vollhardt observed that the benzocyclyne (which is a DBA, term which will be defined in Chapter 1.3.1) **119** explodes violently when heated to 250 °C and the resulting products included bucky tubes and bucky onions that are "all carbon materials".[21] Compound **120**, which is a structural isomer of **119**, decomposed at 50 °C to give an insoluble residual carbon rich material, the structure of which still not yet known.[22] Nevertheless, such strained compounds containing deformed triple bonds are very interesting materials and are still a topic of interest for chemists.

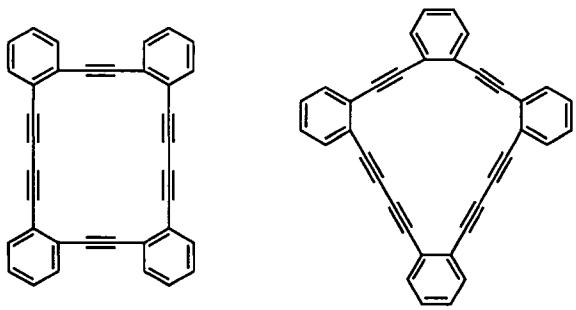

119 120

Figure 1.6 Structure of compounds **119** and **120**

1.3.1. Orthocyclophynes

Dehydrobenzoannulenes (DBAs) are regarded as orthocyclophynes and have been investigated mainly due to their interesting aromatic or antiaromatic character. DBAs can be viewed as dehydrogenated benzannulenes. In the 1980s, DBAs were synthesized to study their diamagnetic ring currents, but it was shown that these currents were weak, so it seemed that this chemistry was obsolete. But once with Vollhardt's discovery,[21] mentioned above, (the transformation to "all carbon materials") a new and fresh perspective towards these "old" molecules appeared and more strained compounds were synthesized. Strained DBAs with acetylene connecting units between the aromatic rings have the general structure depicted in Figure 1.7, where compound **121** is a dibenzo system and compound **122** is a tribenzo system.

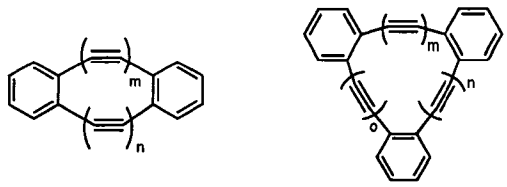

121 122

Figure 1.7 General structures for di- and tri- DBAs **121** and **122**

Di- and tri-benzo systems are important, because the strain of the ring is limited to 8–14 carbon atoms (as in Figure 1.7) and the more strained the structure the more interesting the properties.[23] The strain of the cycle will influence the chemical and physical properties. For DBAs, the deformation of the triple bond will affect the orbital overlap and the cyclic conjugation. One such strained compound is hexadehydrodibenzo[10]annulene **123** where the alignment of the both in-plane and out-of-plane *p* orbitals is perturbed by the bending of the triple bonds (Figure 1.8).[23]

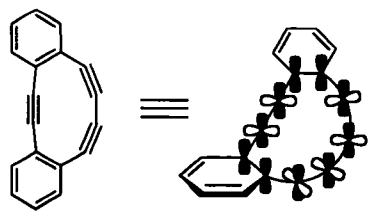

123

Figure 1.8 Representative orbital overlap for hexadehydrodibenzo[10]annulene **123**

One of the first methods used in the synthesis of DBAs is bromination followed by the dehydrobromination (**124**) as presented in Scheme 1.5.[24] Usually for synthesis of DBAs, the classic approaches such as metal-mediated reactions of Hay coupling

(oxidative acetylene homocoupling), Stille coupling, Sonogashira coupling, Suzuki coupling[25] are used either in an intermolecular fashion where the ring closure is done by formation of two or more bonds between two or more pieces or by intramolecular fashion where only one bond is formed in the same piece.

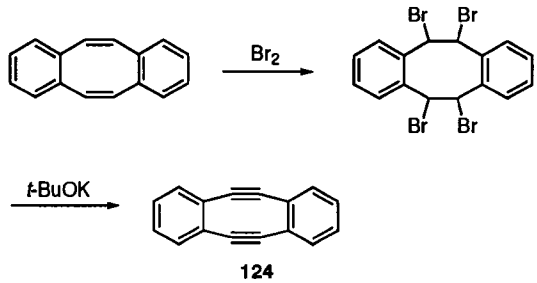

124

Scheme 1.5 Synthesis of benzoannulenes **124** involving bromination and dehydrobromination

Tobe, who is a major player in this field, has used this coupling chemistry, but in order to get more strained unsymmetrical compounds, he has developed an ingenious method discussed below. Because Tobe's work had such a big impact upon this chemistry field I chose to discuss the synthesis of compound **125**, which in my opinion illustrates the most clever idea for incorporating strained alkynes. Compound **125** (octadehydrodibenzo[12]annulene) is a very good example of a strained DBA and was synthesized by Tobe et al. following the procedure presented in the Scheme 1.6.[23] Due to its highly strained structure, complete characterization was not possible, although its presence was proved by UV–vis and FTIR spectroscopies. Tobe developed an interesting method, in which the UV irradiation, of a propellatriene derivatives results in a [2 + 2] fragmentation, leaving behind a new triple bond.[26] The synthesis starts with compound **126**, that is deprotected *in situ*, then coupled with compound **127** (diiodotolane) under phase transfer conditions. Irradiation of compound **128** should presumably form

compound **125**. Although compound **125** is probably formed, only compound **129** (18% yield) is isolated, which is formed most probably by a [4 + 2] cyclization between compound **128** and the desired intermediate, compound **125**. Irradiation of compound **128** in furan yields compound **130**. As proven by X–ray crystallography, the addition takes place at the central triple bond, which was predicted to be the most strained at 147.1°.

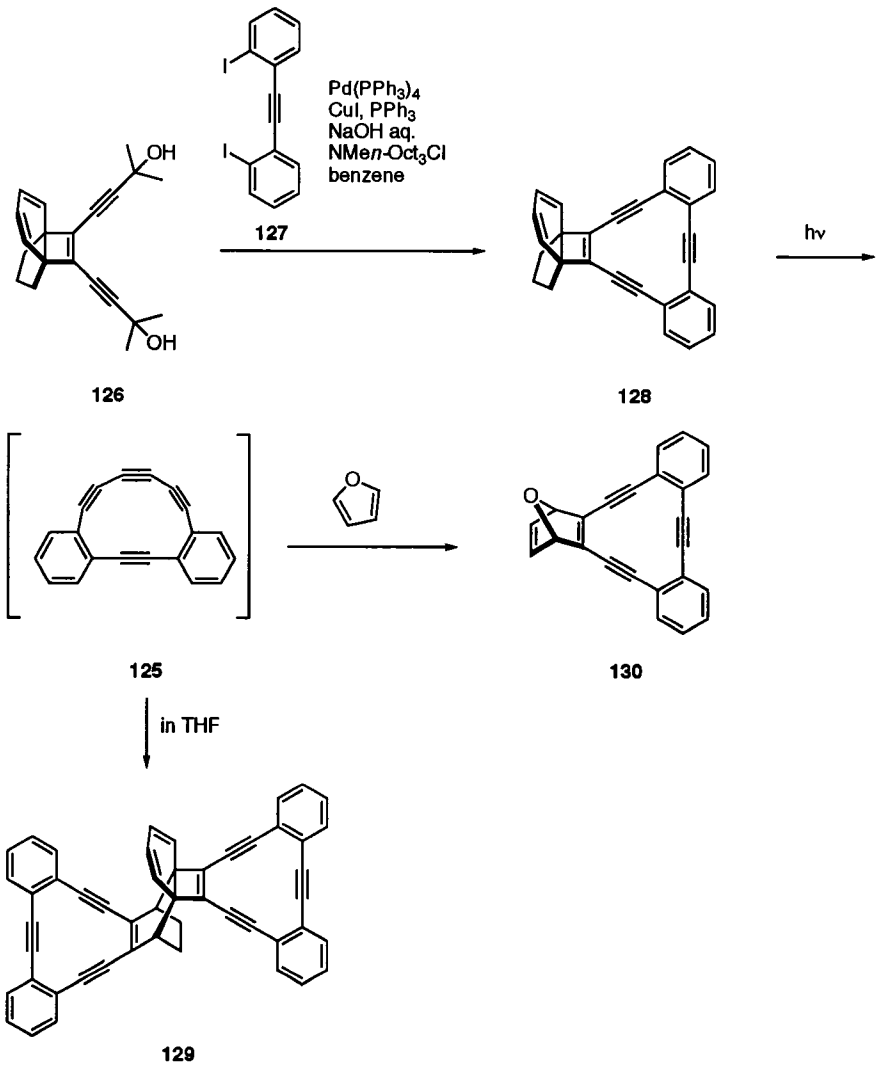

Scheme 1.6 Synthesis of **125** and its pathways of reactivity

1.3.2. Paracyclophynes

Paracyclophynes possess a belt-like rigid structure and are characterized by well defined cavities (Figure 1.9).[6] Paracyclopynes can be included in the same category of fully π-conjugated compounds as cyclo[*n*]carbons, cycloacenes or oligoparaphenylenes and they are important from many points of view, including synthetic and theoretical targets, and also as host molecules. The first compound of this class compound **131** (Figure 1.9) is a [2_6]paracyclophyne and it is synthesized by Oda[5] and the second compound from this series, **132**, is synthesized by Tsuji and is a [4_6]paracyclophyne.[27]

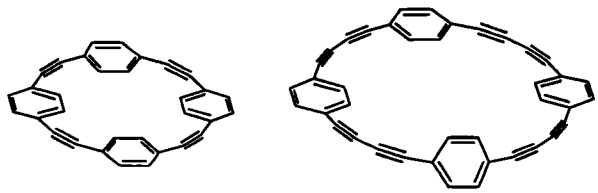

131 132

Figure 1.9 Structures of paracyclophynes **131** and **132**

Compounds **133a** and **133b** are very important members of the highly unsaturated paracyclophyne family due to their very strained structure. Furthermore it is believed that under certain conditions, they might form C_{36}, which has a fullerene-like structure.[28] The synthesis of compounds **133a** and **133b**, depicted in Scheme 1.7, was accomplished by palladium catalyzed coupling of propellanediyne **134** with 1,4-diiodobenzene, yielding compounds **135a** and **135b**. Subsequent deprotection of the TMS protected alkynes followed by copper catalyzed coupling under very dilute conditions resulted in compounds **136a** and **136b**. Unfortunately when compound **136a** was irradiated in THF a

polymeric material was isolated. In order for the intermediate to be trapped as a [4 + 2] adduct the reaction was conducted in furan, but compound **137** was formed and compound **138** was eliminated as a possible product due to its instability. It is still not understood why compound **133,** will not react with furan in a Diels–Alder manner, despite known precedent.[23] Compound **136a** under mass spectrometry conditions did not yield C_{36}^{-} but rather only $C_{36}H_8^{-}$, which failed to undergo dehydrogenation. On the other hand more promising results appeared from compound **136b**, which contains weaker C-Cl bonds and underwent the expected transformation yielding C_{36}^{-}. The desired peak (of C_{36}^{-}) from LD-TOF spectrum is considerably larger than $C_{36}Cl^{-}$, $C_{36}Cl_2^{-}$.

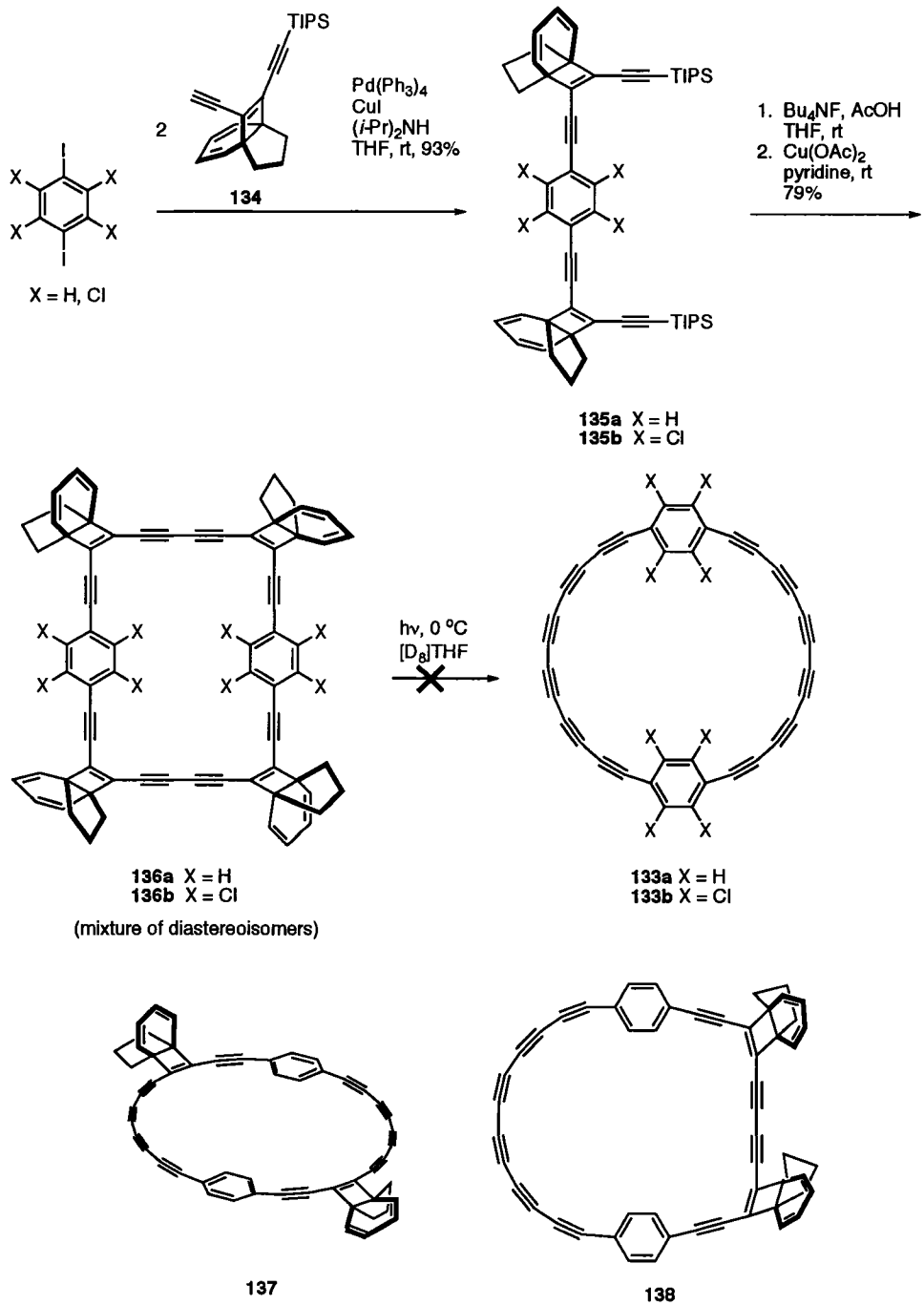

Scheme 1.7 Attempted synthesis of compounds **133a** and **133b**

1.4. Cyclo[*n*]carbons

As mentioned previously, cyclo[*n*]carbons are precursors of fullerenes, therefore the synthesis of such kind of compounds has been a highlight recently, as the fullerenes were in the 1990s. Cyclo[*n*]carbons are *n*-membered monocyclic rings of sp-hybridized C-atoms that posses a unique electronic feature resulting from two perpendicular systems of conjugated π-orbitals, one in-plane and one out-of-plane. Cyclo[*18*]carbon is expected to show Huckel-aromatization stabilization due to the two orthogonal (4n+2)π electron systems.[29] The structural nature of the cyclo[*n*]carbons is still debated, although they are mainly recognized as being formed by alternating C—C and C≡≡C bonds (Figure 1.10), although some older references depicting a cumulenic structure are known.[29,30]

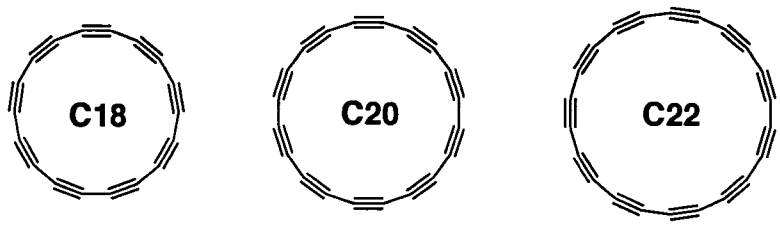

Figure 1.10 Predicted structure of cyclo[*18*]–, [*20*] – and [*22*]carbons

Synthetic efforts towards these still elusive cyclo[*n*]carbons have been conducted over the past 20 years and the results are less than satisfactory. Although it was reported that the formation of cyclo[*n*]carbons was detected in gas phase,[29] macroscopic quantities are still needed for characterization.

The pioneers of this subtle chemistry are Diederich and Tobe, and their approaches towards this attractive subject will be described in detail. In order to synthesize cyclo-C_{18}, C_{24} and C_{30} Diederich used mainly three methods, a) CO

elimination from compound **139**,[31] b) a retro-Diels-Alder elimination of anthracene for compound **140**, and c) removal of the μ-(hexacarbonyl)dicobalt by oxidation, alkyne-ligand exchange or flash vacuum pyrolysis from compound **141**.[29] All the three precursors (Figure 1.11) showed evidence in the formation of cyclo[*n*]carbons, however, isolable quantities of the desired compounds were not obtained.

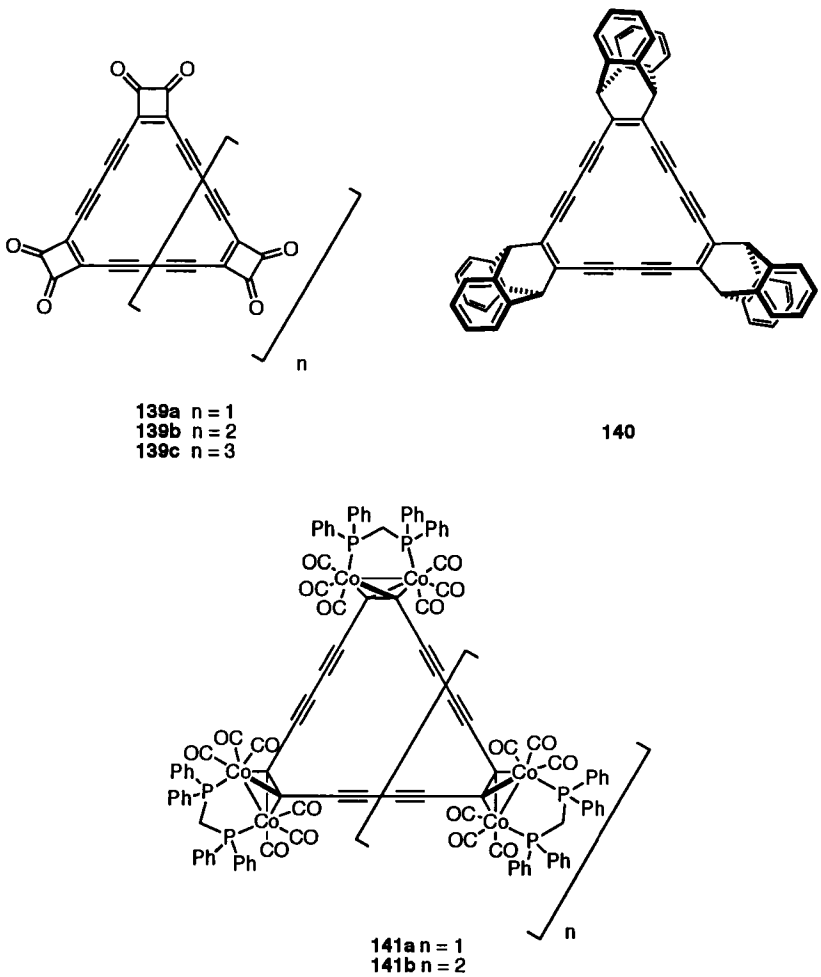

Figure 1.11 Precursors of cyclo[*n*]carbons

Carbon oxides **139a–c** showed promising results in the formation of C_{18}, C_{24} and C_{30}. In order for the elimination of carbon monoxide to take place, compounds **139a–c** had to be irradiated with two wavelengths, one necessary for the formation of the diketene intermediates and the second one being used for the elimination of carbon monoxide (Scheme 1.8). The starting material showed a strong IR absorption at 1792 cm^{-1}, which is specific to the carbonyl group from the cyclobutenedione, and after 4 minutes of irradiation at a wavelength of 388 nm, this absorption disappeared completely and a strong new absorption appeared at 2115 cm^{-1} which is usually associated with ketenes. Under the second irradiation light (280 nm) the diketene released carbon monoxide, which absorbs at 2138 cm^{-1}. Unfortunately no conclusive IR–results for the formation of C_{18} were found, although it was expected that the cyclo[*n*]carbon would lack any strong IR absorptions due to its high symmetry and lack of dipole moment. The formation of both positive and negative ions of C_{18}, C_{24}, C_{30} was observed in the positive and negative modes, respectively, of FT-TOF mass spectra.

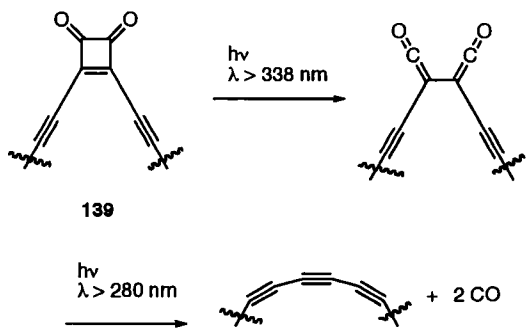

Scheme 1.8 Photochemical rearrangement of compound **139**

Compounds **139a–c** also have been subjected to LD-FTMS in both positive and negative modes.[31] In the negative mode of LD-FTMS, compounds **139a** and **139b** showed the C_{18}^- and C_{24}^- peaks, respectively, in contrast with **139c**, which did not show C_{30}^-, but rather an

abundant peak of C_{10}^-. These results can be attributed to the fact that C_{18} and C_{24} are more stable then C_{30}, which undergoes decomposition due to the fact that it is more reactive. In the positive mode of LD-FTMS, all three compounds **139a–c** showed the complete decarbonylation with the formation of: a) C_{18}^+, C_{24}^+ and C_{30}^+, b) the dimers, and c) fullerenoid ions: C_{50}^+, C_{60}^+ and C_{70}^+. All these results were noticed with only one laser pulse and the higher carbon clusters such as C_{50}^+, C_{60}^+ and C_{70}^+ were formed by the reaction in the gas phase of the respective cyclo[*n*]carbons, followed by successive C_2 losses, rather than by some other ionic species formed in a second laser pulse. This piece of information helped solve the puzzle of fullerene formation by showing indeed that the cyclo[*n*]carbons were precursors and involved in the mechanism of fullerene formation.

Compound **140** (Figure 1.11) was passed into the gas phase by laser-flash heating and eliminated three molecules of anthracene in a retro Diels-Alder fashion. Cyclo[*18*]carbon was detected as a neutral product using resonant two-photon-ionization time of flight mass spectrometry.[29] Unfortunately, the attempt to synthesize C_{18} by flash-vacuum pyrolysis yielded only anthracene and a polymeric material. Compound **141** (Figure 1.11), which possed masked triple bonds due to the complexation with Co did not afford cyclo[*18*]carbon for $n = 1$ or cyclo[*24*]carbon for $n = 2$ due to unexpected problems during decomplexation.

Tobe's approach towards the synthesis of the cyclo[*n*]carbons depended upon [2 + 2] photochemical rearrangements of compounds **142**.[3] The results of these types of reactions under LD TOF positive mode conditions were unexpected because only the signal from the indane fragment was seen upon reaction of **142**. On the other hand, in negative mode the parent ion $C_{18}R_3^-$ (where R is the indane fragment) and the anions

resulting from successive losses of one, two and all three indane fragments were seen, in addition to C_{36}^- and C_{54}^-. These represent the dimer and trimer of C_{18}^-, which were also seen, but fullerene formation was not observed. For n = 2, the same pattern was observed under LD TOF analysis.

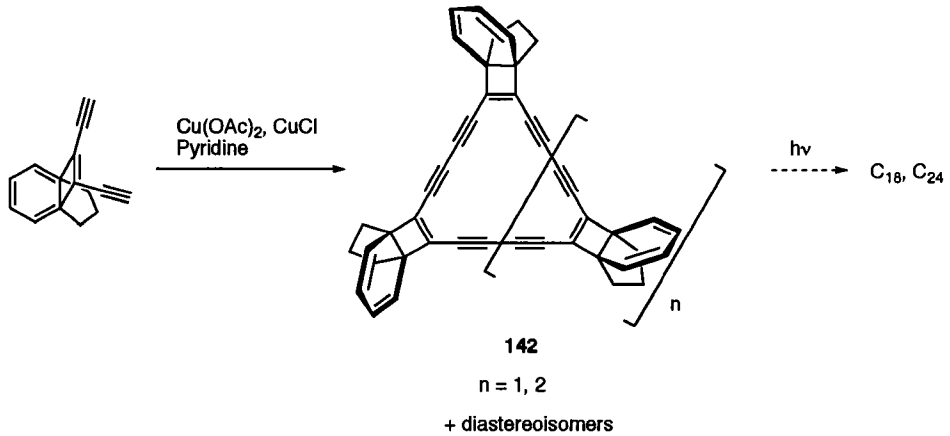

142

n = 1, 2

+ diastereoisomers

Scheme 1.9 Synthesis of compound **142**

The [2 + 2] reaction described above is advantageous to some extent for synthesizing the trimer (n = 1) and tetramer (n = 2) of **142**, but due to the small angle (ca. 90°) between the triple bonds and diethynyl[4.3.2]propellatetrine unit, larger dehydrooligomers such as the pentamer (n = 3) or hexamer (n = 4) were not obtained. To overcome this inconvenience a new method was developed by Tobe,[32] based on rearrangement of vinylidenes to alkynes and a [2 + 1] chelotropic fragmentation of dialkynylmethylenebicyclo[4.3.1]deca-1,3,5-triene derivatives. The mechanism of rearrangement of vinylidenes is shown in Scheme 1.10. The bond angle on the exo methylene carbon in structure **II** was found to be close to 120° so larger dehydrooligomers were formed.

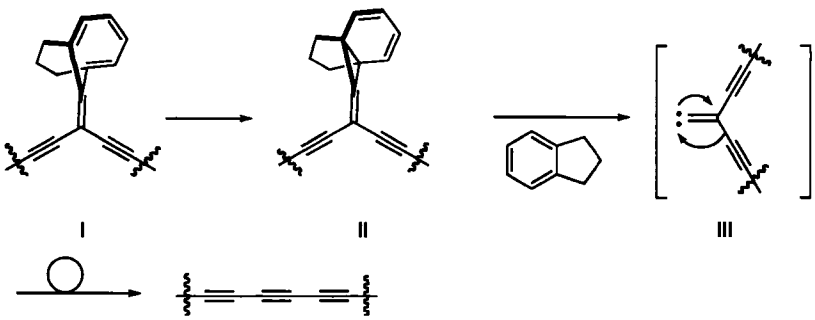

Scheme 1.10 Mechanism of rearrangement of vinylidenes to triple bonds

This time the sequence of reactions (Scheme 1.11) towards the cyclo[*n*]carbons started from compound **143**, which is readily available from the reaction of dibromocarbene and dihydroindane. Compound **143** afforded compound **144**, and lithium-halogen exchange of compound **144** followed by the treatment with 1,5-bis(trimethylsilyl)penta-1,4-diyn-3-one and then protection with TMSCl afforded compound **145**. Compound 145 was treated with *t*-BuLi and TMSCl resulting compound **146**, which after deprotection and oxidative coupling afforded the trimer (3%), tetramer (33%), pentamer (15%), and hexamer (7%).

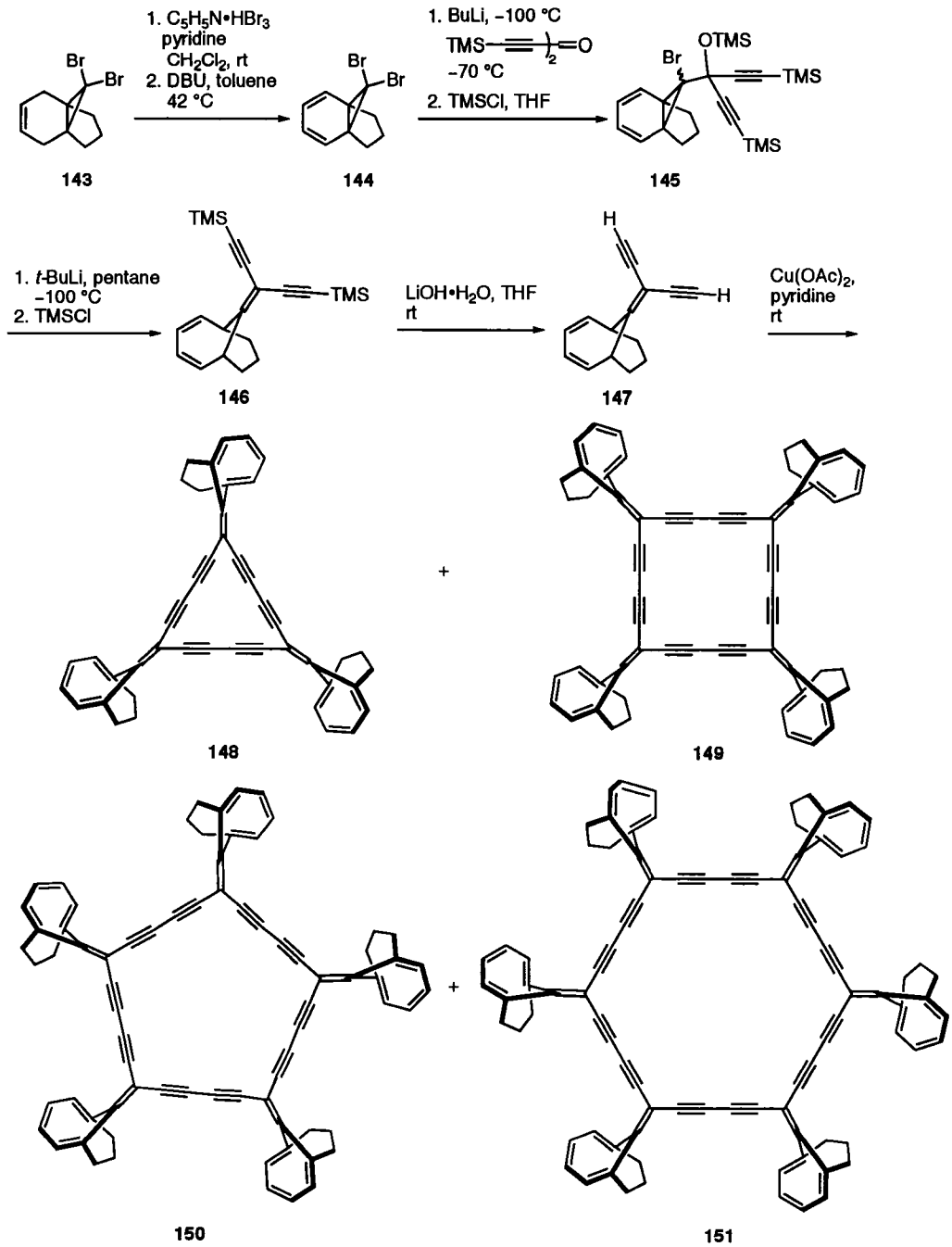

Scheme 1.11 Synthesis of cyclo[*n*]carbons precursors (**148–151** as diastereoisomers, only the most symmetrical diastereoisomers shown)

Compounds **148–151** were subjected to LD TOF in the negative mode and the spectra showed the formation of cyclo[*n*]carbon anions (*n* = 18, 24, 30, 36) formed by stepwise

loss of aromatic fragments. In this series, C_{36}^- had a different behavior since its peak intensity was weaker than in the other cases presented above, maybe due to the fact that its structure was a cluster rather than a monocyclic ring such as C_{18}, C_{24} and C_{30}.

Rees's approach[33] towards cyclo[*n*]carbons was based upon the formation of precursor **152** that was supposed to undergo a mild deprotection of the amino-1,2,3-traiazole unit in the presence of $Pb(OAc)_4$ and CH_2Cl_2 at –78 °C. Using this synthetic route had its challenges, but also the benefit of using large scale (at least 1 g each step), the exception being the cyclo-oligomerization step where compounds **152** were formed. The synthesis (Scheme 1.12) started with compound **153**, which was subjected to a reaction with a highly electrophilic–aminating agent, MSH (mesitylenesulfonyl-*O*-hydroxylamine), the reaction was carried at a 60 g scale and two isomers were formed (**154**). The next step was the protection of the amino group, which resulted isomers **155** and **156** were separated by fractional crystallization. The desired isomer **155** was coupled with trimethylsilylacetylene affording compounds **157** and **158**. Compound **158** was obtained as a byproduct due to a migration of the *N*-substituent from the 1– to the 2–position although the reason for this secondary reaction was not known. Deprotection of compound **157** afforded compound **159** that was further subjected to Hay coupling conditions to give a mixture of trimer, tetramer and pentamer in a ratio of 2:2:1. Unfortunately the last step the deprotection showed to be very difficult and the C_{18}^+ peak was not observed in the FAB mass spectrum.

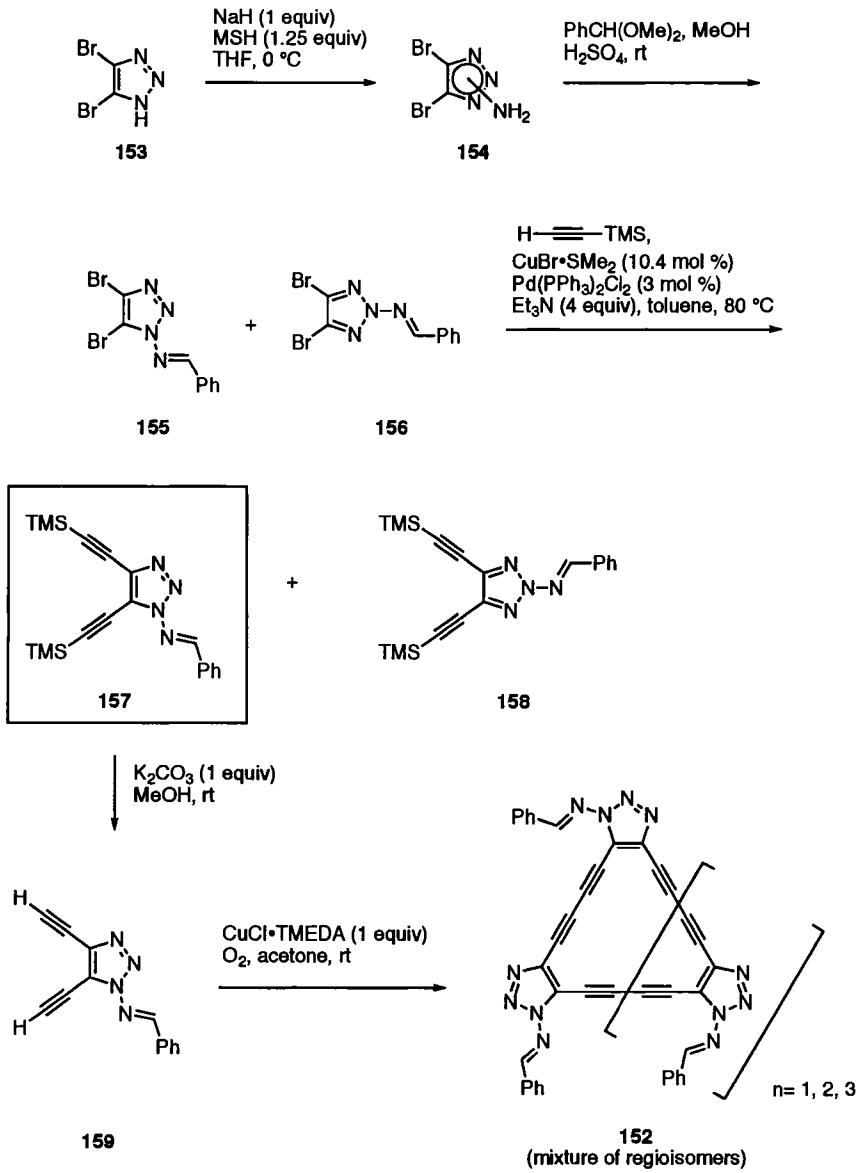

Scheme 1.12 Rees' synthesis towards cyclo[*n*]carbons

1.5. Conclusions

Because the synthesis of the cyclo[*n*]carbons has yet to be accomplished, we envisioned a new approach toward these intriguing molecules, would based on a four-fold Fritsch-Buttenberg-Wiechell (FBW) rearrangement effected on compound **160**, a procedure that has shown very good results in our group (Scheme 1.13). Unfortunately the precursor of cyclo[*22*]carbon, compound **160** could not be obtained due to solubility problems. Because this solubility problem could not be avoided, a new project was born namely the synthesis of strained cyclic tetraynes **I** from precursors **II** with only a two-fold FBW rearrangement (Scheme 1.14).

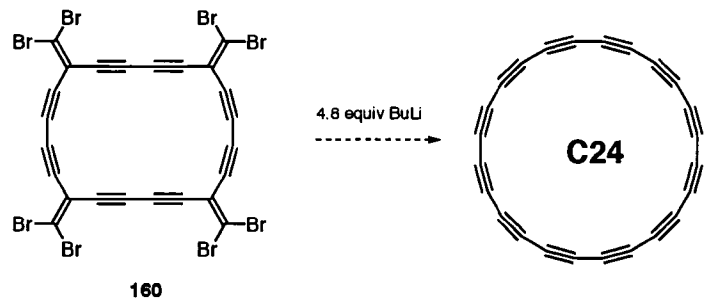

Scheme 1.13 Proposed synthesis of C_{24}

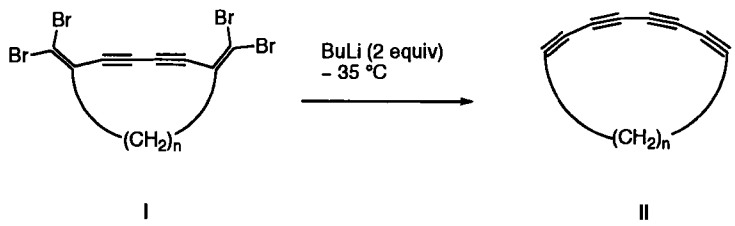

Scheme 1.14 Synthesis of model compound **II**

The angle of bending of sp-hybridized carbon atoms in this new class of compounds is calculated to be comparable to the bending encountered in the cyclo[*n*]carbons. Trying to increase the triple bond bending as much as possible by reducing the length of alkyl chain could provide insight as to whether the synthesis of cyclo[*n*]carbons via the FBW rearrangement would be a feasible project. Furthermore, the characterization of strained cyclic tetraynes is currently not known. In conclusion there is room for growth in the chemistry of cyclic strained cycloalkynes and our efforts towards achieving these goals will be discussed in the next chapter.

2. Synthetic approach towards cyclotetraynes

2.1. Introduction

The discovery of C_{60} as a stable carbon allotrope[34] proved to be an invigorating step in acetylene chemistry. Because it was thought that strained alkynes could undergo fullerene formation[35] numerous interesting precursors were synthesized in the hope of deciphering the enigma of fullerene formation. As was mentioned in Chapter 1, great examples of strained acetylenes were synthesized and the boundary represented by 180° bond angle specific to sp-hybridization was passed. Together with the remarkably strained compounds (e.g., **123**, **125**, **133a** or **133b**) discussed in Chapter 1, strained cyclic tetraynes (Figure 2.1) represent a class of compounds that could offer insight into another important question: To what degree can a triple bond be bent?

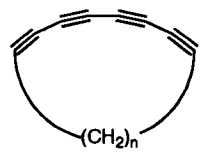

Figure 2.1 General structure of conjugated tetraynes

Attempting to solve this problem, Fallis synthesized compound **201** (Figure 2.2). [36] It was proposed that this compound was formed, but due to its significant ring strain, it was not stable enough for characterization. In principle compound **201** was, however the first member of a new class of chemical compounds: allenyl-ethynyl-phenyl-cyclophane. To the best of my knowledge compound **201** is the only conjugated cyclic tetrayne mentioned in the literature.

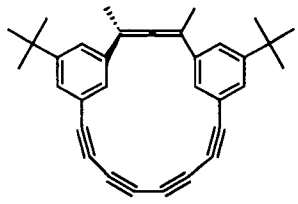

201

Figure 2.2 Structure of compound **201**

Because complete characterization of this type of molecule (cyclotetraynes) is desirable, our approach and interest have been directed towards developing a relatively simple and rational synthesis of cyclic tetraynes, which could afford a quantity of the samples sufficient for complete characterization (Figure 2.1). Hereafter, this chapter describes the synthesis of three relatively strained cyclic tetraynes (**202–204**) and one linear tetrayne (**205**) as a model compound (Figure 2.3).

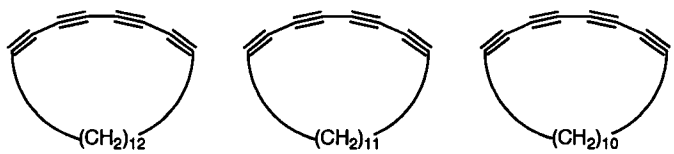

202 203 204

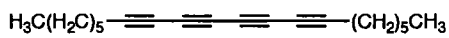

205

Figure 2.3 Structure of compounds **202–205**

Alkyl chains were used to tether the ends of the tetrayne unit due to the fact that by playing with the number of methylene (CH_2) groups, one may influence in a logical and organized manner the strain of the cycle. By decreasing the number of methylene groups (*n* designates the number of methylene groups, Figure 2.1) one by one and

through analysis of the resultant effect on a particular property, trends may be discovered that will provide insight regarding the results of strained triple bonds. Taking all this information into account, the first step toward these molecules is to decide which range of methylene groups would produce the desired level of ring strain in these cycles.

One of the easiest ways to determine if a molecule is strained is to try to build it with a simple model set. Building of the molecules with Darling models showed, to some extent, that the cycle containing n = 15 methylene units, did not have the desired strain although a small amount of deformation of the triple bonds was observed (Figure 2.4). The next compound built, with n = 14 methylene units, showed that the strain was not as great as expected. The same result was found for the model that contained n = 13 methylene units. But as can be seen in Figure 2.3, the compound with n = 12 methylene units (compound **202**) showed a relatively high deformation of the triple bonds, and this therefore, was the first cyclic tetrayne to be synthesized. The success or failure of this synthesis then set the stage for our strategy: if compound **202** was obtained then we would focus on the next smaller compound of the series n = 11, whereas if compound **202** proved to be too strained, then the next larger compound to be attempted with n = 13.

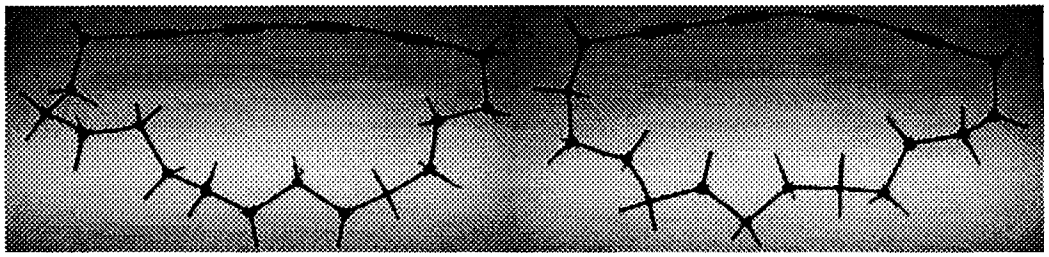

$(CH_2)_{15}$ $(CH_2)_{14}$

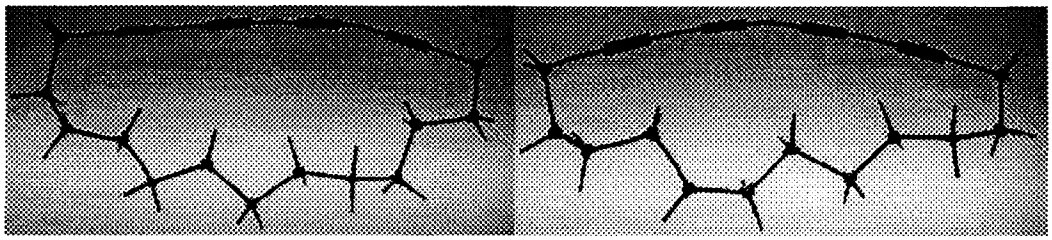

$(CH_2)_{13}$ $(CH_2)_{12}$

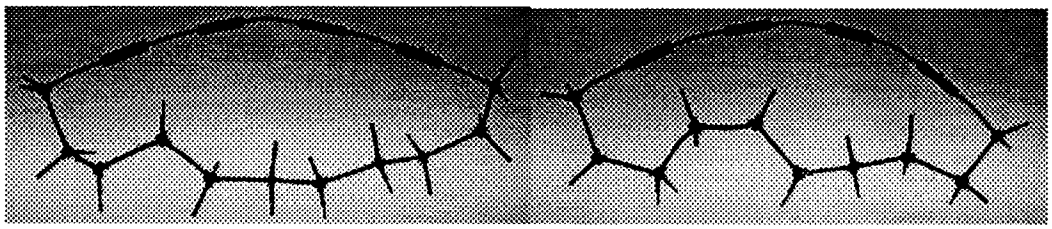

$(CH_2)_{11}$ $(CH_2)_{10}$

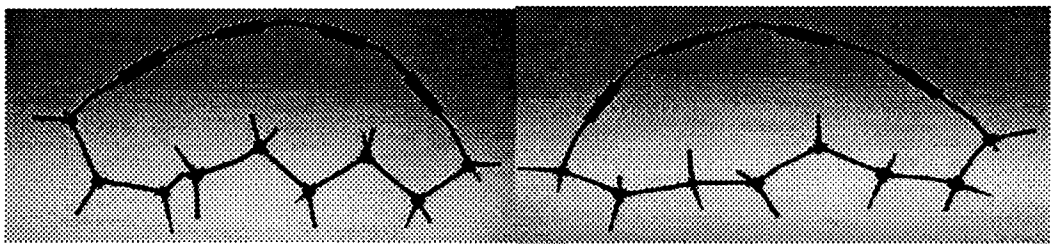

$(CH_2)_9$ $(CH_2)_8$

Figure 2.4 Darling models for cyclotetraynes with n = 15–8

As can be seen in the Figure 2.4 the most strained cyclotetrayne built with the Darling models had eight methylene units. Further trials of increasing the ring strain by reducing the number of sp^3-hybridized atoms resulted in the destruction of these models,

which were only made to show the normal linear geometry of the triple bond and are not made to sustain this kind of strain.

The Darling models showed us where the cyclic strain begins, but a more detailed structural analysis of these compounds was obtained with the aid of MacSpartan.[37] MacSpartan is a reduced version of Spartan, which runs only for Unix computers, programed for Mac computer users. This version of the program provides standard molecular mechanics, semi-empirical, and *ab initio* methods and is intended to be used by synthetic chemists that do not have knowledge in molecular mechanics calculations, myself included in this category.

Using calculation at the **3-21G*** level of MacSpartan, cyclic tetraynes with varying alkyl chain tethers have been modeled, and theoretically predicted bond angles obtained for the tetraynes. Calculations were done for compounds containing from twelve to ten methylene units and only one representative minimized structure of each of the resulting structures is presented in Figure 2.5. Unfortunately, every time the same molecule was modeled, a slightly different set of bond angles for the triple bonds was displayed (the range is given in Table 2.1). Therefore, seven different calculation runs were done for each molecule and the averaged bond angles of the triple bonds for each individual minimized structure ware calculated (Table 2.2).

Table 2.1 Range of obtained angles (°) using MacSpartan

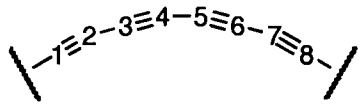

n	1–2–3	2–3–4	3–4–5	4–5–6	5–6–7	6–7–8
12	166.1–168.3	165.8–168.5	167.1–169.1	166.6–170.1	167.4–171.0	166.3–173.5
11	164.7–170.8	163.6–168.1	163.8–167.9	165.1–167.0	165.2–168.6	165.8–171.4
10	160.5–167.3	159.8–165.6	160.7–164.9	163.0–164.9	162.7–166.2	163.3–170.0

Table 2.2 Calculated average angles (°) over all the bonds for each minimized structure [(1–2–3 + 2–3–4 + 3–4–5 + 4–5–6 + 5–6–7 + 6–7–8) / 6]

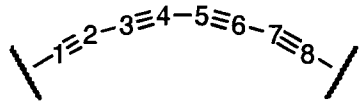

n	Structure 1	Structure 2	Structure 3	Structure 4	Structure 5	Structure 6	Structure 7
12	169.0	169.4	168.4	168.9	167.0	168.9	169.9
11	166.5	166.3	167.9	167.3	168.3	167.2	165.7
10	165.2	162.8	165.9	165.9	164.7	164.3	165.3

As can be seen from Table 2.1, the bond angles deviates from the normal 180° to 168.6° for the angle formed by carbon atoms 1–2–3 (as noted in the figure above the table) for $n = 12$. A more pronounced decrease in the bond angle is noticed for the angles 3–4–5 and 4–5–6 where the difference between the most strained and the most unstrained compound is more then 10°. All the structures, with their angle values are presented in Appendix 1 at the end of the thesis.

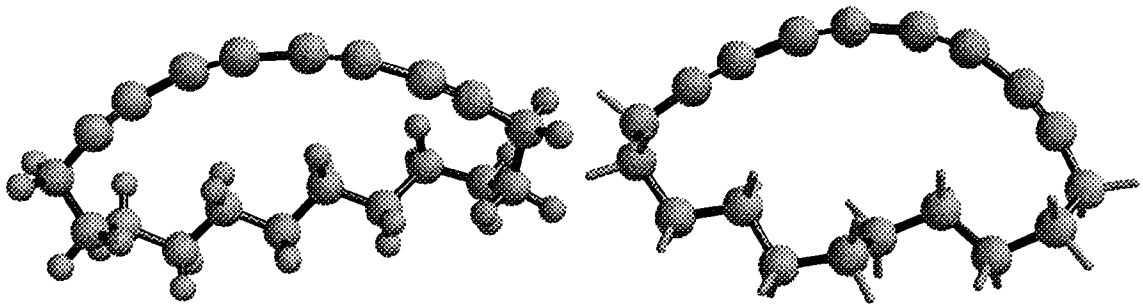

$(CH_2)_{12}$ $(CH_2)_{11}$

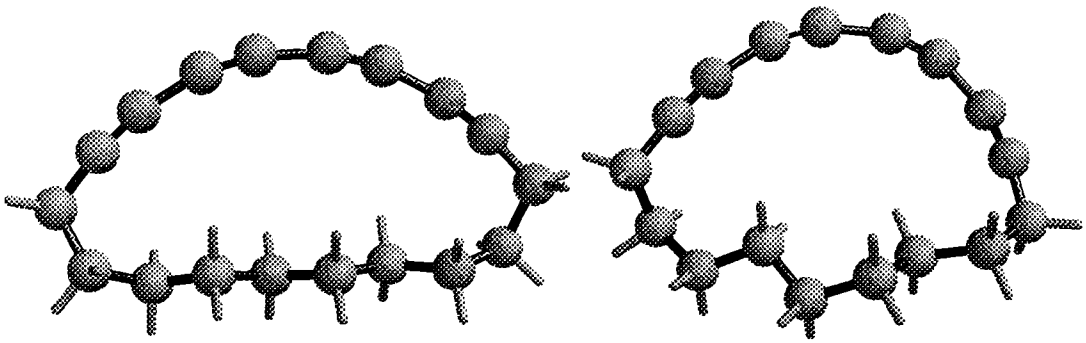

$(CH_2)_{10}$ $(CH_2)_9$

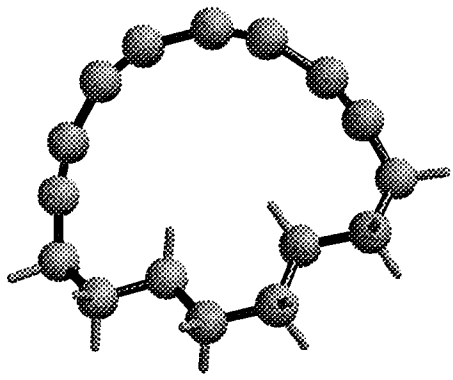

$(CH_2)_8$

Figure 2.5 MacSpartan minimized structures for compounds having n = 12–8

2.2. Synthetic approach toward cyclotetraynes

Once the computational part of this project was accomplished with the aid of MacSpartan, a synthetic approach toward cyclotetraynes was devised. The plan toward cyclic tetraynes involved six reaction types that are outlined in Scheme 2.1. Starting from the corresponding diacid (**I**), treatment with either PCl_3 or $SOCl_2$ would afford acyl chloride (**II**), Friedel-Crafts acylation would afford diketone (**III**),[38,39] and subsequent Corey-Fuchs dibromoolefination[40] would provide tetrabromide (**IV**). The deprotection of the silyl alkynes and homocoupling under Hay conditions[41,42] would afford the cyclic tetrayne precursor **V**. The cyclic compound **V** is then rearranged according to the Fritsch-Buttenberg-Wiechell (FBW) rearrangement,[43-46] to yield the desired compound **VI.** The design of this synthetic approach seemed to be straightforward although problems appeared even with the first reaction, the Friedel-Crafts acylation. The first step in the acylation was the transformation of the respective acid to the acyl chloride. For this purpose, thionyl chloride ($SOCl_2$) was used. Unfortunately industrial production and export from the USA of thionyl chloride was controlled under the Chemical Weapons convention, limiting my access to this reagent. So this simple reagent, used for a single sequence, had to be replaced with phosphorus trichloride (PCl_3). Thus, although the final product was the same, the procedure was modified in order to accommodate this new reagent.

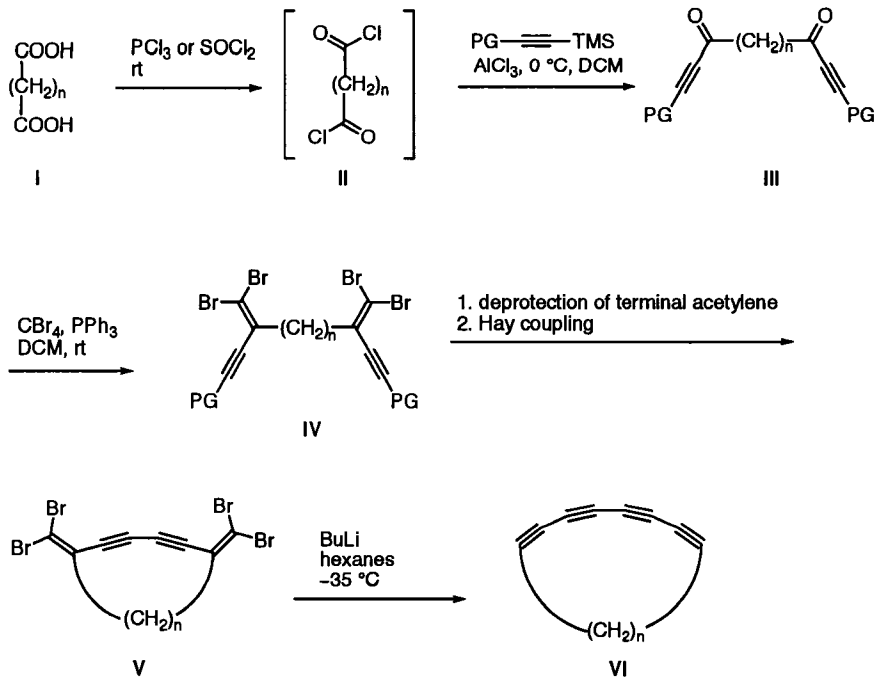

Scheme 2.1 Strategy toward cyclic tetraynes where PG is either a TBDMS or TMS protecting groups

2.2.1. Synthesis of compound 202 (n = 12)

To accomplish the synthesis of the cyclotetrayne that contains twelve methylene units (Scheme 2.2) the synthesis started with tetradecanedioic acid (**206**). The diacid was converted to the acyl chloride using $SOCl_2$ and the uncharacterized acyl chloride was reacted with *tert*-butyldimethyl-trimethylsilyl-acetylene and aluminum trichloride. The resulting compound **207** was obtained with a satisfactory yield of 75% (Scheme 2.2). *Tert*-butyldimethylsilyl was the initial protective group of choice for the alkyne group due to its stability.

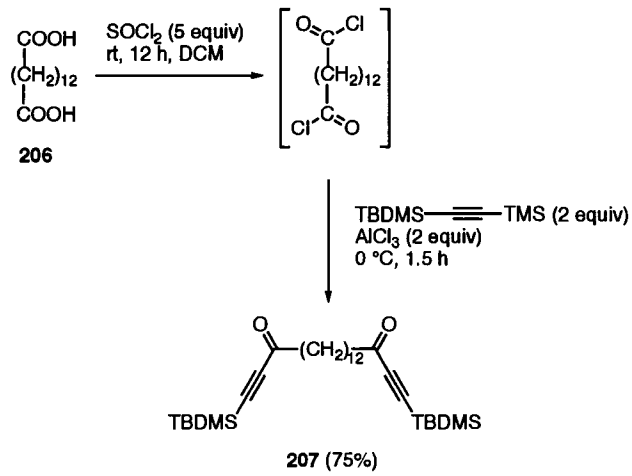

Scheme 2.2 Synthesis of compound **207**

The next step in the sequence of reaction was the synthesis of the tetrabromide **208**. Following the traditional procedure,[40] this reaction proved to be quite easy and high yielding 82% (Scheme 2.3).

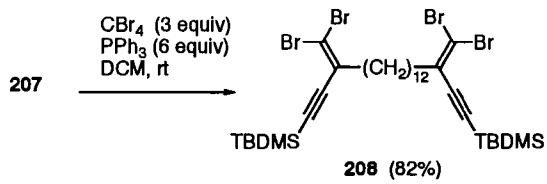

Scheme 2.3 Generation of tetrabromide **208**

Once the tetrabromide was obtained, the next step was the removal of the TBDMS group in the presence of TBAF, using wet THF as a solvent, Scheme 2.4.

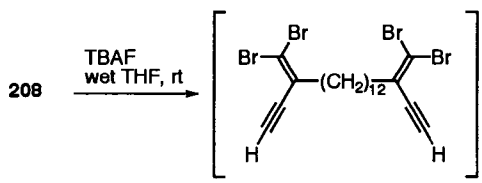

Scheme 2.4 Deprotection of tetrabromide **208**

Unfortunately the alkyne was not very stable during deprotection, as was seen by TLC analysis (Figure 2.6). The TLC plate showed the newly formed terminal alkyne and also a considerable baseline spot. But this was intuitive because after the addition of TBAF to the solution, which was initially pale yellow in color, it turned immediately dark purple. Attempts at improving the outcome of deprotection failed (by increasing the volume of the solvent or by a rapid quench of the reaction).

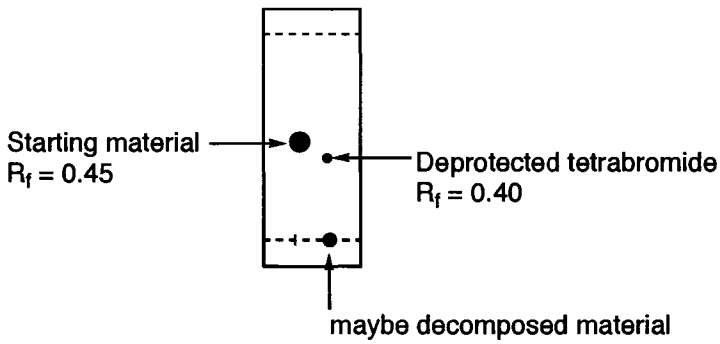

Figure 2.6 TLC on silica gel of compound **208** and its deprotected form, eluent used: hexanes (co-spot is not shown)

It is worth noting that after deprotection, an aqueous work-up was required as well as drying of solution. The newly formed terminal alkyne was not stable neat, and this was observed during removal of the THF solvent completely, which resulted in the formation of dark red oil. Upon TLC analysis even further decomposition of the desired compound was revealed. Although the results of the deprotection step were not great, trials of homocoupling of the terminal alkynes to form a cycle were attempted. Unfortunately the yields were less than satisfactory (2–3%). Therefore this synthetic sequence was abandoned.

It was realized that the protecting group used (TBDMS) was not the best choice, although the yields of the initial reactions were satisfactory. Thus, a new protecting group

was chosen, trimethylsilyl (TMS), which was expected to be easier to remove. The sequence of reactions started from the same diacid (tetradecandioic acid, **206**), but in the acylation step *tert*-butyldimethyl-trimethylsilyl-acetylene was replaced with *bis*-trimethylsilyl-acetylene, yielding compound **209** (Scheme 2.5). The yield of this reaction was 64%. The Corey-Fuchs dibromoolefination yielded compound **210** with a 51% yield.

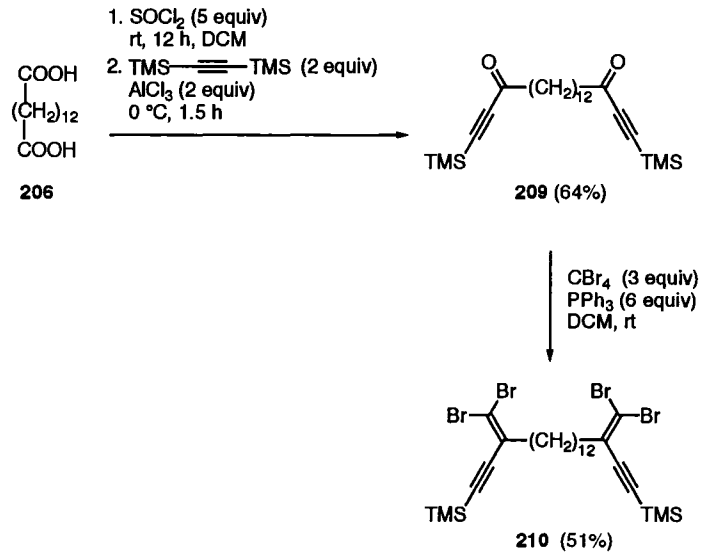

Scheme 2.5 Synthesis of compounds **209** and **210**

Yields proved to be lower in this case compared with the previous reactions (with TBDMS as substrate) and this was mainly attributed to the fact that the TMS protective group was more labile. In some cases, the monodeprotected diketone (**209a**) (Scheme 2.6) was formed in the reaction together with the desired material (**209**). Column chromatography was used to separate these two diketones, but this step proved to be difficult due to the fact that monodeprotection took place even during column chromatography. In principle column chromatography afforded the purified compounds **209** and **209a**, but a certain portion of the mixture was not separated due to coelution.

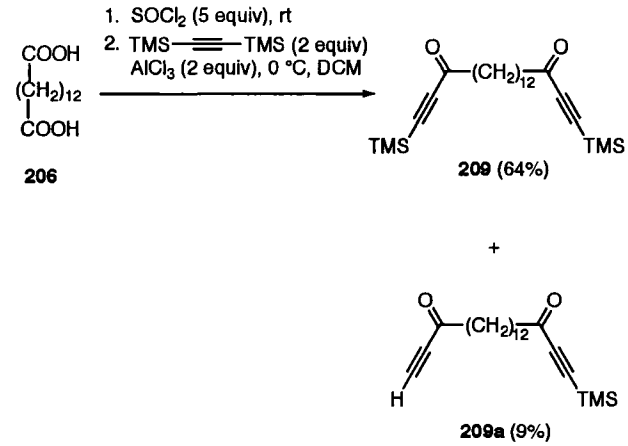

Scheme 2.6 Formation of diketone **209**

In order not to waste valuable starting materials, the resulting mixture (**209** and **209a**) was subjected to Corey-Fuchs dibromoolefination (Scheme 2.7). Most probably both compounds **210** and **210a** were formed. Subsequent desilylation of presumed mixture ultimately afforded compound **210b**. TLC analyses during the deprotection reaction were crucial toward determining that the Corey-Fuchs reaction and subsequent desilylation could be done even without purification of compounds **209** and **209a** (Figure 2.7). Therefore it is safe to assume that even without separation of compounds **209** and **209a**, the mixture can undergo the Corey-Fuchs reaction without any problems.

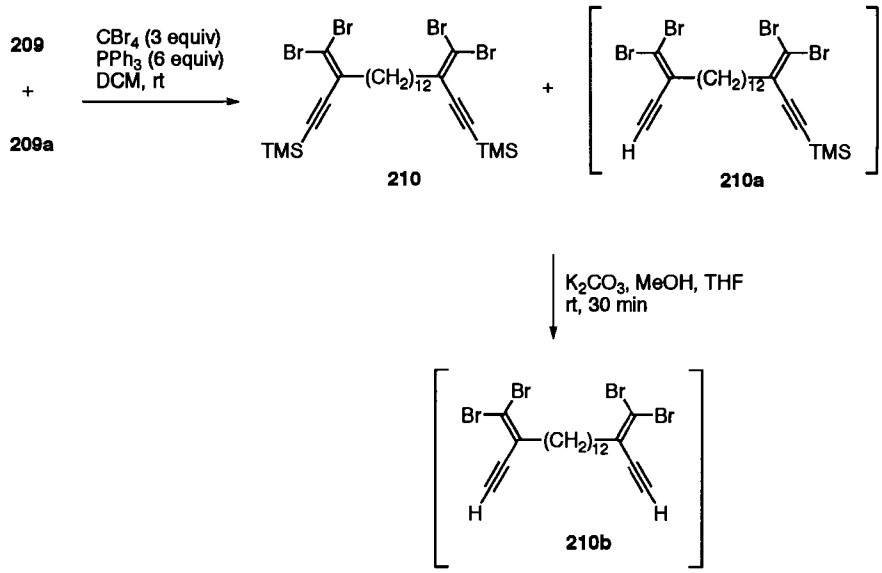

Scheme 2.7 Schematic representation of what was believed to occur during synthesis of compound **210b**

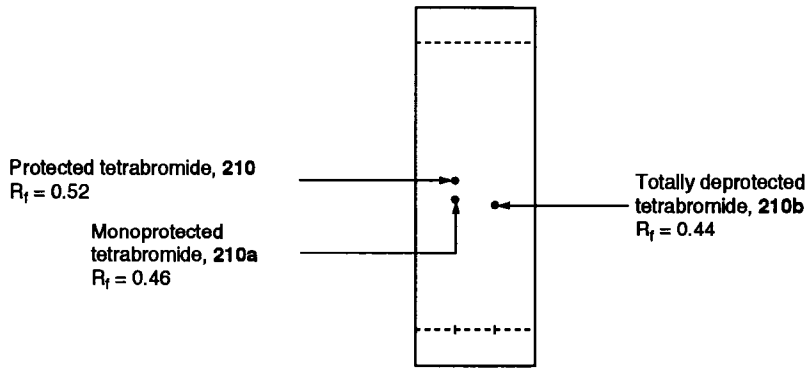

Figure 2.7 TLC on silica gel of the deprotection of compounds **210** and **210a**, eluent used: hexanes (co-spot not shown)

Having solved the problems that occurred in the acylation step and obtaining the linear tetrabromide **210** as a pure compound, the next step was the Hay coupling.[41] The Hay coupling was used because this is one of the most encountered reactions in the synthesis of cyclic diacetylenes, forming carbon-carbon bond *via* oxidative coupling of terminal acetylenes. The pre-catalyst in the Hay coupling is Cu(I), which is oxidized to

Cu(II) in the catalytic cycle by oxygen that is bubbled into the flask during the reaction. *N,N,N,N*-Tetramethylethane-1,2-diamine (TMEDA) is used in this type of reaction because it forms a complex with copper that is soluble in a wide variety of solvents. As a solvent we chose DCM because it has given good results for coupling of terminal alkynes in our group.[43] From the beginning, it was clear that in order to obtain the cyclic monomer from the terminal dialkyne, the reaction conditions would have to be changed from the standard ones. The question was, how dilute did the reaction mixture need to be in order to maximize the formation of the desired monomer (Scheme 2.8)?

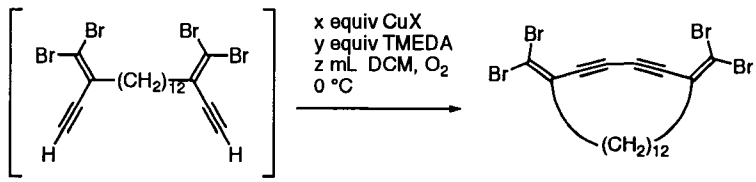

210b **211**

Scheme 2.8 Schematic representation of Hay coupling yielding compound **211** (x, y and z equiv because the required quantities were not yet known)

Having found a protecting group that can be easily removed (TMS) without decomposition of the terminal dialkyne, screening for the best Hay conditions began. The Hay catalyst was prepared by mixing CuCl with TMEDA in a solution of DCM for 10–15 minutes in the presence of air. The terminal dialkyne (0.47 mmol) was dissolved in 25–30 mL of DCM and added drop-wise to the solution containing the catalyst over a short period of time (5 min). The most important conditions and results when using CuCl as catalyst are summarized in Table 2.3.

Table 2.3 Conditions and results for different catalyst loading and dilution conditions

Entry	Terminal dialkyne (mmol)	CuCl (mmol)	TMEDA (mmol)	Time of addition of terminal dialkyne	DCM (mL)	Yield (%)
1	0.47	0.47	0.47	10 min	100	~5% Mainly polymerization occurred
2	0.47	0.47	0.47	10 min	200	~12%
3	0.47	0.47	0.47	30 min	500	Very slow reaction
4	0.47	1.41	1.41	N/A	500	25-30%

As it can be seen in **Entry 1**, the volume of DCM that I started with was 100 mL, unfortunately the solution was too concentrated and polymerization took place (the reaction was allowed to mix for 2 hours). When the volume of DCM was doubled (**Entry 2**) the yield was not satisfactory, possibly because the addition of the terminal dialkyne to the reaction mixture was too fast and polymerization also took place. Not yet realizing that the addition time of the deprotected dyine to the reaction mixture was also a very important factor, I changed the volume of DCM to 500 mL (**Entry 3**) and, unfortunately, the reaction was too slow and only the starting material was seen on TLC plate over a period of 2 hours. After careful monitoring of the reaction for over 2 hours, I realized that it was not going to go to completion, so another two equivalents of CuCl were added, bringing the total sum of catalyst to three equivalents (**Entry 4**). The amount of TMEDA was also changed in accordance with the catalyst. The cyclic monomer (**211**) was

obtained in a yield of 25%. A second run with the same reaction conditions provided compound **211** in 30% yield, which was encouraging. In this reaction, I noticed that the reaction was not going to completion, and according to the TLC analysis the spot belonging to the terminal dialkyne was still present after two hours. So either the catalyst loading was insufficient or the dilution conditions were exaggerated.

Usually the choice of Cu(I) is almost arbitrary, it can be either CuCl or CuI. By changing the catalyst from CuCl to CuI, due to personal preference, I noticed that reaction times were relatively faster. Using the same reaction conditions as in **Entry 4** with CuI, a new compound was isolated, with a crystalline white appearance and it was thought to be the cyclic dimer (**212**) (Figure 2.8). Unfortunately mass spectroscopy could not give any information about the molecular weight so conclusive identification of **212** was not possible. ^{13}C NMR shifts for sp^2 (two signals) and sp (two signals) hybridized carbon atoms for **212** were close to those of compound **211**. The only difference appeared in the chemical shifts of sp^3-hybridized carbons (six signals), where those of the cyclic dimer **212** showed slightly downfield values (Figure 2.9)

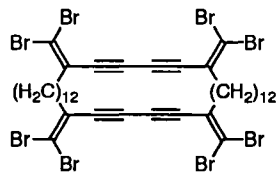

212

Figure 2.8 Assigned structure for compound **212**

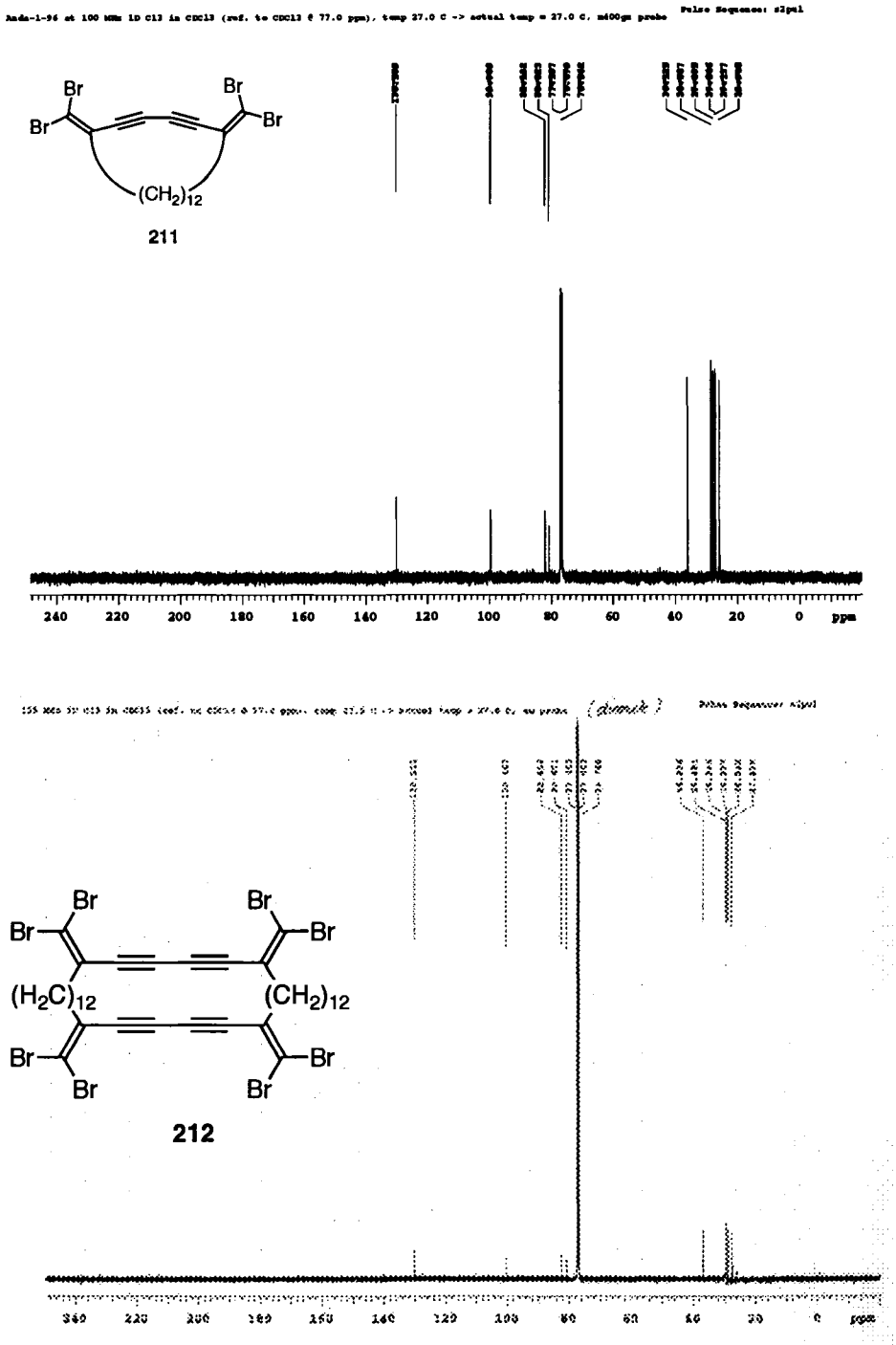

Figure 2.9 ^{13}C NMR spectra of compounds **211** (100 MHz, $CDCl_3$) and **212** (125 MHz, $CDCl_3$)

Overall, this reaction ultimately gave the cyclic monomer **211** (31%), dimer **212** (13%), an uncertain amount of unreacted starting material (not isolated), and baseline material. The TLC of this reaction is presented in Figure 2.10.

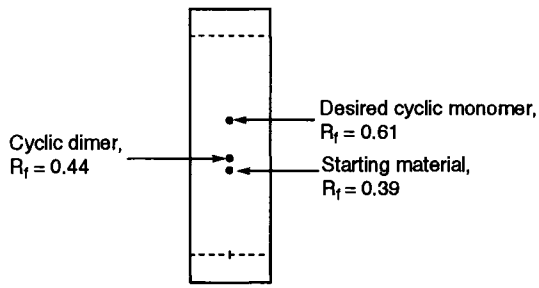

Figure 2.10 TLC on silica gel, representing the Hay coupling reaction using conditions from **Entry 4**, eluent used: hexanes (co-spot not shown)

Using the conditions from **Entry 4** (Table 2.3), afforded not only the desired compound, but also the perplexing result of having the dimer formed and residual starting material. Then I realized that the solution containing the terminal alkyne added to the DCM that contained the catalyst was too concentrated. Therefore, the time for addition of terminal alkyne to the catalyst solution was increased from 5 to 20 minutes, and the amount of solvent used to dissolve the terminal alkyne was also increased to about 150 mL. Due to the fact that many reactions were run in order to optimize the conditions and a fair amount of compound **211** was obtained, further trials to increase the yield were not tried.

The next step in the synthetic approach to the cyclic tetrayne was the FBW rearrangement. It has been shown in our group that alkyne moieties readily undergo 1,2-shifts through an intermediate alkylidene carbenoid species.[43,47] In this reaction lithium-halogen exchange between BuLi and 1,1-dibromoolefin initiates a Fritsch-Buttenberg-Wiechell (FBW) rearrangement and affords new polyynes. It has been shown in our

group that dibromoolefinic precursors substituted with alkyl chains undergo FBW rearrangement with an excellent rate of success not even expected by the authors,[48] yielding compounds such as **213a** and **213b** in almost incredible yields of 83% and 71%.

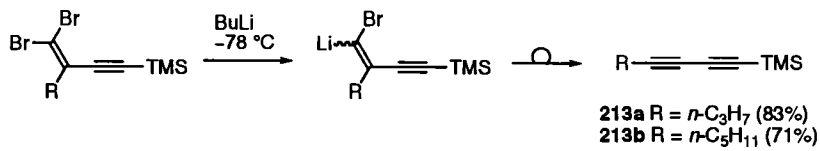

Scheme 2.9 Alkyl substituents incorporated to the enyne framework and their yields

In the same work it was shown that multiple FBW rearrangements could take place. The two-fold rearrangement yielded compounds **214a** and **214b** high yields of 67% and 66% (Scheme 2.10).

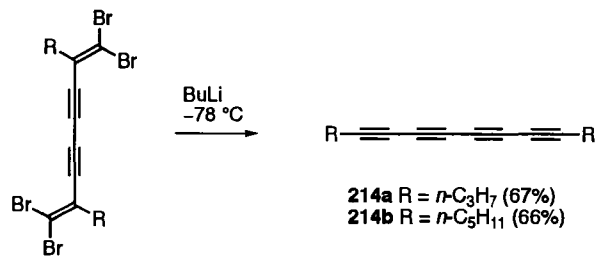

Scheme 2.10 Literature precedent for a two-fold rearrangement

With the knowledge that the two-fold FBW rearrangement worked well and that pendant alkyl groups were suitable candidates for this particular reaction, the only thing that remained was to attempt this reaction on the cyclic precursor **211** (Scheme 2.11). The cyclic tetrabromide **211** was dissolved in dry hexanes, the temperature decreased to about –35 °C, and 2.1 equivalents of BuLi were added drop-wise over a period of 2 minutes. The solubility of compound **211** in hexanes at lower temperatures was quite low, and care was therefore taken when the solution was cooled down and the amount of solvent was

increased as necessary. With the addition of each drop of BuLi, the solution changed the color to a dark yellow-brown. After addition of BuLi was complete the solution was quenched carefully at –10 °C with aqueous ammonium chloride, usually ca. 25–30 minutes after the addition of BuLi.

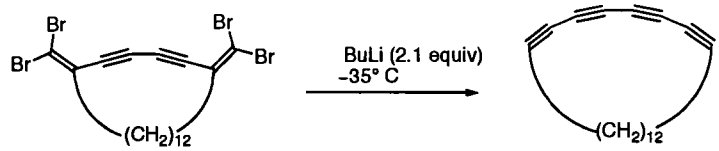

211 202

Scheme 2.11 FBW rearrangement of compound **202**

Compound **202** proved to be unstable neat and had to be stored as a solution. Subsequent to workup and purification (column chromatography), the complete removal of solvent yielded a dark red solution. As mentioned, upon complete removal of solvent, compound **202** decomposed, presumably into a carbon rich material that was not characterized. EI mass analysis failed to give a conclusive answer regarding the molecular formula of **202**, which should be $C_{20}H_{24}$, but rather an unexpected molecular peak was observed at an *m/z* that corresponds to $C_{24}H_{34}$. This byproduct was presumably the result of butylation that takes place during the FWB rearrangement. Fortunately, this byproduct decomposed faster when neat than the desired compound **202**, so complete removal of solvent followed by a second round of column chromatography to remove the newly formed baseline material yielded the pure compound **202**. On the other hand, the trial of removing of the much less unstable butylated product through concentration had unwanted consequences; the desired compound (**202**) decomposed as well, but at a slower rate. It was observed by TLC analysis that after the removal of the byproduct, the

purified compound **202** decomposed yielding a new baseline material. Compound **202** proved, however, to be stable for longer periods of time if stored in hexanes and at 0 °C. The ^{13}C NMR spectrum of **202**, however, was consistent with the desired structure (Figure 2.11). As expected in the NMR spectrum of **202** there are four sp-hybridized carbons that resonate between 91.8 and 64.2 ppm and six sp^3-hybridized carbons that are clustered together in the region of 31.4–20.3 ppm.

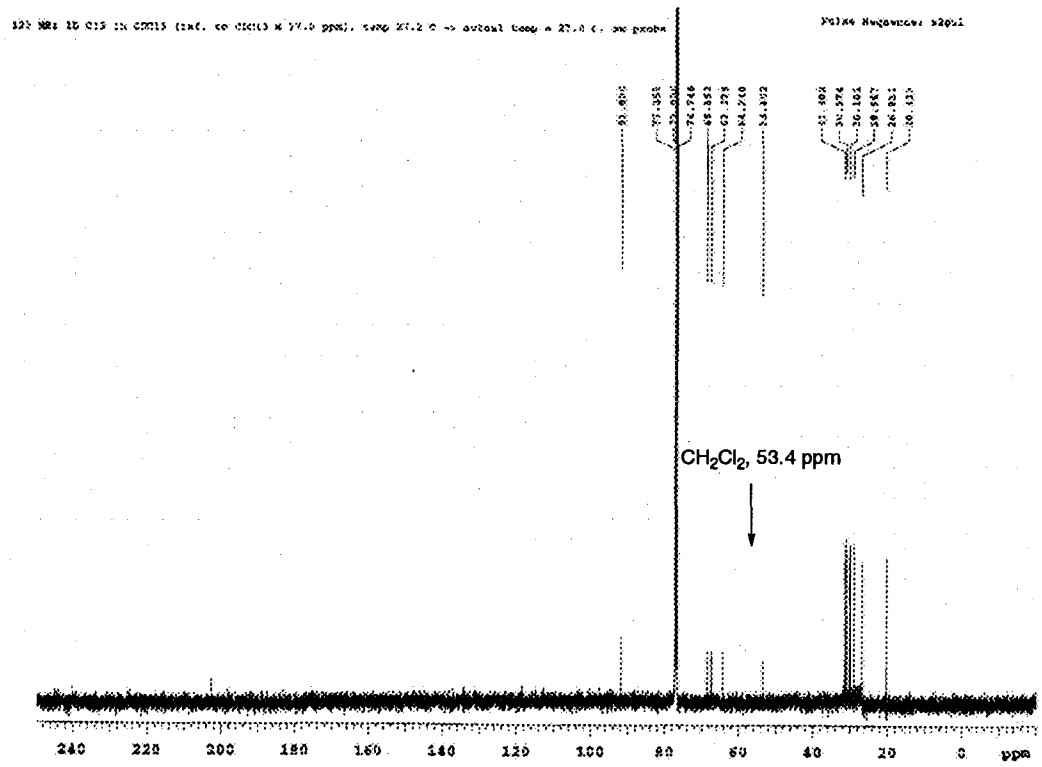

Figure 2.11 ^{13}C NMR spectrum (100 MHz, $CDCl_3$) of compound **202** (DCM also present)

2.2.2. Synthesis of compound 203 (n = 11)

We next directed our attention toward the synthesis of cyclic tetrayne **203**, which has one CH_2 unit less than compound **202**. Being familiarized with all the reactions involved in this type of synthesis, the reaction sequence was more easily accomplished (Scheme 2.12). Starting with diacid **215** the first step, as usual was the formation of the acyl chloride followed, by the Friedel-Crafts acylation that afforded diketone **216** in a 65% yield, which was reasonable for a two-step reaction sequence. Diketone **216** smoothly underwent dibromoolefination, resulting in tetrabromide **217** (60% yield). Scaling up the Hay coupling reaction gave compound **218** in a disappointing yield of 17%, but the amount isolated was sufficient for the subsequent FBW step. Therefore trials to improve this yield were not attempted.

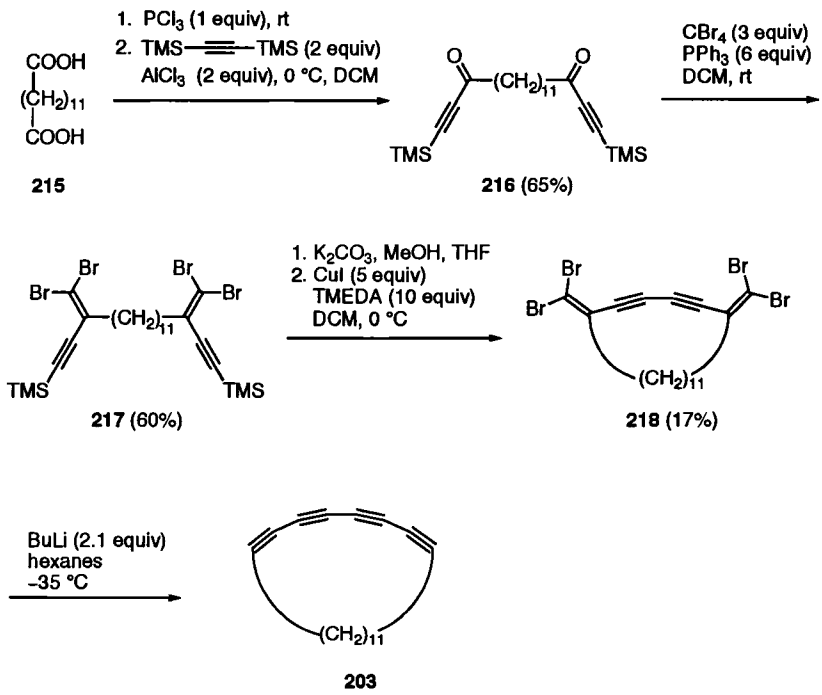

Scheme 2.12 Synthesis of compound **203**

The ^{13}C NMR spectrum of **203** (Figure 2.12) provided evidence that the desired compound was formed, showing four signals for sp-hybridized carbon atoms and six signals for sp^3-hybridized carbon atoms. Once again EI mass analysis proved useless for this type of compound, and the molecular peak was not observed. No other MS methods were attempted.

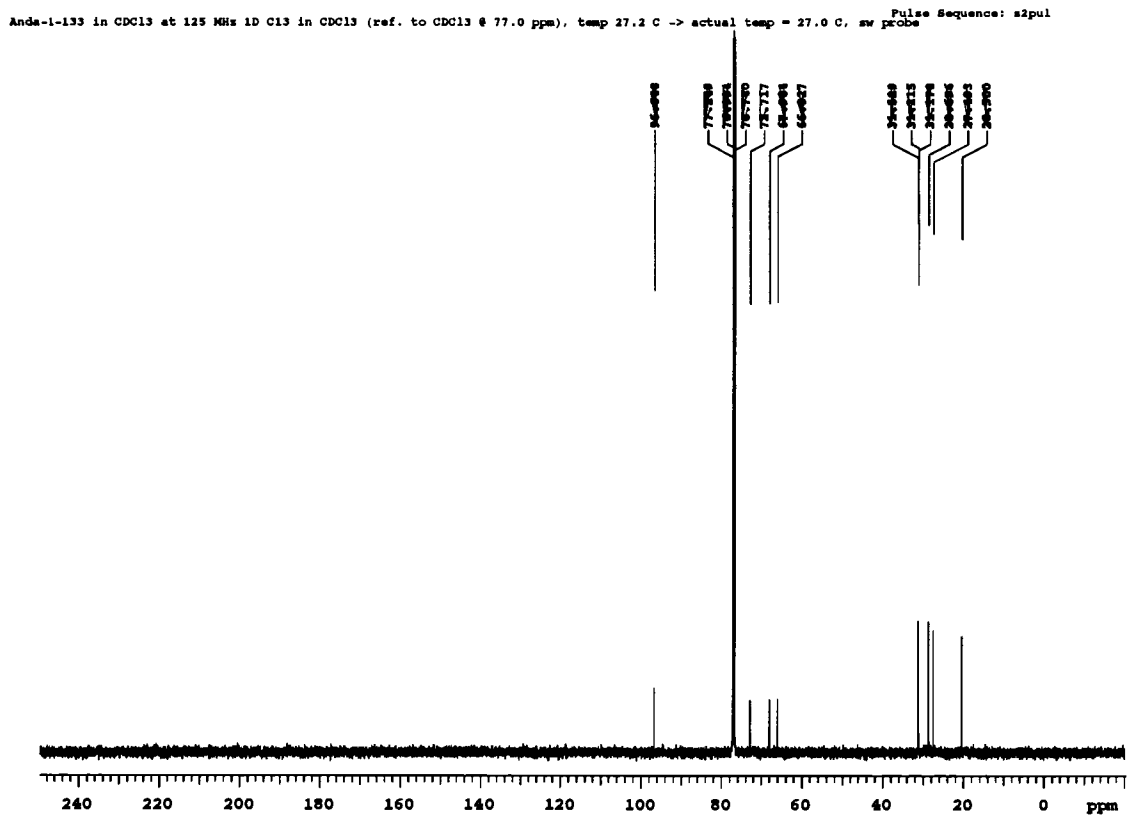

Figure 2.12 ^{13}C NMR spectrum (125 MHz, $CDCl_3$) of compound **203**

2.2.3. Synthesis of compound 204 (n = 10)

Having successfully synthesized two cyclic tetraynes (**202** and **203**) our attention was focused into preparing the next strained macrocycle, which contained only ten methylene units. Its synthesis was essentially identical to the two previous cases

discussed (Scheme 2.13). The uncharacterized acyl chloride was subjected to Friedel-Crafts acylation and diketone **220** was produced in an almost incredible yield of 96%. The subsequent dibromoolefination yielded compound **221** in 60% yield, and the tetrabromide **221** was desilylated using the standard procedure. The resulting terminal alkyne was dissolved in ca. 500 ml of DCM. Meanwhile the catalyst solution, prepared by dissolving 5 equivalents of CuI and 10 equivalents of TMEDA in ca. 1500 mL of DCM was cooled down to 0 °C. Using a dropping funnel, the terminal alkyne was added to the freshly prepared catalyst solution for over a period of 30 minutes. Compound **222** was obtained in 74% yield. Finally, careful addition of BuLi to compound **222** in a solution of dried and cooled hexanes yielded compound **204**, which was purified via flash chromatography (silica gel, hexanes).

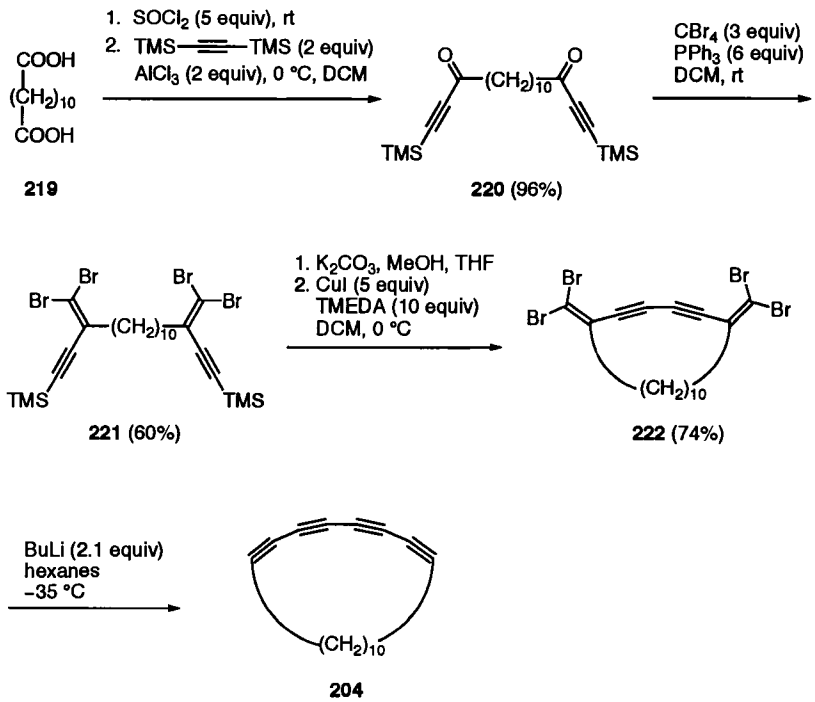

Scheme 2.13 Synthesis of compound **204**

Compound **204** did not prove to be as robust as its predecessors, compounds **202** (n = 12) and **203** (n = 11). Complete removal of the solvent left behind an almost completely decomposed material. NMR spectroscopic analysis consistently showed a small amount of hexanes, which could not be removed even though numerous trials of replacing it with chloroform were tried. Shown in Figure 2.13 is the ^{13}C NMR spectrum of compound **204**. All its characteristic signals are observed, including four signals due to sp-hybridized carbons and five others carbon atoms in the sp^3-region.

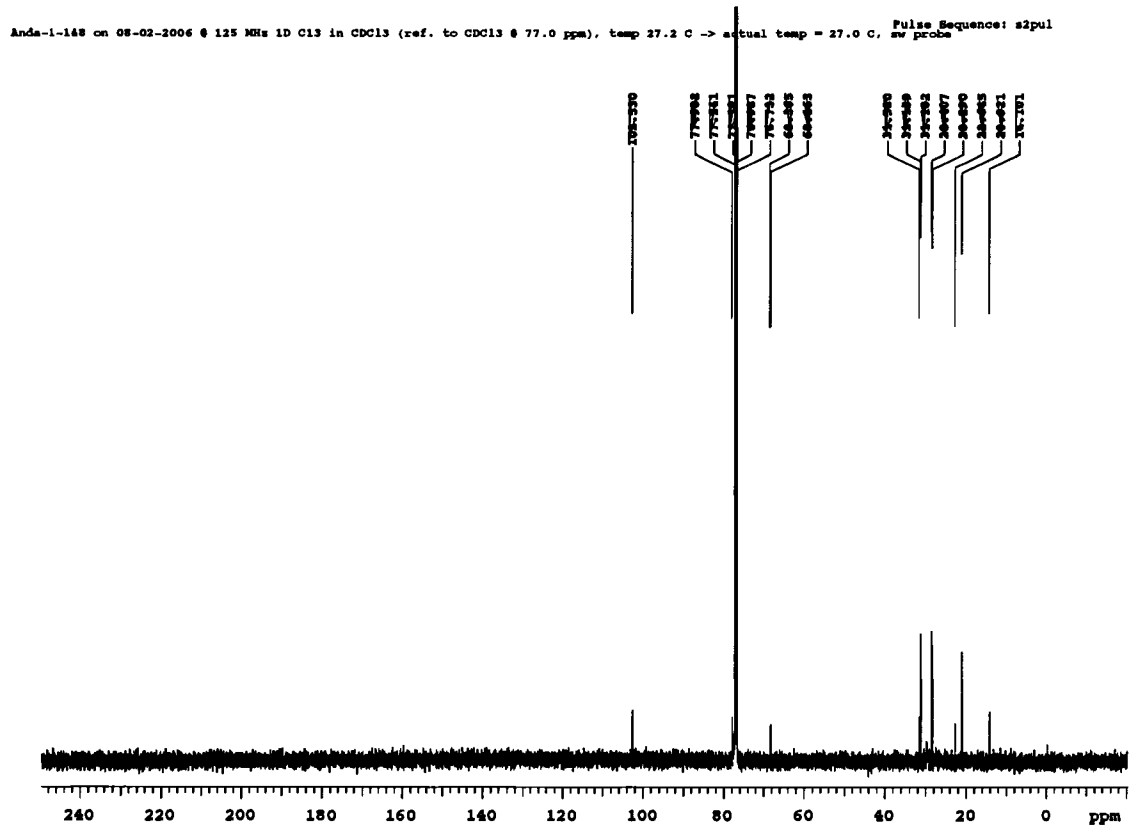

Figure 2.13 ^{13}C NMR spectrum (125 MHz, $CDCl_3$) of compound **204** (hexane impurities at 31.6, 22.6 and 14.1 ppm)

2.2.4. Synthesis of linear compound 205

Following to the successful synthesis of three cyclic tetraynes compounds **202** (*n* = 12), **203** (*n* = 11) and **204** (*n* = 10), it was time to synthesize and characterize a model acyclic compound, **205**. Scheme 2.14 illustrates the synthetic pathway that finally gave the desired product. The synthesis began with the readily available heptanoic acid **223**, which was treated with $SOCl_2$ and then subjected to Friedel-Crafts acylation to give monoketone **224** in 49% yield. The Corey-Fuchs dibromoolefination afforded compound **225** in 67%. Subsequent desilylation and homocoupling afforded compound **226** in a modest yield of 40%. Compound **226** was subjected to a two-fold FBW rearrangement and yielded compound **205** in 79%. In comparison to its cyclic homologs, compound **205** can be stored neat and was isolated as light yellow oil that showed no signs of decomposition.

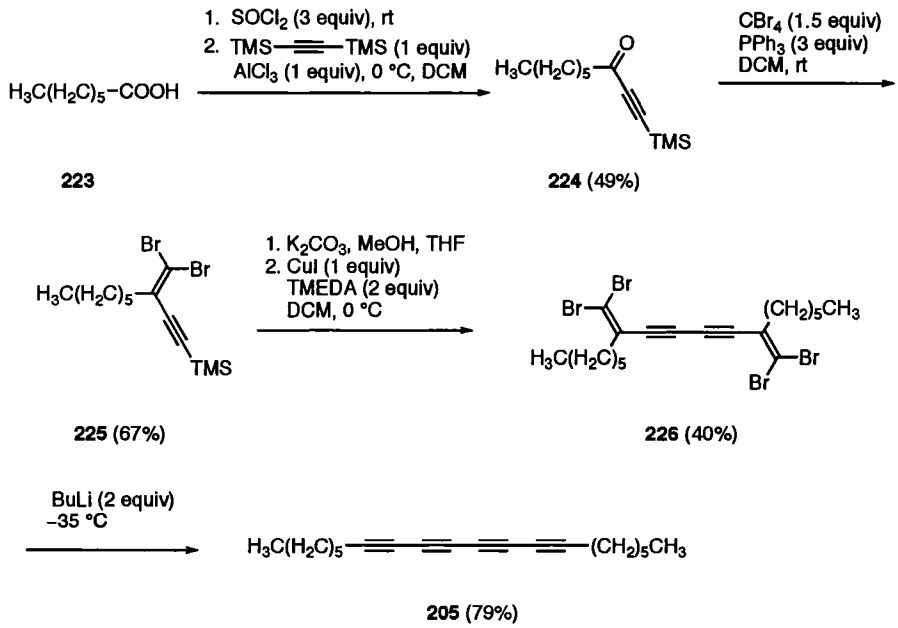

Scheme 2.14 Synthesis of compound **205**

The ^{13}C NMR spectrum (Figure 2.14) of compound **205** appears to look more like cyclic compound **202** (n = 12). A more detailed comparison between the cyclic tetraynes and the linear tetrayne will be presented in the next chapter.

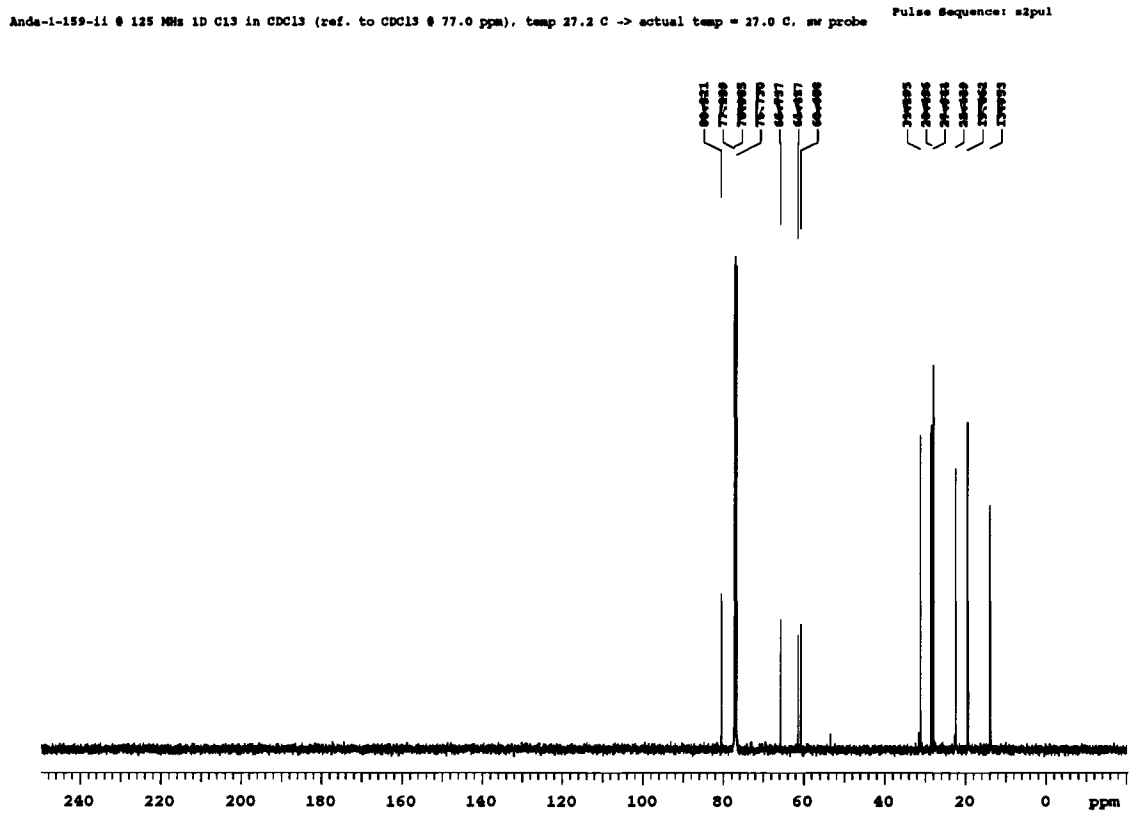

Figure 2.14 ^{13}C NMR spectrum (125 MHz, $CDCl_3$) of compound **205**

The synthetic strategy toward the cyclic tetraynes proved successful, providing a series of three strained cycles and one linear compound in order to compare their properties. We then became intrigued by the synthesis of the much more strained compounds **227** and **228** (Figure 2.15).

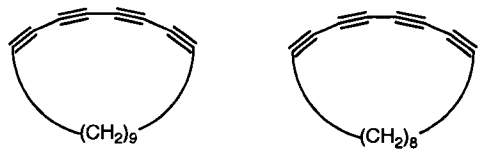

227 228

Figure 2.15 Structure of compounds **227** and **228**

Due to a lack of time, the FBW rearrangements have not yet been completed, but the precursors have been synthesized in good yields (Scheme 2.15). The starting point of the synthesis was once again the formation of the respective acyl chlorides from the diacids **229** and **230**. Subsequent acylation afforded the diketones in good yields (**231** and **232**), Corey-Fuchs reaction gave **233** and **234**, which were deprotected and homocoupled to form cyclic diynes **235** and **236.**

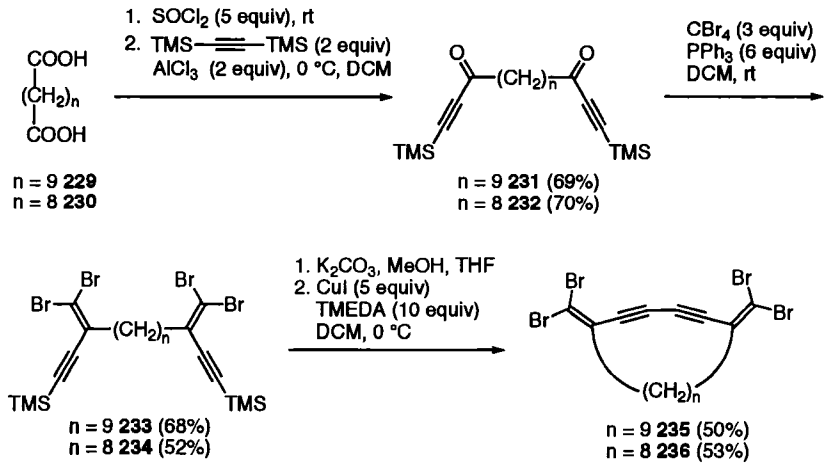

Scheme 2.15 Synthesis of precursors for compounds **227** and **228**

2.3. Conclusion and Future Work

In this chapter the synthesis of three cyclic tetraynes (**202–204**) and an acyclic analog (**205**) was discussed together with those of their precursors. Optimization of conditions needed for their synthesis has also been presented. The most difficult step was the development of conditions for the Hay coupling to provide the cyclic precursors. For this reaction it was found that the best results required: 5–6 equiv. of CuI and 18 equiv. of TMEDA dissolved in 1500 mL DCM and stirred at atmospheric pressure for ca. 15 minutes until the color of the solution turns pale blue. A previously desilylated tetrabromide (3.5 mmol) was dissolved in ca. 400 mL DCM and added drop-wise to the catalyst mixture over a 30 min period. Why this relatively large-scale reaction? This corresponds to a little more or less than 2 g of the tetrabromides, used to ensure a yield of ca. 0.7 g of the desired diyne-macrocycle precursor. Due to the fact that during FBW rearrangement four bromine atoms are lost and the stability of cyclotetraynes is questionable, there is a need for at least one-gram scale reactions. The future of this project rests in the ability to synthesize the cyclic tetraynes through the FBW rearrangement of compounds **235** and **236**, which will create even more strained cyclotetraynes.

3. Discussion

In this chapter two separate problems will be discussed, the first involves the analysis of some unexpected characteristics of the cyclic tetrabromide precoursors. Second, is an evaluation of what has been discovered by characterization of cyclotetraynes and looking at trends as a function of ring strain.

3.1. Tetrabromides

It has to be noted that the successful synthesis of the cyclic tetrabromides represented a milestone in the synthesis of cyclotetraynes, from my point of view. Careful monitoring of the Hay coupling reactions and numerous changes in reaction conditions to optimize the yield represented meticulous work over a period of many months. Adding to this effort was extensive solution state characterization.

HMBC NMR spectroscopy was used to identify, as much as possible, each sp^3-hybridized carbon atom of the alkyl chain. This analysis also provided another interesting trend. Initially it was thought that the endocyclic sp^2-carbon atoms resonated around 100 ppm and exocyclic sp^2-carbon atoms, bearing two electronegative bromine atoms, resonated around 140 ppm. HMBC NMR analysis showed the opposite. Figure 3.1 contains one HMBC spectrum (compound **235**), all the other HMBC spectra are attached in Appendix 2. As can be seen, the carbon atom that resonates at around 130 ppm is correlated with two types of hydrogen atoms (^2J and ^3J, respectively). This particular carbon resonance corresponds to the endocyclic (sp^2) carbon atom because it is the only one likely to couple to both the allylic and homoallylic methylene protons (schematic representation in Figure 3.2). On the other hand, for the carbon atoms that resonate near

100 and 80 ppm, only the coupling with allylic methylene protons (^3J) is observed (Figure 3.1). So can it be determined which one of these two carbon atoms is an acetylenic sp- carbon and which one is the exocyclic sp^2-hybridized carbon? A literature search revealed that compound **I** (Figure 3.3) possesses some characteristic features similar to my macrocyclic tetrabromides.[49] First of all, this particular molecule contains two symmetrically positioned exocyclic sp^2-hybridized carbon atoms that are directly connected to two bromines atoms and two endocyclic sp^2-hybridized carbon atoms. The endocyclic sp^2-hybridized carbon atoms resonate at 139.2 ppm. On the other hand, the exocyclic sp^2-hybridized carbon atoms resonate around 90.2 ppm. Because this latter value, for compound **I** is almost 9 ppm lower then the one thought to belong to the analogous carbon of the cyclic tetrabromides: **211**, **218**, **222**, **235**, **236**, it is still not safe to assign that the signal presented around 99 ppm for these compounds belongs to the exocyclic sp^2-hybridized carbon atom. Another interesting comparison compound, that has the same functional groups as my macrocyclic tetrabromides and can be used for comparison, is compound **II** (Figure 3.3). Compound **II** represents a precursor in a synthetic pathway of a graduate student from our group, Thanh Luu. As can be seen from Figure 3.3 compound **II** posses one dibromoolefin moiety and also a triple bond. The assignment of NMR resonances is, to a certain extent, easy. For example the hydrogen substituted sp-hybridized carbon atom has a height that cannot be ignored in comparison with the other sp-hybridized carbon atom. Tracing back the resonances for the sp^2-hybridized carbon atoms I found the protected precursor of compound **II** in the form of compound **III** (Figure 3.3). As can be seen from Figure 3.3 the only difference between compound **II** and **III**, regarding the NMR spectroscopy is the major shift of almost 15

ppm when comparing the alkyne moiety in the silyl protected and unprotected form. The sp^2-hybridized carbon atoms show little or no response to the deprotection. In the view of all this data, I think it is safe to say for my compounds: **211**, **218**, **222**, **235**, **236** that a) the resonances present between 96 and 100 ppm are characteristic for exocyclic sp^2-hybridized carbon atoms and b) the two resonances presented upfield are characteristic to the sp-hybridized carbon atoms. Unfortunately, although the resonances assigned to the sp-hybridized carbon atoms should be differentiated by the correlation pattern of the HMBC NMR technique, I am not able to assign, with confidence which carbon atom is which, due to resolution difficulties. For example compound **236** ($n = 8$) has a significant difference between the resonances of sp-hybridized carbon atoms of exactly 4 ppm, and still this is not enough to overcome the resolution problem. To better understand the variation between chemical resonances of the sp and sp^2-hybridized carbon atoms of the cyclic tetrabromides they are summarized in Table 3.1. The upfield shift of the exocyclic alkylidene carbon atom may be explained by "the heavy atom effect".[49] The bromine atoms affect the resonance of the carbon atom bonded directly to the heavy atom (e.g., bromine or iodine), shifting the resonance upfield.

Table 3.1 Summary ^{13}C NMR resonances belonging to the sp- and sp^2-hybridized carbon atoms of the cyclic tetrabromides

	endocyclic sp^2-hybridized carbon atom	exocyclic sp^2-hybridized carbon atom	acetylenic resonance	acetylenic resonance
Compound **211** $n = 12$	130.2 ppm	99.7 ppm	82.1 ppm	80.4 ppm
Compound **218** $n = 11$	130.1 ppm	100.0 ppm	82.9 ppm	81.1 ppm
Compound **222** $n = 10$	130.1 ppm	99.8 ppm	83.3 ppm	81.5 ppm
Compound **235** $n = 9$	130.3 ppm	99.5 ppm	84.1 ppm	82.0 ppm
Compound **236** $n = 8$	130. 3 ppm	98.6 ppm	86.5 ppm	82.5 ppm
Compound **226** (linear)	130.1 ppm	100.1 ppm	82.3 ppm	80.5 ppm

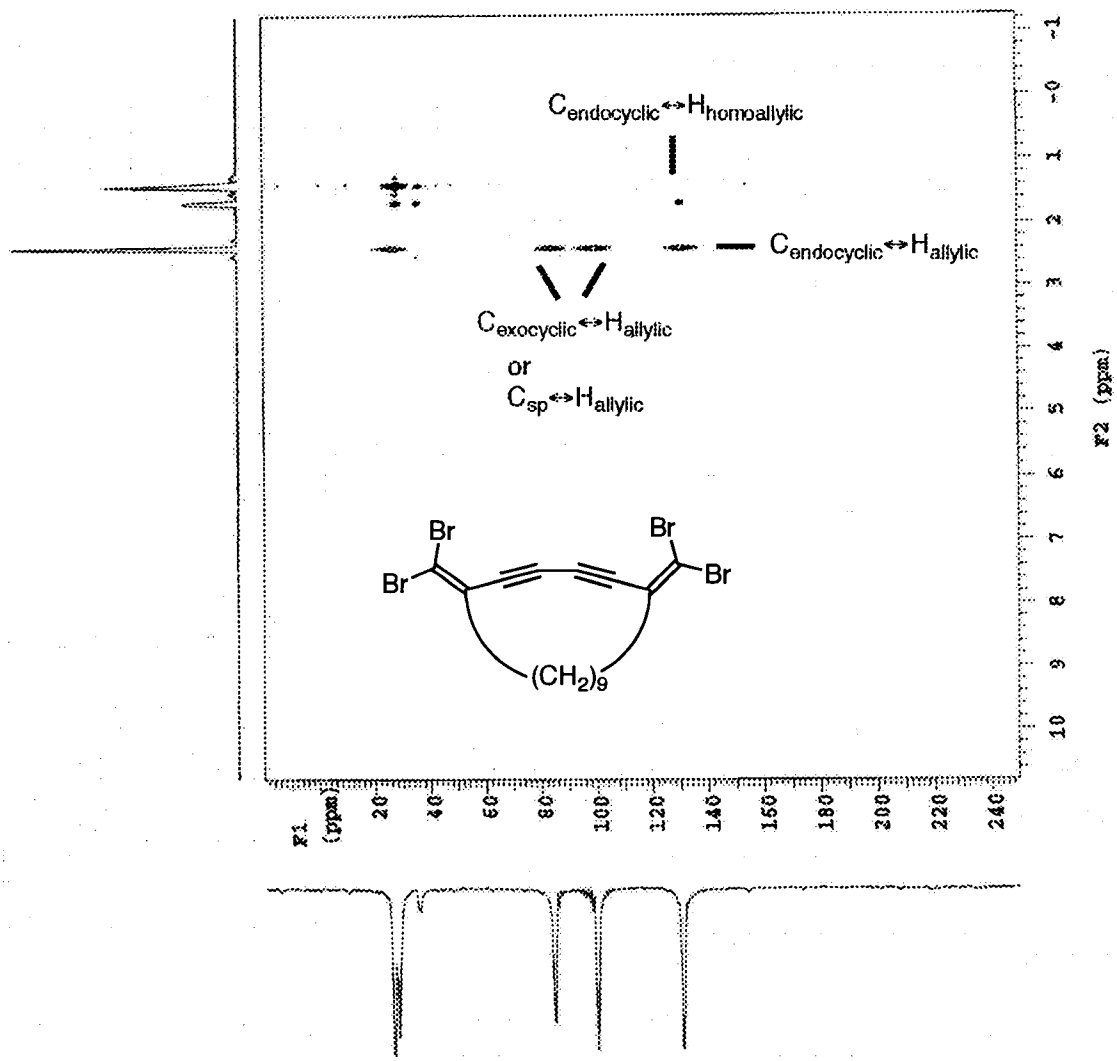

Figure 3.1 HMBC NMR spectrum of compound **235** (500 MHz, $CDCl_3$), showing the correlations for the endocyclic vinylic carbon atom and the allylic and homoallylic protons and the correlation between the exocyclic carbon atom and allylic protons.

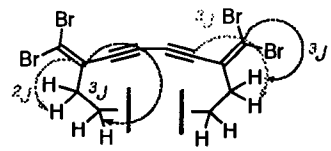

Figure 3.2 Schematic representation of coupling pattern of the sp-hybridized carbon atom, endocyclic and exocyclic sp^2-hybridized carbon atoms.

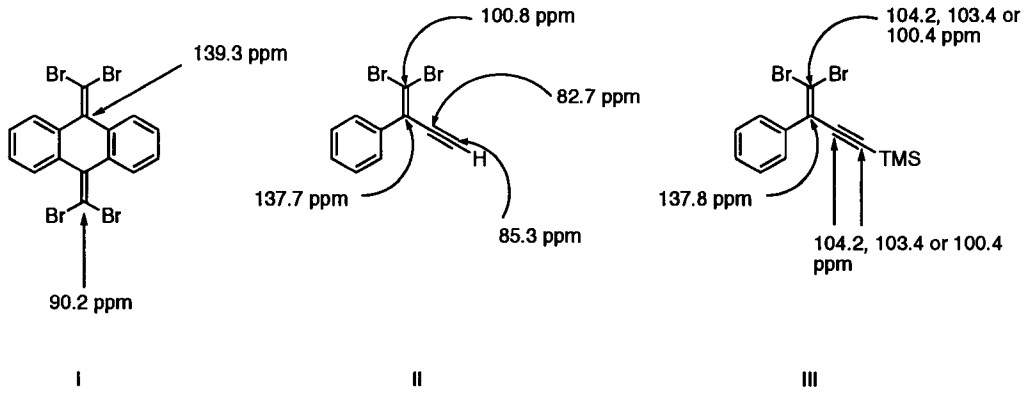

Figure 3.3 Structures and some important chemical resonances for compounds **I**, **II** and **III**

All the correlations observed in the HMBC NMR spectra of the tetrabromo-macrocycles are summarized in Table 3.2. Unfortunately, the correlations between the sp^3-hybridized carbons and the hydrogen atoms were more difficult to determine. All the sp^3-carbon atoms were clustered together and the hydrogen atoms that correlated with the respective carbon atoms appeared as multiplets, therefore the correlations were not determined.

Table 3.2 HMBC correlation table showing the values (ppm) for the hydrogen atoms and carbon atoms.

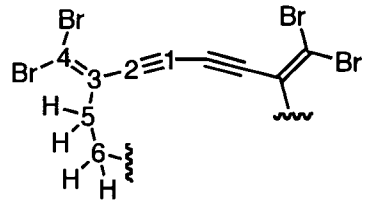

	$5CH_2 \leftrightarrow 3C$	$5CH_2 \leftrightarrow 4C$	$6CH_2 \leftrightarrow 3C$	$5CH_2 \leftrightarrow 1C$	$5CH_2 \leftrightarrow 2C$	$6CH_2 \leftrightarrow 1C$
211	2.35↔130.2	2.35↔99.7	1.60↔130.2	x	2.35↔82.1	x
218	2.41↔130.1	2.41↔100	1.63↔130.1	x	2.41↔82.9	x
222	2.40↔130.1	2.40↔99.8	1.40↔130.1	x	2.40↔83.5	x
235	2.38↔130.2	2.38↔99.5	1.66↔130.2	x	2.38↔84.1	x
236	2.43↔130.3	2.43↔98.6	1.64↔130.3	x	2.43↔86.5	x

Once the correlations regarding the sp- and sp^2-hybridized carbon atoms and allylic and homoallylic protons were determined, it was the time to determine if the ring size influenced the resonance of carbon atoms. As can be seen from Table 3.1, the resonances of the sp and sp^2-carbon have no noticeable trend. The exocyclic sp^2-carbon atoms showed almost identical values of either 130.1 or 130.2 ppm. The endocyclic sp^2-carbon atoms showed a slight difference and the linear compound (**226**) showed this particular signal the most downfield at 100.1 ppm, whereas the most strained compound (**236**) had this resonance at 98.6 ppm. A much more noticeable difference is in regard with the most downfield sp-hybridized carbon atoms (identified as 2C, Table 3.2). The difference between the most strained compound and the linear compound in this case was 4.2 ppm. Fortunately, a linear relationship between the ring size and carbon resonances belonging to the sp-hybridized carbon atoms can be established (Figure 3.4) (the linear compound was neglected).

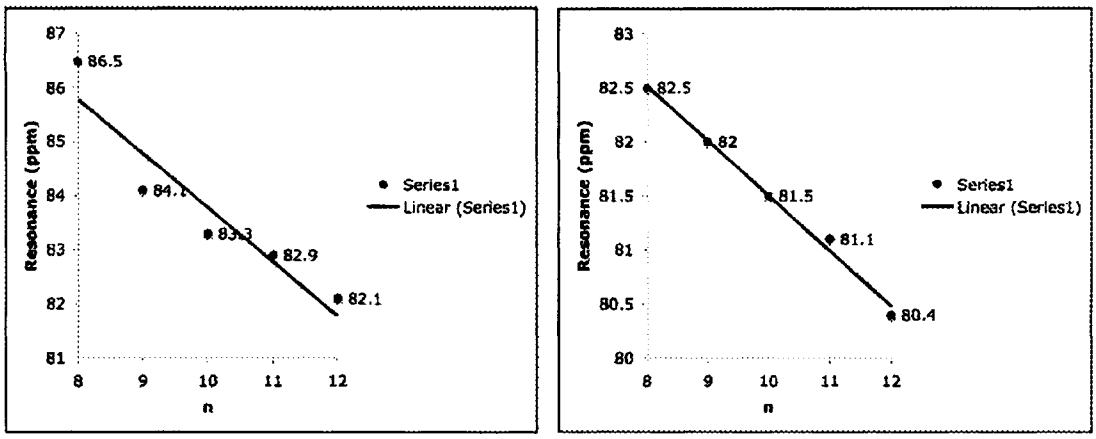

Figure 3.4 Plot of ^{13}C NMR chemical shift for the sp-hybridized carbon atoms versus the ring size (n) (left $R^2 = 0.8828$, right $R^2 = 0.9927$)

In addition to characterization in solution (e.g., ^{13}C NMR and ^{1}H NMR spectroscopy), the cyclic tetrabromides are highly crystalline substances that produced crystals suitable for solid-state characterization (X-ray analysis). Single crystals for compounds **222** (n = 10) and **236** (n = 8) were obtained by slow evaporation from a mixture of DCM and hexanes at room temperature. The ORTEP representations for these two compounds are presented in Figures 3.5. and 3.6. Because the structural reports regarding these two compounds are attached as Appendix III, I will mention only that a) the bond angle value for C(1)-C(2)-C(3) for compound **236** (n = 8) which is 173.2° (Figure 3.5) and b) the bond angle value for C(4)-C(5)-C(6) of compound **222** (n = 10) which is 177.4° (Figure 3.6). These bond angle values are presented because they reflect the best the effect of distortion of the sp-hybridized carbon atoms bonds by the decrease of methylene units. Unfortunately the rest of cyclic tetrabromides, although very crystalline substances, gave crystals unsuitable for X-ray analysis.

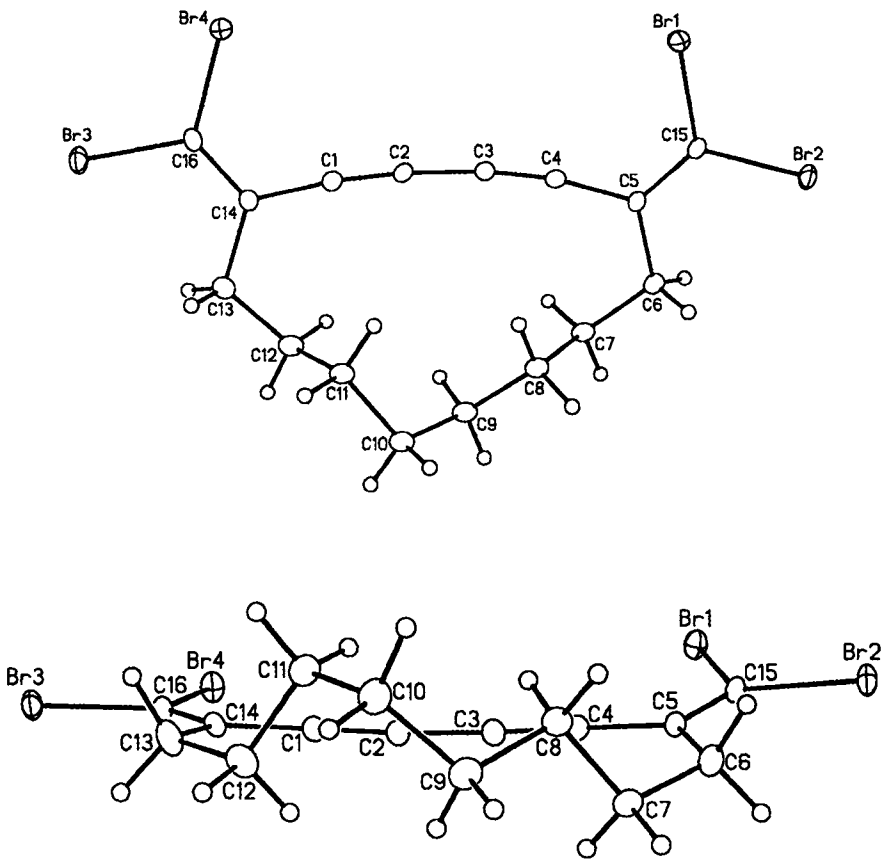

Figure 3.5 Top structure is the perspective view of **236** showing the atom-labelling scheme. Non-hydrogen atoms are represented by Gaussian ellipsoids at the 20% probability level. Hydrogen atoms are shown with arbitrarily small thermal parameters. Second structure is an alternate view of the molecule from the side.

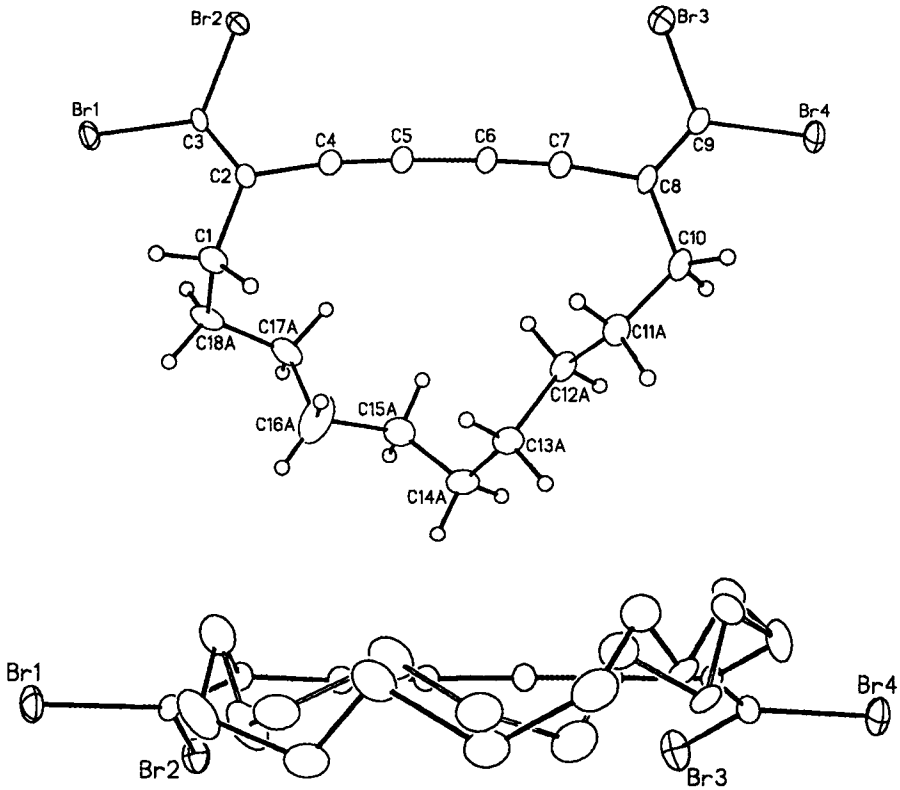

Figure 3.6 Top structure is the perspective view of **222** showing the atom-labeling scheme. Non-hydrogen atoms are represented by Gaussian ellipsoids at the 20% probability level. Hydrogen atoms are shown with arbitrarily small thermal parameters. Second structure is an alternate view of the molecule. Second structure is an alternate view showing the disordered decamethylene group. Major (70%) form is indicated by the solid bonds; minor (30%) form is indicated by the open bonds

3.2. Cyclotetraynes

Although the synthesis of cyclic tetrabromides represented a difficult step in achieving the final cyclotetraynes, the final goal of this project was to find and to define trends among this new series of compounds. As described, three cyclic tetrayne compounds have been obtained, as well as one acyclic analogue. Unfortunately no crystals suitable for X-ray analysis have been grown for these tetraynes, a fact hampered by the fact that the cyclotetraynes prefer to decompose rather than crystallize. This was observed on many occasions in NMR tubes, which were setup as a crystallization chambers. Therefore at this time only solution-state characterization is available.

3.2.1. Trends found with the aid of ^{13}C NMR spectroscopy

In our group, a previous student of Prof. Tykwinski, Dr. Sara Eisler, synthesized a series of molecules called dendralenes **112** (Figure 3.7).[12] This work has shown that endocyclic sp^2-hybridized carbon atoms are deshielded when the ring strain is increased, possibly due to bond rehybridization of the carbon framework. My work can, in part, be compared to this dendralene work.

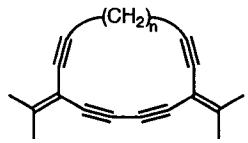

112

n = 2, 3, 4, 5, 7

Figure 3.7 Structure of dendralenes **112**

First of all we sought to identify individual resonances of the carbon atoms in ^{13}C NMR spectra. Once again HMBC NMR proved a powerful tool. HMBC NMR analysis of compound **202** (n = 12) and of the linear compound **205** showed that the most

downfield carbon atom resonance (δ 91.8) belongs to the first sp-hybridized atom from the series of eight carbon atoms (Figure 3.8). As it can be seen from the HMBC spectrum, the most downfield sp-hybridized carbon atom is able "to see" two types of hydrogen atoms (^2J and ^3J) i.e, the propargylic and homopropargylic protons. Therefore this carbon atom is identified as C(1). The next two carbon atoms (δ 68.5 and 67.4) couple with the propargylic protons (^3J and ^4J), therefore these particular carbon atoms are identified as C(2) and C(3). Unfortunately I can not assign which one is C(2) and which one is C(3) by just looking at the intensity of the correlation although one might guess that C(2) is δ 68.5 and C(3) is δ 67.4 . The good news is that C(4) does not appear in the HMBC-NMR spectrum, therefore I can say with a certain conviction that the signal at δ 60.7 is C(4). The ^{13}C NMR spectra of the cyclotetraynes (**202–204**) and model linear compound (**205**) have been shown in the previous chapter, and here we analyze trends observed in these resonances. Below is the graph of the observed ^{13}C NMR resonances plotted for each of the individual compounds. As can be seen, the most strained cyclotetrayne, compound **204** (n = 10), has all the sp-hybridized carbon atoms resonating at higher frequencies in comparison with the other members of the series. The trend continues in compounds **202–205** showing that the more strained the cyclotetrayne, the higher the respective frequency of the sp-hybridized carbon atoms. It is interesting to see that the strain in the alkyl tether is not seen in the of ^{13}C NMR spectrum because the chemical shift for the propargylic carbon atoms is almost identical (30-31 ppm) for all the cyclotetraynes synthesized (**202–204**).

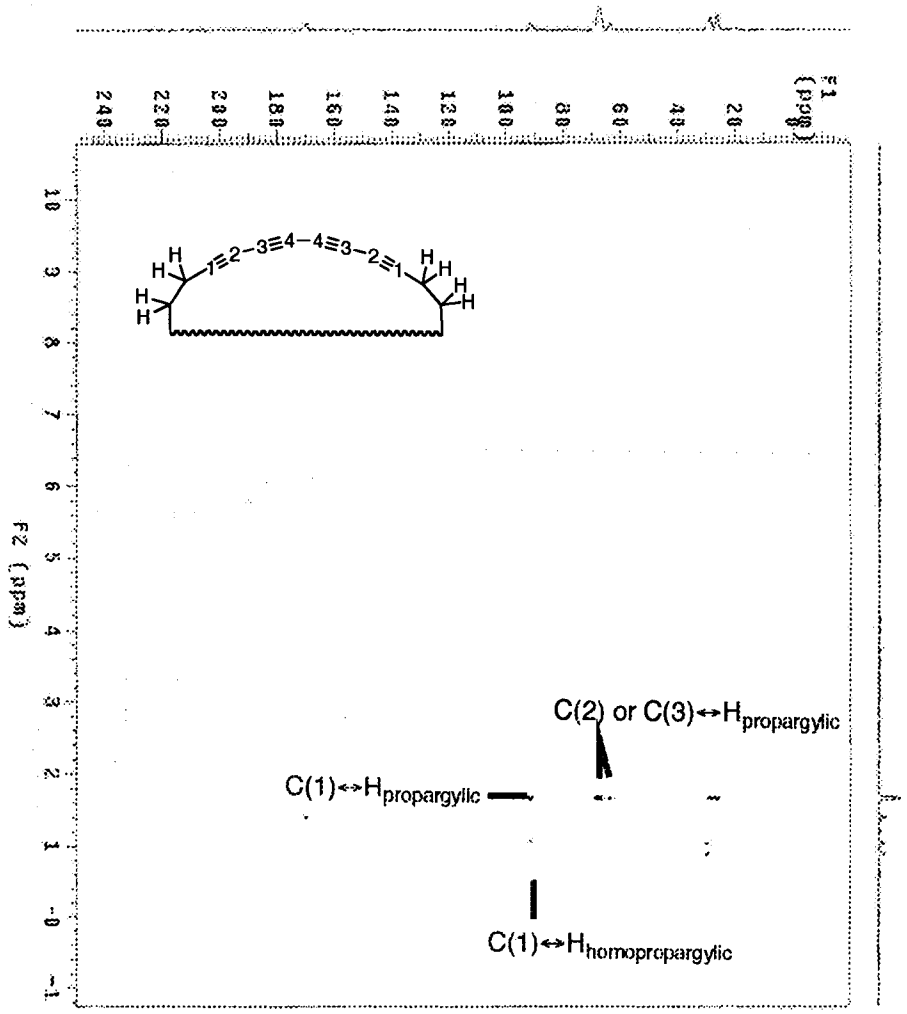

Figure 3.8 HMBC spectrum of compound **202**

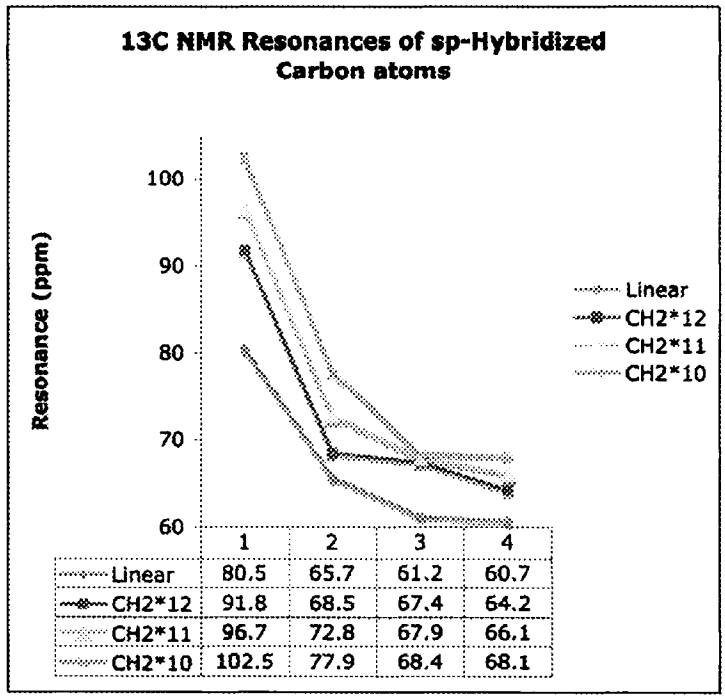

	1	2	3	4
Linear	80.5	65.7	61.2	60.7
CH2*12	91.8	68.5	67.4	64.2
CH2*11	96.7	72.8	67.9	66.1
CH2*10	102.5	77.9	68.4	68.1

Figure 3.9 Graphic representation ^{13}C resonances of each individual compound

As can be seen from the graph, the most drastic change is observed in the shift of the C(1) carbon resonance where there is a difference of more than 20 ppm between the most strained compound **204** (n = 10) and linear compound **205**. The same trend is noticed for all the other sp-hybridized carbon atoms.

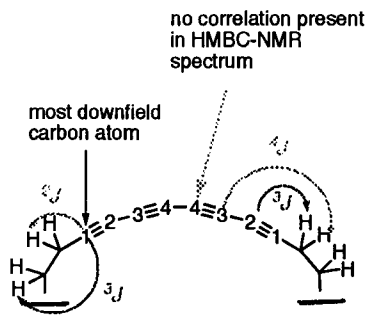

Figure 3.10 Schematic representation of coupling pattern of carbon atoms as seen in HMBC NMR analysis

Figure 3.11 represents the relationship between the calculated bond angle α for the most downfield carbon atom and the ^{13}C NMR resonances observed for compounds **202–205**. As can be seen from the linear relationship (Figure 3.11), the acetylenic carbon experience a serious deshielding as ring strain is increased. Due to space reasons, graphs depicting the linear relation-ship between all the other sp-hybridized carbon atoms versus the ring size are not shown, furthermore I chose to show only the most dramatic change regarding the chemical shift versus the ring size.

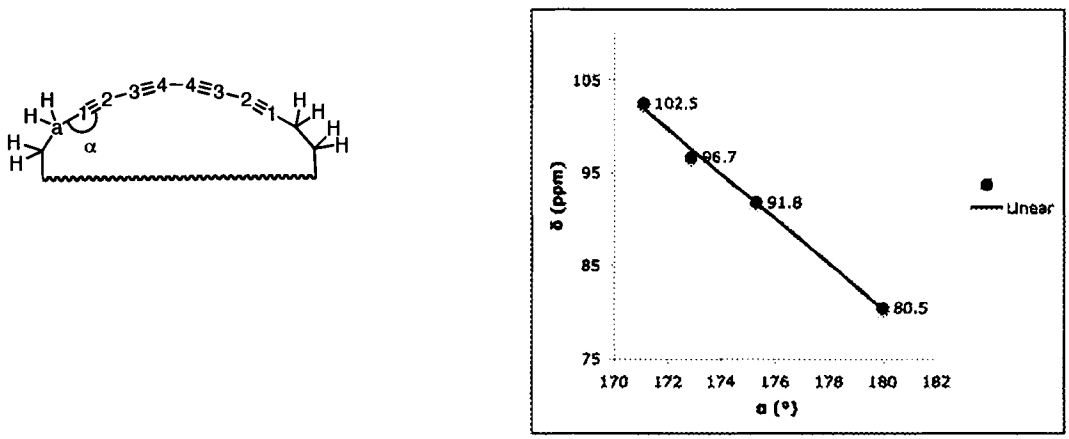

Figure 3.11 Plot of ^{13}C NMR chemical shift for C(1) versus calculated bond angle (R^2 = 0.9958)

Once the trend in chemical shift of the α-acetylene carbon had been identified, one considers the reason for the change in chemical shift for the terminal sp-hybridized carbons in sterically strained cyclotetraynes. Possibly, the induced magnetic field from the tetrayne functionality is differently affecting the terminal sp-hybridized carbon atom depending on the deviation from the tetrayne axis. Another reason might be hypeconjugation with the CH bond from the adjacent methylene group, which increases

the electronic density of the tetrayne functionality (Scheme 3.1). Gleiter found similar results when he analyzed, with the aid of photoelectron spectroscopy, σ–π electron interactions for 1,5-cyclooctadiyne and 1,6-cyclodecadiyne.[51] 1,5-Cyclooctadiyne (eight membered ring) was compared with 1,6-cyclodecadiyne (ten membred ring) and it was found that there was a difference in ^{13}C NMR resonace for acetylenic carbons of almost 13 ppm between the more strained and less strained compounds. As described by Gleiter, presumably hyperconjugation plays a role because the out of plane π-orbitals have the correct geometry to interact with the adjacent σ-orbitals (CH). Furthermore in the same work it was shown that C–C σ-orbitals (from the alkyl chain) have the correct geometry to interact with the in plane π-orbitals. At this moment, although a trend in the chemical shifts of the sp-hybridized carbon atoms has been determined, it is not possible to state conclusively the factors that dictate this behavior.

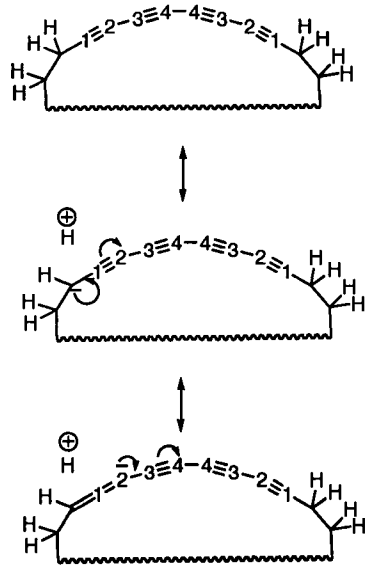

Scheme 3.1 Schematic representation of how hyperconjugation can explain the shift to downfield values in ^{13}C NMR spectroscopy of tetraynes **202–205**

3.2.2. Trends found with the aid of UV–vis spectroscopy

In addition to NMR spectroscopy, UV–vis spectroscopy is routinely used in the characterization of conjugated organic compounds, therefore the results from these experiments will be discussed. Before an analysis of trends within the cyclic tetraynes, the UV–vis spectroscopy had to be compared to a linear analogues. Fortunately, there are examples of linear tetraynes in the literature, in particular the work by Balova.[52] The UV–vis spectra of the series of compounds in Figure 3.12 has been reported. The λ_{max} (nm) values do not to differ with chain length and are essentially equivalent for all of the compounds examined showing as a series of absorption at: 217, 228 and 239 nm (hexanes). These results match the values found for the linear compound **205** in my study.

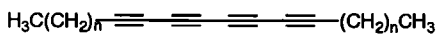

205 n = 5
301a n = 7
301b n = 9
301c n = 11

Figure 3.12 Linear tetraynes (**205**, **301a–c**) reported by Balova[52]

With the confirmation that absorption values for the linear compound **205** were similar to that of other analogues, the differences for the cyclotetraynes synthesized in my study could be analyzed. In Figure 3.13 the absorption spectra for compounds **202–205** are plotted.

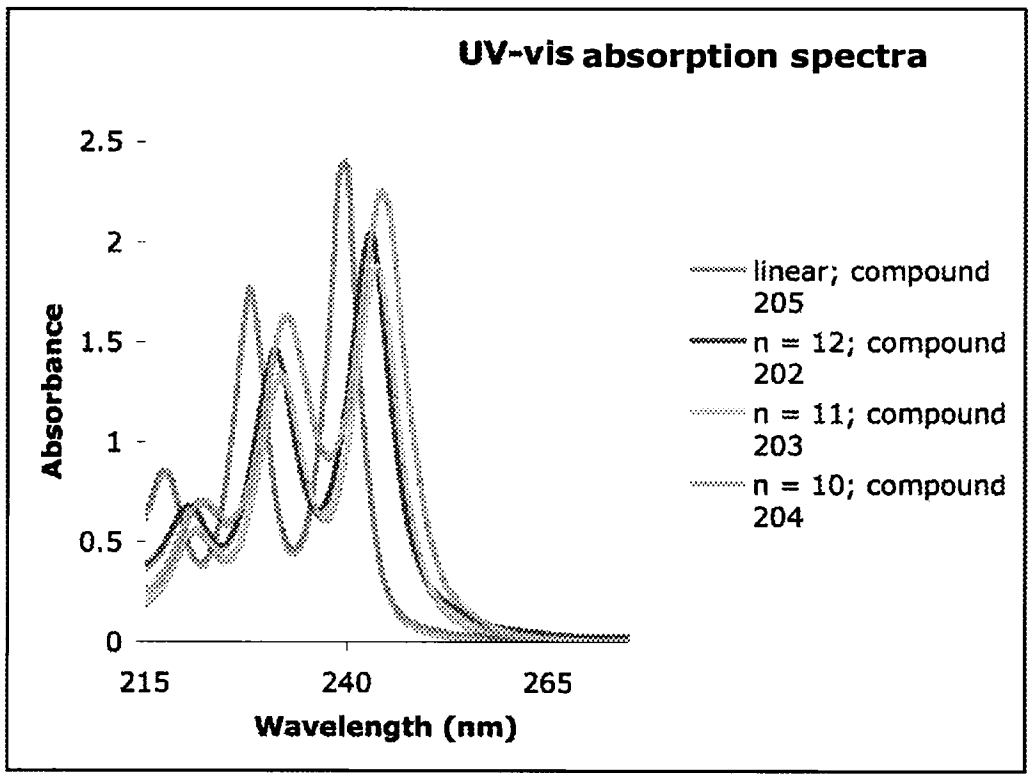

Figure 3.13 Absorption spectra for compounds **202–205** in hexanes solution

At first glance there is not a significant difference between the spectra. The only difference is a slight bathchromic shift of 5 nm for the cyclic compound **204** ($(CH_2)_{10}$) in comparison to the linear compound **205**. The values of λ_{max} are summarized in Table 3.2, showing the differences between the linear compound **205** and the cyclotetraynes **202–204**.

Table 3.3 Selected UV absorption data for compounds: **202–205** (absorption maxima, λ_{max})

Compound	Absorption maxima, λ_{max} (nm) in DCM
205	217, 228, 240
202	220, 231, 243
203	221, 232, 244
204	222, 233, 244

Due to the fact that the cyclotetraynes were not stable neat, concentrations could not be obtained in order to calculate ε values. Therefore many trials of measuring the UV–vis absorbance were done. During the numerous data collection for the UV–vis spectra, I noticed that, for more concentrated solutions of cyclotetrayne, an additional set of absorption bands with much lower intensity was observed at lower energy (Figure 3.14). At the time, I did not know if this new band was a result of my compounds or was a sign of decomposition.

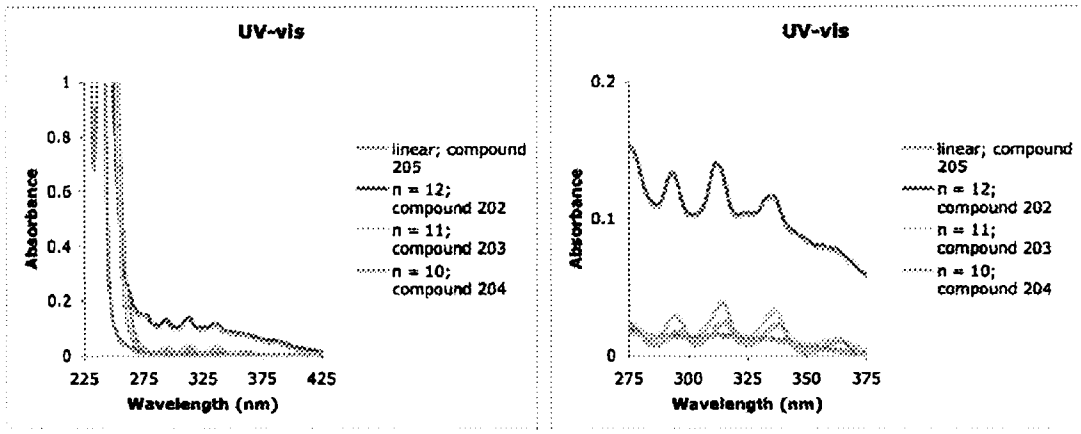

Figure 3.14 (Left) UV-vis spectra of concentrated solutions of compounds **202–205** in hexanes and magnification of the first graph, 275-375 nm (right)

A careful literature search showed that this set of absorption had been prevoiusly observed for linear tetraynes.[53] In the work published by Armitage et al. "Research on Acetylenic Compounds. Part XXXVII. The Synthesis of Conjugated Tetra-acetylenic Compounds" in 1952, the same trend was observed for compounds **302a–c** (Figure 3.15). The authors reported a high intensity band in the region between 235–240 nm and a medium intensity band at longer wavelengths between 280–360 nm. Interesting enough, the triynes **303a**, **b** (Figure 3.15),[54] showed the same trend, having two absorption sets: one of high intensity at shorter wavelengths and one of medium intensity at longer wavelengths. Given that the triacetylenes **303a**, **b** and the tetraacetylenes **302a–c** showed similar absorption spectra, it was striking to find that the diacetylenes **304a**, **b** (Figure 3.15)[55] showed characteristic sharp bands at 227.5, 238.5 and 253 nm, but the set at lower energy was not observed.[53-55]

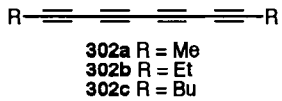

302a R = Me
302b R = Et
302c R = Bu

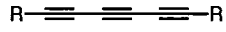

303a R = Me
303b R = Et

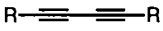

304a R = Et
304b R = Bu

Figure 3.15 Structures of compounds **302–304**

While the linear compound **205** did not show a clear low intensity set of absorption band, between 275–350 nm, cyclic compounds **202**, **203** and **204** did show these absorptions. These low intensity bands showed well-defined lines, but strikingly there was only a small difference between the wavelengths of individual compounds, even though the ring strain had increased quite significantly. All λ_{max} values have been shown in the Table 3.3, and as can be seen, the more strained the compound, the more resolved signals are and more absorption maxima can therefore be reported.

Table 3.4 Selected UV absorption data (in nm) for the lower intensity band absorption for compounds **202–205**

Compound	Absorption maxima (λ_{max}) (nm)
205	293, 313, 334
202	293, 312, 335
203	295, 314, 337, 363
204	296, 316, 338, 364, 392

Still it was interesting to note that by plotting the highest energy absorption of significant intensity against the calculated bond angle, a linear relationship was found

(Figure 3.16, left). Also by plotting the third value of absorptions (Table 3.3) from the set of low intensity absorption (low energy) against the same calculated bond angle, a linear relation ship was also found (Figure 3.16, right). While there would seem to be a trend relating strain to the observed UV–vis absorptions, it is tenuous plotting all the other absorptions bands versus the calculated bond angle, because they gave less significant fits. This may be a result, however, of the resolution of the apparatus.

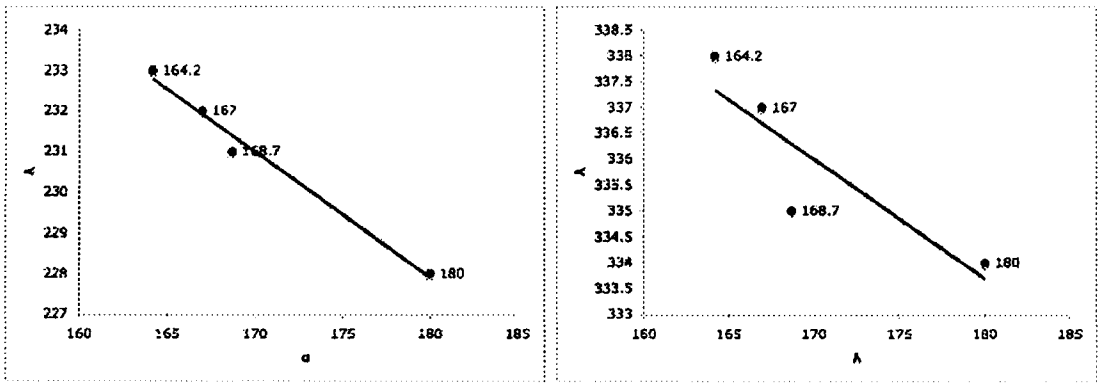

Figure 3.16 Plot of UV-vis absorption λ (nm) versus the calculated averaged bond angle for the high intensity band (R^2 = 0.9932) (left) and for the medium intensity band (R^2 = 0.8751) (right)

One of the differences between the cyclic tetraynes **202–204** and the linear compounds **302–304**, regarding the "unexpected" low intensity absorption band, is that the compounds synthesized in the present study show more defined peaks once the ring strain is increased. The linear compounds show multiple peaks in this region, but these signals are less resolved.

Once the UV–vis spectra of compounds **202–205** had been compared to the reported linear analogs, a trend was defined for λ_{max} as a slight bathochromic shift of 5 nm between the most strained compound (**204**) and the linear model compound (**205**).

The cyclic compounds **202–204** have a low intensity band, consisting of more defined absorption maxima, when compared to the linear compounds and once again there is a slight bathochromic shift of 3 nm between the most strained compound **204** and the linear compound **205**.

The logical next step is to compare my compounds with other cyclic acetylenic analogues. Compounds **108a** and **108b**[12] (Figure 3.17) discussed briefly in the introduction chapter are perfect candidates for this task of comparing UV-vis spectra resulting from strained polyynes. The UV–vis spectrum of compound **108b**, practically strain free, exhibits characteristic fine structure, whereas the more strained compound **108a** shows a broad absorption maximum. For both spectra, the absorption bands are observed in the range of 210-270 nm. The broad absorption maximum presented by compound **108a** was attributed to ring strain. This result is contrary to my results, where the greater the ring strain, the more defined the absorption maxima. The authors did not give much attention to the absorption band at higher wavelength (285 nm) for compound **108b** due to its low intensity. The fact that the absorption maxima for compounds **108a** and **108b** do not vary significantly is not surprising, in view of the results I found for the analysis of λ_{max} for **202** and **203**.

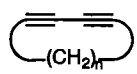

108a n = 9
108b n = 10

Figure 3.17 Structures of compounds **108a** and **108b**

In the same work[12] the synthesis and UV–vis spectroscopic characterization of the series of compounds presented in Figure 3.18 was reported, where compound **107b** was

regarded as the most strained. As expected there was a bathchromic shift in λ_{max} as ring strain increased. It was observed that, as the ring strain increased, the vibrational structure disappeared, again opposite to that observed for my compounds. For compounds **107** this observation was explained by the distortion of the two chromophores, and transannular interactions (between acetylenes and phenyl groups) were also believed to play a major role. Knowing that the cyclotetraynes presented in this work posses neither two types of chromophores nor transannular interactions, it is plausible that the fine vibrational lines are more defined as the ring strained is increased, even though opposite trend is mentioned in the literature for [*m*,*n*]paracyclophanes[56] and for [*m*,*n*]paracyclophadiynes.[12]

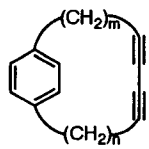

107a m = 2, n = 4
107b m = n = 3
107c m = 3, n = 4
107d m = n = 4
107e m = n = 5

Figure 3.18 Structure of compounds **107a–e**

On the other hand, the work of Tykwinski and coworkers[43] on dendralenes, shows a similar trend to that observed in my study. In this work, the linear compound (**305**) is compared to the dendralenes (**112**, Figure 3.19). The linear compound **305** has broadened signals and lower values for ε, attributed to the rotational freedom of the alkylidine units about the butadiyene moiety. A comparison of compounds **112a–e** shows peak broadening for relatively unstrained molecules **112d,e** in comparison with the more rigid and strained molecules **112a,b**. A bathochromic shift is also observed for the more rigid

molecules **112a,b** and is attributed to the ring strain rather than to the homoconjugation. Regarding UV–vis analysis, the work with dendralenes **112** is the closest to my study. Although compounds **112** are to some extent very different in comparison with compounds **202–204** a similar trend is found in the UV–vis absorption characteristics and that the more strained the cycle, the more defined the absorption signals.

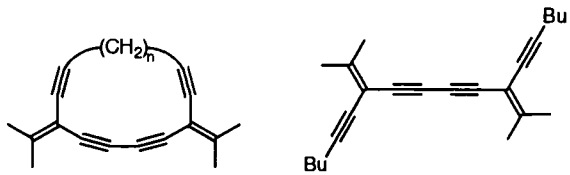

112a n = 2
112b n = 3
112c n = 4
112d n = 5
112e n = 7

305

Figure 3.19 Structures of compounds **112** and **305**

In conclusion, the UV–vis spectra of conjugated tetraynes reported in this thesis show a slight batochromic shift of 5 nm between the linear compound **205** and the most strained compound **204**, a fact attributed to the ring strain in the molecules, the same trend is valid also for the low intensity band of absorptions where more defined peaks are found with the increasing of the ring strain.

3.3. Conclusion

Chapter 3 contains discussions regarding two different classes of compounds: cyclic enediynes and cyclotetraynes. With the aid of characterization in the solution-state, some trends have been defined regarding ring strain. While the failure to obtain X–ray analysis for the conjugated cyclotetraynes was a drawback of this project, NMR spectroscopic study, UV–vis analysis and MacSpartan calculations in the case of cycloteraynes revealed important insight in this unprecedented class of compounds.

4. Experimental section

4.1. General experimental details

Column chromatography: silica gel-60 (230-400 mesh) from *Silicycle*. Thin layer chromatography (TLC): plastic sheet coated with *silica gel–60 (*mesh 40–63*)* from *Macherey-Nagel*: visualization by UV light (254 nm). Melting point: Gallenkamp or *Fischer–Johnes* apparatus: uncorrected. UV–vis spectra: *Varian Cary 400* at ambient temperature; λ in nm. IR spectra (cm^{-1}): *Nicolet Magna-IR* (neat–microscope, or DCM cast). ^{1}H and ^{13}C NMR: *Varian Gemini–400, or–500* MHz instruments, at 27 °C in $CDCl_3$; solvent peaks (7.24 ppm for ^{1}H and 77.0 ppm, for ^{13}C) as reference. EI MS (70 eV): *Kratos MS 50* instrument. The Microanalytical Service, Department of Chemistry-University of Alberta, performed elemental analyses. ^{13}C NMR spectra are broadband decoupled. Coupling constants *J* are reported as observed. For IR data, useful functional groups and 3–4 of the strongest absorptions are reported, including but not limited to C-H, C=C and C≡C, C=O bond stretches. All solvents ratios reported are volume, unless otherwise noted.

4.2. General experimental methods

Reagents were purchased reagent grade from commercial suppliers. DCM and hexanes were distilled from CaH_2 before use. A drying tube (containing anhydrous calcium sulfate) and flame-dried glassware were used for the formation of acyl chlorides. A positive pressure of N_2 was used for Friedel-Crafs acylations. Vigorously flame dried glassware and a positive N_2 pressures were used for FBW rearrangements. Anhydrous

$MgSO_4$ was used after aqueous workup as drying agent. Evaporation and concentration *in vacuo* was done with an H_2O-aspirator pressure.

General Procedure A – Friedel-Crafts Acylation.[38,48] Unless otherwise noted in the individual procedures, thionyl chloride (72 mmol) was added to the dicarboxylic acid (18.0 mmol), dissolved previously in freshly distilled DCM, in a dry flask protected from moisture with a drying tube containing Dryerite, and the mixture allowed to stir for 12 h at rt. The excess thionyl chloride was then removed *in vacuo* to provide the acyl chloride. Freshly distilled DCM (100 mL) was added and the temperature of the solution lowered to 0 °C (ice and water mixture). Bis(trimethylsilyl)acetylene (37.0 mmol) and $AlCl_3$ (37.0 mmol) were added and the reaction mixture warmed to rt over 3 h. The reaction was carefully quenched by the addition of the reaction to 10% HCl (50 mL) in ice (50 mL). Hexanes (50 mL) were added, the organic layer separated, washed with satd. aq. $NaHCO_3$ (3 × 20 mL), NaCl (2 × 20 mL), dried ($MgSO_4$), filtered and the solvent removed *in vacuo*. Column chromatography (silica gel) provided the pure diketone.

General Procedure B – Friedel-Crafts Acylation.[38] Unless otherwise noted in the individual procedures, PCl_3 (18.0 mmol) was added to a solution made of the dicarboxylic acid (18.0 mmol) dissolved in freshly distilled DCM (50 mL), under inert atmosphere of N_2 and the mixture was allowed to stir for 12 h. The temperature of the solution was lowered to 0 °C (ice and water mixture). Bis(trimethylsilyl)acetylene (37.0 mmol) and $AlCl_3$ (37.0 mmol) were added and the reaction mixture warmed to rt over 3 h. The reaction was carefully quenched by the addition to the reaction of an ice and

water mixture (50 mL). Hexanes (50 mL) were added, the organic layer separated, washed with satd. aq. $NaHCO_3$ (3 × 20 mL), NaCl (2 × 20 mL), dried ($MgSO_4$), filtered, and the solvent removed *in vacuo*. Column chromatography (silica gel) provided the pure diketone.

General Procedure C – Dibromoolefination.[40,48] Unless otherwise noted in the individual procedures, CBr_4 (26.1 mmol) and PPh_3 (52.2 mmol) were added to freshly distilled CH_2Cl_2 (100 mL) and allowed to stir for 5 min at rt under an inert atmosphere of N_2 until the mixture turned bright orange. The diketone (8.6 mmol) in CH_2Cl_2 (10 mL) was slowly added to the CBr_4/PPh_3 mixture over a period of 5 min. The reaction mixture turned a dark brown color upon addition of the diketone. TLC analysis was used to monitor the reaction, indicating that dibromoolefination was typically complete almost immediately. The solvent was reduced to *ca.* 20 mL, hexanes added (100 mL), the inhomogeneous mixture filtered through silica gel and the solvent removed *in vacuo*. Column chromatography (silica gel) provided the pure tetrabromides.

General Procedure D – Oxidative (Hay) Coupling.[41,48] A mixture of the trimethylsilyl-protected acetylene (3.5 mmol) and K_2CO_3 (0.70 mmol) in wet THF/MeOH (30 mL, 1:1 *v/v*) was stirred for 1 h until monitoring by TLC revealed that the deprotection reaction was complete. Hexanes (50 mL) and satd. aq. NH_4Cl (30 mL) were added, the organic phase separated, washed with satd. aq. NH_4Cl (2 × 20 mL), dried ($MgSO_4$) and the solvent reduced to *ca.* 50 mL. The terminal acetylene was added to a solution of the Hay catalyst [CuI (17.5 mmol, ca. 6 equiv, and TMEDA (53 mmol)) in CH_2Cl_2 (2000 mL],

previously stirred until homogeneous). This mixture was stirred at 0 °C (ice and water mixture) until TLC analysis no longer showed the starting material (*ca.* 1.5 h). Satd. aq. NH_4Cl (200 mL) was added, the organic phase separated. The solvent was reduced to 200 mL then washed with satd. aq. NH_4Cl (2 x 20 mL), dried ($MgSO_4$), filtered and the solvent removed *in vacuo*. Column chromatography (silica gel) gave the desired product.

General Procedure E – FBW rearrangement of Dibromoolefins to Alkynes.[48,44-46] Unless otherwise noted in the individual procedures, a solution of the tetrabromide (0.41 mmol) in hexanes (125 mL) under an inert atmosphere of N_2 was cooled to –35 °C (dry ice and acetone). BuLi (2.1 equiv) was slowly added over a period of ca. 5 min. The reaction mixture turned an orange color. TLC analysis was used to monitor the reaction until starting material was no longer present. The reaction was warmed to approximately –5 °C over a period of 20 min and then was quenched with satd. aq. NH_4Cl (10 mL) or wet THF, and the reaction mixture was then let to stir under ambient conditions for 5 min. The solvent was removed in vacuo. The crude reaction was passed through a plug of silica to remove baseline material. Column chromatography (silica gel) gave the desired product.

4.3. Experimental details

Cycloicosa-1,3,5,7-tetrayne

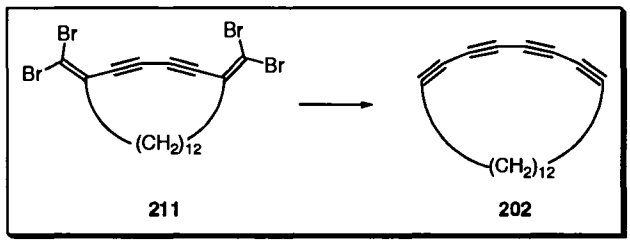

Tetrabromide **211** (0.18 g, 0.31 mmol) in hexanes (50 mL) was subjected to rearrangement according to general procedure E using BuLi (2.5 M in hexanes, 0.26 mL, 0.65 mmol) to afford **202** as an unstable red compound. Decomposition could be minimized if the compound was kept in solution (hexanes); R_f = 0.48 (hexanes); UV–vis (hexanes) λ_{max} 220, 231, 243, 293, 312, 335; IR (CH_2Cl_2 cast) 3114, 2187, 1433 cm^{-1}; ^1H NMR (500 MHz, $CDCl_3$) δ 2.31 (pseudo t, virtual J = 6 Hz, 2H), 1.67 (pseudo t, virtual J = 5.5 Hz, 2H), 1.54-1.49 (m, 4H), 1.23 (m, 4H); ^{13}C NMR (125 MHz, $CDCl_3$) δ 91.8, 77.3, 68.5, 67.4, 31.4, 31.0, 30.1, 28.9, 26.8, 20.3; EIMS analysis was unsuccessful; Chemical formula: $C_{20}H_{24}$;

Cyclononadeca-1,3,5,7-tetrayne

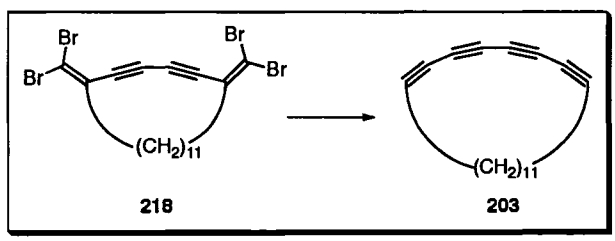

Tetrabromide **218** (0.15 g, 0.26 mmol) in hexanes (50 mL) was subjected to rearrangement according to general procedure E using BuLi (2.5 M in hexanes, 0.22 mL,

0.55 mmol) to afford **203** as an unstable red compound. Decomposition could be minimized if the compound was kept in solution (hexanes); R_f = 0.47 (hexanes); UV–vis (hexanes) λ_{max} 221, 232, 244, 295, 314, 337, 363; IR (CH_2Cl_2 cast) 2926, 2853, 2222, 2181, 1465, 720 cm^{-1}; ^1H NMR (500 MHz, $CDCl_3$) δ 2.35 (*pseudo*-t, virtual J = 6 Hz, 2H), 1.68–1.65 (m, 4H), 1.54–1.51 (m, 4H), 1.35–1.27 (m, 10H), 0.90–0.86 (m, 2H); ^{13}C NMR (125 MHz, $CDCl_3$) δ 96.6, 72.7, 67.9, 66.0, 31.3, 31.2, 31.1, 28.7, 27.5, 20.5. EIMS analysis was unsuccessful; Chemical formula: $C_{19}H_{22}$.

Cyclooctadeca-1,3,5,7-tetrayne

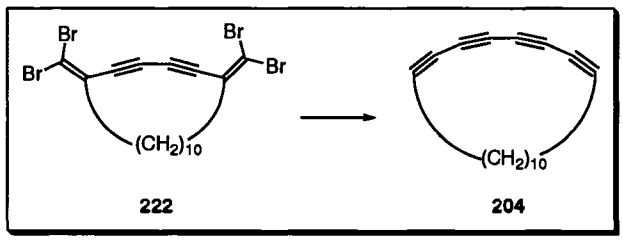

222 204

Tetrabromide **222** (0.15 g, 0.27 mmol) in hexanes (50 mL) was subjected to rearrangement according to general procedure E using BuLi (2.5 M in hexanes, 0.23 mL, 0.57 mmol) to afford **204** as an unstable red compound. Decomposition could be minimized if the compound was kept in a solution of hexanes; R_f = 0.48 (hexanes); UV–vis (hexanes) λ_{max} 222, 233, 244, 296, 316, 338, 364, 392; IR (CH_2Cl_2 cast) 2926, 2854, 2224, 1461, 1158, 727 cm^{-1}; ^1H NMR (500 MHz, $CDCl_3$) δ 2.36 (*pseudo*-t, virtual J = 6.5 Hz, 4H), 1.67 (*pseudo*-p, virtual J = 7.0 Hz, 4H), 1.54–1.49 (m, 6H), 1.41–1.35 (m, 6H); ^{13}C NMR (125 MHz, $CDCl_3$) δ 102.5, 77.9, 68.4, 68.0, 31.1, 31.1, 28.4, 28.3, 20.9. EIMS analysis was unsuccessful; Chemical formula: $C_{18}H_{20}$.

Icosa-7,9,11,13-tetrayne[57]

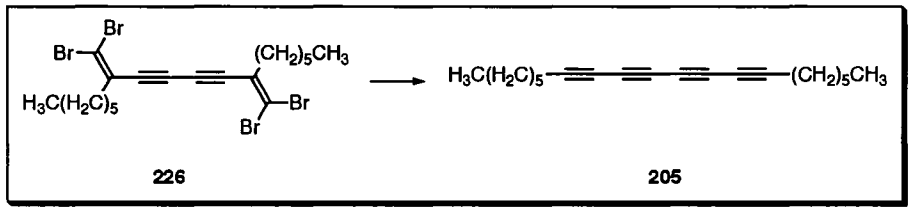

Tetrabromide **226** (0.090 g, 0.15 mmol) in hexanes (20 mL) was subjected to rearrangement according to general procedure E using BuLi (2.5 M in hexanes, 0.13 mL, 0.20 mmol) to afford **205** (0.031g, 79%) as a stable yellow oil; R_f = 0.52 (hexanes); UV–vis (hexanes) λ_{max} 217, 228, 240, 293, 313, 334; IR (CH_2Cl_2 cast) 2956, 2930, 2858, 2226, 1466, 724 cm^{-1}; ^1H NMR (500 MHz, $CDCl_3$) δ 2.31 (*pseudo*-t, virtual J = 7 Hz, 2H), 1.54 (*pseudo*-p, virtual J = 7 Hz, 2H), 1.39 (*pseudo*-p, J = 7.5, 2H), 1.37–1.29 (m, 4H), 0.89 (*pseudo*-t, J = 7 Hz, 3H); ^{13}C NMR (125 MHz, $CDCl_3$) δ 80.5, 65.7, 61.5, 60.7, 31.2, 28.5, 27.9, 22.4, 19.5, 13.9; EI HRMS *m/z* calcd. for $C_{20}H_{26}$ (M^+) 266.2034, found 266.2033. Spectral data consistent with that reported.[57]

1,18-bis(*tert*-butyldimethylsilyl)octadeca-1,17-diyne-3,16-dione

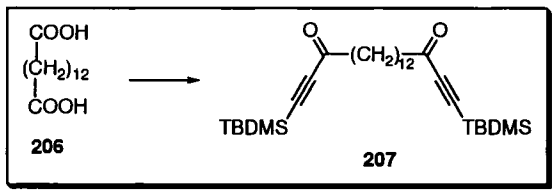

Tetradecanedioic acid **206** (2.00 g, 7.74 mmol) was subjected to Friedel-Crafts acylation according to general procedure A using $SOCl_2$ (2.78 mL, 4.56 g, 38.7 mmol), *tert*-butyldimethyl(trimethylsilyl)acetylene (3.29 g, 15.5 mmol) and $AlCl_3$ (2.07 g, 15.5 mmol) in CH_2Cl_2 (50 mL). Purification by column chromatography (silica gel,

hexanes/ethyl acetate 9:1) afforded **207** (2.92 g, 75%) as a light yellow oil: R_f = 0.63 (hexanes/ethyl acetate 9:1); IR (film cast) 2928, 2856, 2148, 1621, 1470, 1251, 722 cm^{-1}; ^1H NMR (400 MHz, $CDCl_3$) δ 2.53 (*pseudo*-t, virtual J = 7.2 Hz, 2H), 1.68–1.65 (m, 2H), 1.26–1.23 (m, 9H), 0.18 (s, 6H), 0.16 (s, 6H); ^{13}C NMR (125 MHz, $CDCl_3$,) δ 187.9, 102.8, 97.4, 45.2, 29.4, 29.3, 29.2, 28.8, 23.8, –5.2; EI HRMS *m/z* calcd. for $C_{29}H_{51}O_2Si_2$ ($[M–CH_3]^+$) 487.3428 found 487.3427.

(3,16-bis(dibromomethylene)octadeca-1,17-diyne-1,18-diyl)bis(*tert*-butyldimethylsilane)

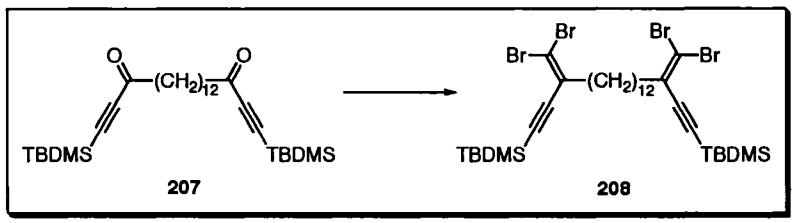

Diketone **207** (2.00 g, 3.98 mmol) in CH_2Cl_2 (25 mL) was subjected to dibromoolefination according to general procedure C using CBr_4 (3.97 g, 12.0 mmol) and PPh_3 (6.28 g, 24.0 mmol) in CH_2Cl_2 (100 mL). Purification by column chromatography (silica gel, hexanes) afforded **208** (2.66 g, 82%) as a light yellow oil: R_f = 0.52 (hexanes); IR (microscope cast) 2959, 2926, 2153, 1463, 1250, 884, 760 cm^{-1}; ^1H NMR (400 MHz, $CDCl_3$) δ 2.32 (*pseudo*-t, virtual J = 7.2 Hz, 4H), 1.58 (pseudo-p, virtual J = 6.8 Hz, 4H), 1.30–1.28 (m, 16H), 0.99 (s, 18H), 0.16 (s, 12H); ^{13}C NMR (125 MHz, $CDCl_3$) δ 131.2, 103.2, 101.7, 97.4, 36.8, 29.6, 29.5, 29.4, 28.9, 27.5, 26.1, 16.6, –4.8. EIMS analysis was unsuccessful; Chemical formula: $C_{32}H_{52}Br_4Si_2$.

1,18-Bis(trimethylsilyl)octadeca-1,17-diyne-3,16-dione (209)

1-(Trimethylsilyl)octadeca-1,17-diyne-3,16-dione (209a)

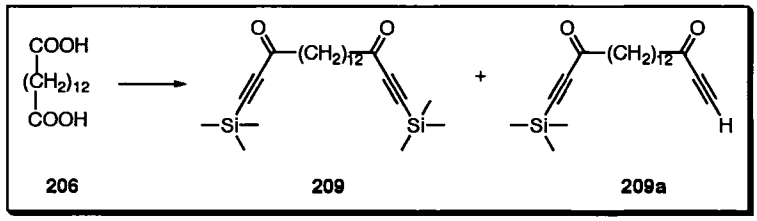

Tetradecanedioic acid **206** (1.00 g, 3.87 mmol) was subjected to Friedel-Crafts acylation according to general procedure A using $SOCl_2$ (1.9 mL, 2.31 g, 19.4 mmol), bis(trimethylsilyl)acetylene (1.31 g, 7.74 mmol) and $AlCl_3$ (1.03 g, 7.74 mmol) in CH_2Cl_2 (50 mL). Purification by column chromatography (silica gel, hexanes/ethyl acetate 9:1) afforded **209** (1.04 g, 64%) as a light yellow oil, R_f = 0.57 (hexanes/ethyl acetate 9:1); and **209a** (0.12 g, 9.1%) as a light yellow oil: R_f = 0.49 (hexanes/ethyl acetate 9:1);

209: IR (film cast) 2926, 2854, 2150, 1678, 1465, 1252, 1086, 847 cm^{-1}; ^1H NMR (500 MHz, $CDCl_3$) δ 2.47 (*pseudo*-t, J = 7.5 Hz, 4H), 1.59–1.56 (m, 4H), 1.21–1.19 (m, 16H), 0.17 (s, 18H); ^{13}C NMR (125 MHz, $CDCl_3$,) δ 187.6, 102.1, 97.2, 45.2, 29.4, 29.3, 29.2, 28.8, 23.8, –0.8; Anal. calcd. for $C_{24}H_{42}O_2Si_2$: C, 68.84, H, 10.11, found C, 70.34, H, 10.33; EI MS *m/z* 418.3 ($[M]^+$, 12), 403.2 ($[M - CH_3]^+$, 29), 345.2 ($[M - C_3H_9Si]^+$, 26), 73.04 ($[TMS]^+$, 100); EI HRMS *m/z* calcd. for $C_{24}H_{42}O_2Si_2$ (M^+) 418.2723, found 418.2724.

209a: IR (film cast) 3253, 2927, 2854, 2150, 2092, 1680, 1465, 1253, 847 cm^{-1}; ^1H NMR (500 MHz, $CDCl_3$) δ 3.21 (s, 1H), 2.57-2.51 (m, 4H), 1.67-1.63 (m, 4H), 1.26 (m, 16H), 0.22 (s, 9H); ^{13}C NMR (125 MHz, $CDCl_3$,) δ 188.0, 187.5, 102.1, 97.5, 81.5, 78.3, 45.4, 45.3, 29.5, 29.4, 29.3, 29.2(7), 29.2(4), 28.9, 28.8, 23.9, 23.7, –0.8; EI MS *m/z* 345.2

([M]$^+$, 1), 331.2 ([M – CH_3]$^+$, 10), 73.04 ([TMS]$^+$, 100); HRMS *m/z* calcd. for $C_{21}H_{33}O_2Si$ (M^+) 345.2093, found 345.2239

(3,16-Bis(dibromomethylene)octadeca-1,17-diyne-1,18-diyl)bis(trimethylsilane)

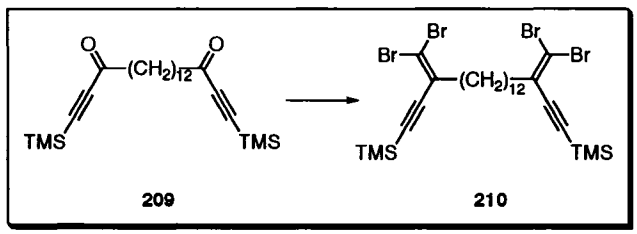

209 210

Diketone **209** (1.59 g, 4.09 mmol) in CH_2Cl_2 (25 mL) was subjected to dibromoolefination according to general procedure C using CBr_4 (3.77 g, 11.4 mmol) and PPh_3 (5.99 g, 22.8 mmol) in CH_2Cl_2 (100 mL). Purification by column chromatography (silica gel, hexanes) afforded **210** (1.43 g, 51%) as a light yellow oil: R_f = 0.52 (hexanes); IR (microscope cast) 2959, 2926, 2153, 1463, 1250, 884; ^{1}H NMR (400 MHz, $CDCl_3$) δ 2.31 (*pseudo*-t, virtual J = 7.2 Hz, 4H), 1.61 (*pseudo*-p, virtual J = 7.2 Hz, 4 H), 1.28-1.22 (m, 16H), 0.22 (s, 18H); ^{13}C NMR (100 MHz, $CDCl_3$) δ 131.1, 103.1, 102.7, 97.5, 36.8, 29.6, 29.5, 29.3, 28.9, 27.4, –0.3; Anal. calcd. for $C_{20}H_{24}SiBr_2Br_2$: C, 42.75; H, 5.80, found C, 41.30; H, 5.54; EI MS *m/z* 729.9 ([M]$^+$, 3), 651.0 ([M – Br]$^+$, 21), 73.04 ([TMS]$^+$, 100); HRMS calc. for $C_{26}H_{42}Si_2{}^{79}Br_2{}^{81}Br_2$ (M^+) 729.9520, found 729.9522.

5,18-bis(dibromomethylene)cyclooctadeca-1,3-diyne (211)

macrocycle (212)

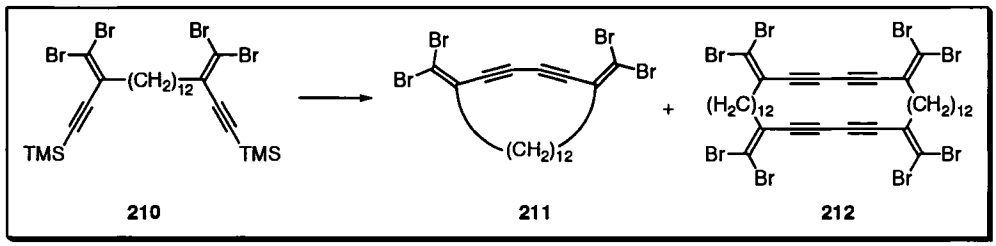

Tetrabromide **210** (1.53 g, 2.19 mmol) was subjected to desilylation and oxidative homocoupling according to general procedure D using K_2CO_3 (0.1 g, 0.7 mmol) in MeOH/THF (20 mL, 1:1 v/v), CuI (1.20 g, 6.65 mmol) and TMEDA (1.2 mL, 13 mmol) in CH_2Cl_2 (2000 mL). Purification by column chromatography (silica gel, hexanes) afforded **211** (0.40 g, 31%) as a white powder: $R_f = 0.61$ (hexanes) and **212** (0.20 g, 13%) as a white powder: $R_f = 0.49$ (hexanes);

211: mp 67-71°C; IR (microscope) 2924, 2854, 1738, 1461, 1377 cm^{-1}; ^1H NMR (400 MHz, $CDCl_3$) δ 2.35 (*pseudo*-t, $J = 7.2$ Hz, 4H), 1.60 (*pseudo*-p, $J = 7.2$ Hz, 4H), 1.38–1.29 (m, 16H); ^{13}C NMR (125 MHz, $CDCl_3$) δ 130.2, 99.7, 82.1, 80.8, 36.1, 28.6, 27.9, 27.3, 27.18 25.9; Anal. calcd. for $C_{20}H_{24}Br_2Br_2$: C, 41.13; H, 4.14; found C, 40.89; H, 4.12; EI HRMS *m/z* calcd. for $C_{20}H_{24}{}^{79}Br_2{}^{81}Br_2$ (M^+) 583.8590, found 583.8570.

212: IR (microscope) 2925, 2852, 1676, 1461, 831 cm^{-1}; ^1H NMR (500 MHz, $CDCl_3$) δ 2.37 (*pseudo*-t, $J = 7.5$ Hz, 4H), 1.60 (m, 4H), 1.33–1.26 (m, 16H); ^{13}C NMR (125 MHz, $CDCl_3$) δ 130.2, 100.2, 82.4, 80.6, 36.8, 29.5, 29.4, 29.3, 28.4, 27.5.

1,17-Bis(trimethylsilyl)heptadeca-1,16-diyne-3,15-dione

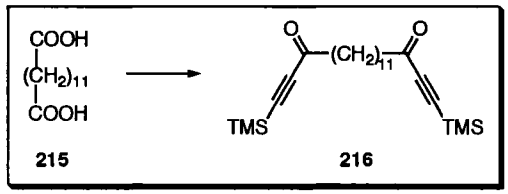

Tridecanedioic acid **215** (3.24 g, 13.3 mmol) was subjected to Friedel-Crafts acylation according to general procedure B using PCl_3 (1.83 g, 13.3 mmol), bis(trimethylsilyl)acetylene (4.53 g, 26.6 mmol) and $AlCl_3$ (3.54 g, 26.6 mmol) in CH_2Cl_2 (50 mL). Purification by column chromatography (silica gel, hexanes/ethyl acetate 9:1) afforded **216** (3.52 g, 65%) as a light yellow oil: $R_f = 0.53$ (hexanes/ethyl acetate 9:1); IR (microscope) 2928, 2855, 2150, 2092, 1679, 1253, 1085, 847 cm^{-1}; ^1H NMR (400 MHz, $CDCl_3$) δ 2.50 (*pseudo*-t, $J = 7.6$ Hz, 4H), 1.62-1.59 (m, 4H), 1.24–1.22 (m, 14H), 0.19 (s, 18H); ^{13}C NMR (100 MHz, $CDCl_3$) δ 187.8, 101.9, 97.3, 45.1, 29.3, 29.2, 29.1, 28.8, 23.8, –0.8; EI MS *m/z* 404.3 ($[M]^+$, 4), 389.2 ($[M–CH_3]^+$, 23), 331.2 ($[M - C_3H_9Si]^+$, 18), 73.04 ($[TMS]^+$, 100); EI HRMS *m/z* calcd. for $C_{23}H_{40}O_2Si_2$ (M^+) 404.2568, found 404.2564.

(3,15-Bis(dibromomethylene)heptadeca-1,16-diyne-1,17-diyl)bis(trimethylsilane)

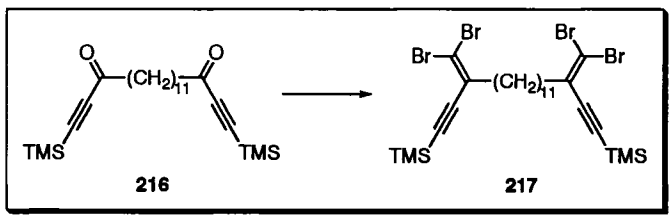

Diketone **216** (3.52 g, 8.69 mmol) in CH_2Cl_2 (10 mL) was subjected to dibromoolefination according to general procedure C using CBr_4 (8.62 g, 26.1 mmol) and PPh_3 (13.7 g, 52.2 mmol) in CH_2Cl_2 (100 mL). Purification by column chromatography (silica gel, hexanes) afforded **217** (3.73 g, 60%) as a light yellow oil: $R_f = 0.47$ (hexanes);

IR (CH_2Cl_2 cast) 2960, 2222, 2197, 2097, 1487 cm^{-1}; ^1H NMR (400 MHz, $CDCl_3$) δ 2.89 (*pseudo*-t, virtual J = 7.2 Hz, 4H), 2.30–2.27 (m, 4H), 1.28–1.26 (m, 14H), 0.19 (s, 18 H); ^{13}C NMR (100 MHz, $CDCl_3$) δ 130.9, 103.0, 102.6, 97.4, 36.6, 29.5, 29.4, 29.2, 28.8, 27.3, –0.4; EI MS *m/z* 715.9 ($[M]^+$, 1), 623.0 ($[M - Br]^+$, 5), 73.04 ($[TMS]^+$, 100); HRMS calc. for $C_{25}H_{40}Si_2{}^{79}Br_2{}^{81}Br_2$ (M^+) 715.9336, found 715.9358.

5,17-bis(dibromomethylene)cycloheptadeca-1,3-diyne

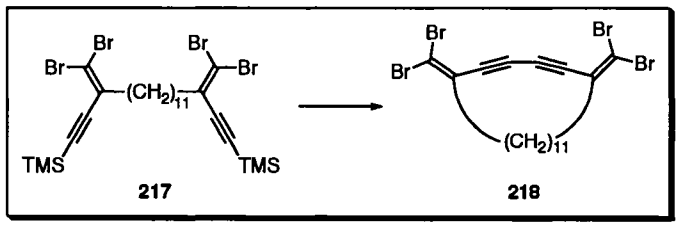

Tetrabromide **217** (1.5 g, 2.1 mmol) was subjected to desilylation and oxidative homocoupling according to general procedure D using K_2CO_3 (0.1 g, 0.7 mmol) in MeOH/THF (20 mL, 1:1 v/v), CuI (1.0 g, 5.3 mmol) and TMEDA (6.4 mL, 10 mmol) in CH_2Cl_2 (30 mL). Purification by column chromatography (silica gel, hexanes) afforded **218** (0.21 g, 18%) as a white powder: R_f = 0.60 (hexanes); mp 97–101°C; IR (microscope) 2924, 2848, 2676, 2194, 1557, 1458, 1368, 871 cm^{-1}; ^1H NMR (400 MHz, $CDCl_3$) δ 2.41 (*pseudo*-t, virtual J = 6.8 Hz, 4H), 1.63 (*pseudo*-p, virtual J = 7.2 Hz, 4H), 1.41–1.33 (m, 14H); ^{13}C NMR (125 MHz, $CDCl_3$) δ 130.1, 100.0, 82.9, 81.1, 35.9, 28.7, 28.0, 27.9, 27.3, 26.5; Anal. calcd. for $C_{19}H_{22}Br_2Br_2$: C, 40.01; H, 3.89; found: C, 39.93; H, 3.85; EI HRMS *m/z* calcd. for $C_{19}H_{22}{}^{79}Br_2{}^{81}Br_2$ (M^+) 569.8414, found 569.8414.

1,16-Bis(trimethylsilyl)hexadeca-1,15-diyne-3,14-dione

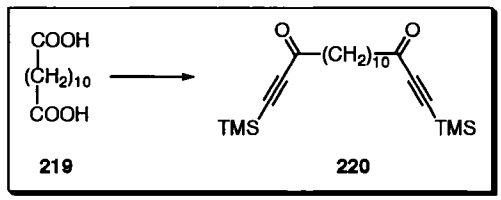

219 220

Dodecanedioic acid **219** (3.98 g, 17.3 mmol) was subjected to Friedel-Crafts acylation according to general procedure A using $SOCl_2$ (3.77 mL, 6.17 g, 51.9 mmol), bis(trimethylsilyl)acetylene (5.89 g, 34.6 mmol) and $AlCl_3$ (4.61 g, 34.6 mmol) in CH_2Cl_2 (50 mL). Purification by column chromatography (silica gel, hexanes/ethyl acetate 9:1) afforded **220** (6.48 g, 96%) as a light yellow oil: $R_f = 0.56$ (hexanes/ethyl acetate 9:1); IR (CH_2Cl_2 cast) 2929, 2856, 2150, 1679, 1226, 847 cm^{-1}; ^1H NMR (500 MHz, $CDCl_3$) δ 2.41 (*pseudo*-t, virtual $J = 7.5$ Hz, 4H), 1.57 (*pseudo*-p, virtual $J = 7$ Hz, 4H), 1.22-1.20 (m, 12H), 0.16 (m, 18H); ^{13}C NMR (125 MHz, $CDCl_3$) δ 187.7, 102.0, 97.2, 45.2, 29.2, 29.1, 28.8, 23.8, -0.8; Anal. calcd. for $C_{22}H_{38}O_2Si_2$: C, 67.63, H, 9.80, found C, 68.75, H, 9.87; EI MS *m/z* 390.2 ($[M]^+$, 5), 375.2 ($[M - CH_3]^+$, 27), 317.2 ($[M - C_3H_9Si]^+$, 19); EI HRMS *m/z* calcd. for $C_{22}H_{38}O_2Si_2$ (M^+) 390.2410, found 390.2406.

(3,14-bis(dibromomethylene)hexadeca-1,15-diyne-1,16-diyl)bis(trimethylsilane)

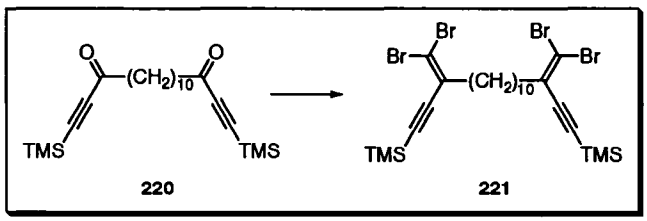

220 221

Diketone **220** (3.08 g, 7.89 mmol) in CH_2Cl_2 (15 mL) was subjected to dibromoolefination according to general procedure C using CBr_4 (7.84 g, 23.7 mmol) and PPh_3 (12.5 g, 47.4 mmol) in CH_2Cl_2 (100 mL). Purification by column chromatography

(silica gel, hexanes) afforded **221** (3.28 g, 60%) as an light yellow oil: R_f = 0.54 (hexanes); IR (CH_2Cl_2 cast) 2960, 2222, 2197, 2097, 1487 cm^{-1}; ^1H NMR (400 MHz, $CDCl_3$) δ 2.31 (*pseudo*-t, virtual J = 7.6 Hz, 4 H), 1.58-1.53 (m, 4H), 1.31 (b s, 12H), 0.22 (s, 18 H); ^{13}C NMR (100 MHz, $CDCl_3$) δ 130.1, 102.1, 101.9, 96.7, 35.8, 28.6, 28.5, 27.9, 26.5, –1.1; EI MS *m/z* 710.9 ($[M]^+$, 2), 623.0 ($[M - Br]^+$, 5), 73.04 ($[TMS]^+$, 100); HRMS calc. for $C_{24}H_{38}Si_2{}^{79}Br_2{}^{81}Br_2$ (M^+) 703.9264, found 703.9263.

5,16-Bis(dibromomethylene)cyclohexadeca-1,3-diyne

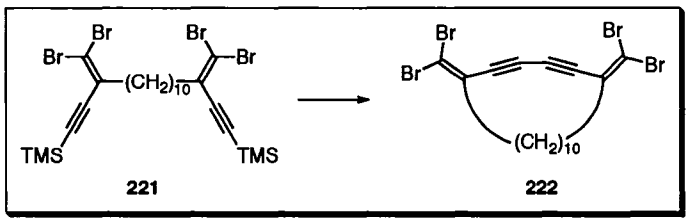

Tetrabromide 221 (0.57 g, 0.82 mmol) was subjected to desilylation and oxidative homocoupling according to general procedure D using K_2CO_3 (0.10 g, 0.70 mmol) in MeOH/THF (20 mL, 1:1 v/v), CuI (0.81 g, 0.82 mmol) and TMEDA (1.2 mL, 8.2 mmol) in CH_2Cl_2 (2000 mL). Purification by column chromatography (silica gel, hexanes) afforded 222 (0.34 g, 74%) as a white powder: R_f = 0.57 (hexanes); mp 122-124°C; IR (microscope) 2926, 2852, 1459, 1332, 850, 791cm^{-1}; ^1H NMR (400 MHz, $CDCl_3$) δ 2.42-2.39 (*pseudo*-t, virtual J = 6.4 Hz, 4H), 1.45-1.35 (m, 12H), 1.68-1.61 (m, 4H); ^{13}C NMR (125 MHz, $CDCl_3$) δ 130.1, 99.8, 83.3, 81.5, 35.4, 28.2, 28.1, 26.9, 26.3; Anal. calcd. for $C_{18}H_{20}Br_4$: C, 38.89; H, 3.63; found C, 38.95; H, 3.68; EI HRMS *m/z* calcd. for $C_{18}H_{20}{}^{79}Br_2{}^{81}Br_2$ (M^+) 555.8257, found 555.8265.

1-(Trimethylsilyl)non-1-yn-3-one[58]

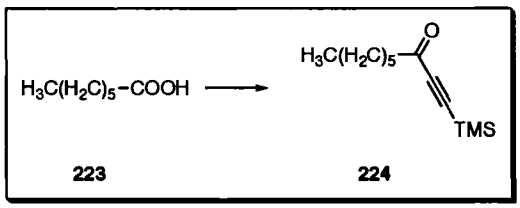

223 224

Heptanoic acid **223** (3.80 g, 29.2 mmol) was subjected to Friedel-Crafts acylation according to general procedure A using thionyl chloride (5.2 mL, 8.6 g, 73 mmol), bis(trimethylsilyl)acetylene (4.92 g, 29.2 mmol) and $AlCl_3$ (3.89 g, 29.2 mmol) in CH_2Cl_2 (50 mL). Purification by column chromatography (silica gel, hexanes/ethyl acetate 9:1) afforded **224** (3.01 g, 49%) as an light yellow oil: R_f = 0.56 (hexanes/ethyl acetate 9:1); IR (CH_2Cl_2 cast) 2959, 2931, 2860, 2150, 1679, 1457, 1252, 847 cm^{-1}; ^1H NMR (500 MHz, $CDCl_3$) δ 2.52 (*pseudo*-t, virtual J = 7.5 Hz, 2H), 1.64 (*pseudo*-p, virtual J = 7.5 Hz, 2H), 1.31-1.26 (m, 6H), 0.87 (*pseudo*-t, virtual J = 7 Hz, 3H), 0.22 (s, 9H); ^{13}C NMR (125 MHz, $CDCl_3$) δ 187.9, 102.1, 97.4, 45.3, 31.5, 28.6, 23.9, 22.4, 13.9, -0.8 ; EI MS *m/z* 195.1 ($[M - CH_3]^+$, 6), 140.1 ($[M - C_5H_{10}]^+$, 68), 125.1 ($[M - C_6H_{12}]^+$, 100). HRMS calcd. for $C_{11}H_{19}OSi$ 195.1205, found 195.1203.

(3-(dibromomethylene)non-1-yne)trimethylsilane

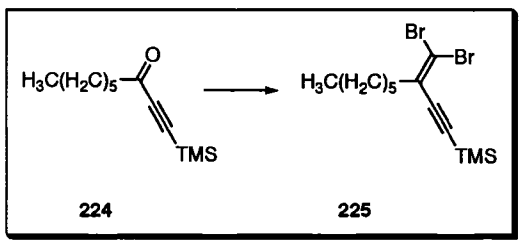

224 225

Monoketone **224** (2.10 g, 10.0 mmol) in CH_2Cl_2 (25 mL) was subjected to dibromoolefination according to general procedure C using CBr_4 (6.62 g, 20.0 mmol) and PPh_3 (10.8 g, 40 mmol) in CH_2Cl_2 (100 mL). Purification by column chromatography

(silica gel, hexanes) afforded **225** (2.52 g, 67%) as an light yellow oil: R_f = 0.74 (hexanes); IR (neat film) 2958, 2929, 2858, 2152, 1466, 1250, 908, 760 cm^{-1}; ^1H NMR (400 MHz, $CDCl_3$) δ 2.32 (*pseudo*-t, virtual J = 7.6 Hz, 2H), 1.61-1.53 (m, 2H), 1.36-1.28 (m, 6H), 0.89 (m, 3H), 0.22 (s, 9H); ^{13}C NMR (100 MHz, $CDCl_3$) δ 131.0, 103.1, 102.8, 97.6, 36.8, 31.6, 28.6, 27.4, 22.6, 14.1, –0.2; Anal. calcd. for $C_{13}H_{22}SiBr_2$: C, 42.64; H, 6.06; found C, 42.38; H, 6.0115; EI MS *m/z* 365.9 (M^+, 6), 280.8 ($[M-C_6H_{13}]^+$, 3), 73.04 ($[TMS]^+$, 100); HRMS calc. for $C_{13}H_{22}Si^{79}Br^{81}Br$ (M^+) 365.9837, found 365.9839

7,12-bis(dibromomethylene)octadeca-8,10-diyne

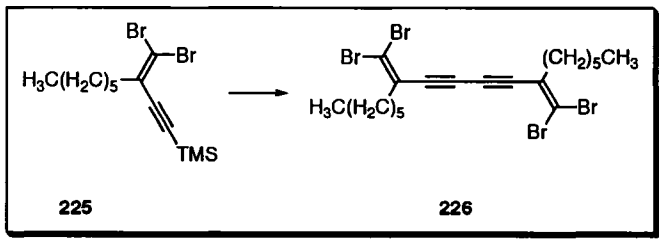

Dibromide **225** (1.61 g, 4.39 mmol) was subjected to desilylation and oxidative homocoupling according to general procedure D using K_2CO_3 (0.022 g, 0.16 mmol) in MeOH/THF (20 mL, 1:1 v/v), CuI (0.44 g, 2.31 mmol) and TMEDA (1.1 mL, 6.6 mmol) in CH_2Cl_2 (50 mL). Purification by column chromatography (silica gel, hexanes) afforded **226** (0.52 g, 40%) as a yellow oil: R_f = 0.64 (hexanes); IR ($CHCl_3$ cast) 2955, 2927, 1460, 833 cm^{-1}; ^1H NMR (400 MHz, $CDCl_3$) δ 2.37 (*pseudo*-t, virtual J = 7.6 Hz, 4H), 1.62-1.55 (m, 4H), 1.32 (M, 12H), 0.92-0.89 (m, 6H); ^{13}C NMR (100 MHz, $CDCl_3$) δ 130.1, 100.1, 82.3, 80.5, 36.8, 31.4, 28.5, 27.4, 22.5, 13.9; EI HRMS *m/z* calcd. for $C_{20}H_{26}{}^{79}Br_2{}^{81}Br_2$ (M^+) 585.8726, found 585.8728.

1,15-Bis(trimethylsilyl)pentadeca-1,14-diyne-3,13-dione

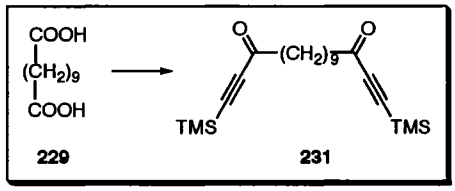

229 231

Undecanedioic acid **229** (1.00 g, 4.62 mmol) was subjected to Friedel-Crafts acylation according to general procedure A using thionyl chloride (1.68 mL, 2.75 g, 23.1 mmol), bis(trimethylsilyl)acetylene (1.57 g, 9.24 mmol) and $AlCl_3$ (1.23 g, 9.24 mmol) in CH_2Cl_2 (50 mL). Purification by column chromatography (silica gel, hexanes/ethyl acetate 9:1) afforded **231** (1.2 g, 69%) as an light yellow oil: R_f = 0.53 (hexanes/ethyl acetate 9:1); IR ($CHCl_3$ cast) 2929, 2857, 2150, 1678, 1252, 846 cm^{-1}; ^1H NMR (500 MHz, $CDCl_3$) δ 2.32 (*pseudo*-t, virtual J = 7.6 Hz, 4H), 1.64-1.58 (m, 4H), 1.27 (b s, 10H), –0.21 (s, 18H); ^{13}C NMR (125 MHz, $CDCl_3$) δ 187.9, 102.1, 97.5, 45.2, 29.2, 29.1, 28.9, 23.9, –0.8; EI MS *m/z* 376.2 (M^+, 7), 361.2 ($[M - CH_3]^+$, 41), 303.2 ($[M - C_3H_9Si]^+$, 23), 73.04 ($[TMS]^+$, 100); EI HRMS *m/z* calcd. for $C_{21}H_{36}O_2Si_2$ (M^+) 376.2253, found 376.2251.

1,14-Bis(trimethylsilyl)tetradeca-1,13-diyne-3,12-dione

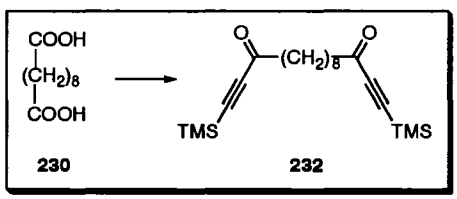

230 232

Decanedioic acid **230** (2.58 g, 12.6 mmol) was subjected to Friedel-Crafts acylation according to general procedure A using thionyl chloride (4.60 mL, 7.5 g, 63.0 mmol), bis(trimethylsilyl)acetylene (4.31 g, 25.3mmol) and $AlCl_3$ (3.38 g, 25.3 mmol) in CH_2Cl_2 (50 mL). Purification by column chromatography (silica gel, hexanes/ethyl acetate 9:1) afforded **232** (3.19 g, 70%) as a light yellow oil: R_f = 0.50 (hexanes/ethyl acetate 9:1); IR

(microscope cast) 2931, 2857, 2151, 1678, 1252,1105, 845 cm^{-1}; ^1H NMR (500 MHz, $CDCl_3$) δ 2.51 (*pseudo*-t, virtual J = 7 Hz, 4H), 2.64–2.60 (m, 4H), 1.28 (b s, 8H), 0.21 (s, 18H); ^{13}C NMR (125 MHz, $CDCl_3$) δ 187.8, 102.0, 97.5, 45.2, 29.0, 28.8, 23.8, –0.7; EI HRMS *m/z* calcd. for $C_{20}H_{34}O_2Si_2$ (M^+) 362.2097, found 362.2091.

(3,13-bis(dibromomethylene)pentadeca-1,14-diyne-1,15-diyl)bis(trimethylsilane)

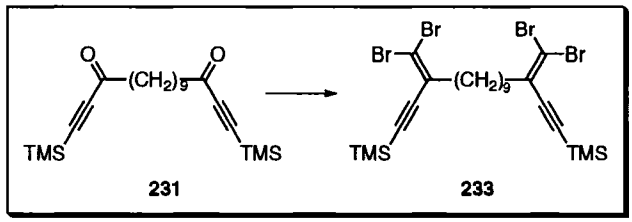

Diketone **231** (0.67 g, 1.8 mmol) in CH_2Cl_2 (25 mL) was subjected to dibromoolefination according to general procedure C using CBr_4 (1.75 g, 5.29 mmol) and PPh_3 (2.77 g, 10.5 mmol) in CH_2Cl_2 (100 mL). Purification by column chromatography (silica gel, hexanes) afforded **233** (0.82 g, 68%) as a light yellow oil: R_f = 0.50 (hexanes); IR (microscope) 2959, 2928, 2856, 2152, 1461, 1250, 884 cm^{-1}; ^1H NMR (400 MHz, $CDCl_3$) δ 2.32 (*pseudo*-t, virtual J = 7.2 Hz, 4H), 1.59–1.53 (m, 4H), 1.32 (s, 10H), 0.22 (s, 18H); ^{13}C NMR (100 MHz, $CDCl_3$) δ 130.9, 103.0, 102.7, 97.5, 36.7, 29.3, 29.2, 28.8, 27.3, –0.3; EI MS *m/z* 687.9 (M^+, 7), 608.9 ([M–Br]$^+$, 12), 73.04 ([TMS]$^+$, 100); EI HRMS *m/z* calcd. for $C_{23}H_{36}Si_2{}^{79}B_2r{}^{81}Br_2$ (M^+) 687.9095, found 687.9047.

(3,12-bis(dibromomethylene)tetradeca-1,13-diyne-1,14-diyl)bis(trimethylsilane)

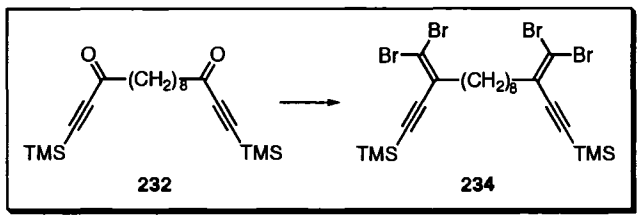

Diketone **232** (2.37 g, 6.55 mmol) in CH_2Cl_2 (25 mL) was subjected to dibromoolefination according to general procedure C using CBr_4 (6.50 g, 19.7 mmol) and PPh_3 (10.3 g, 39.3 mmol) in CH_2Cl_2 (100 mL). Purification by column chromatography (silica gel, hexanes) afforded **234** (2.30 g, 52%) as a light yellow oil: R_f = 0.48 (hexanes); IR ($CHCl_3$ cast) 2927, 2852, 2150, 1432, 1721 cm^{-1}; ^1H NMR (500 MHz, $CDCl_3$) δ 2.31 (*pseudo*-t, virtual J = 7.8 Hz, 4H), 1.59–1.56 (m, 4H), 1.33 (*pseudo*-d, virtual J = 2.0 Hz, 8H), 0.23 (s, 18H); ^{13}C NMR (125 MHz, $CDCl_3$) δ 131.1, 103.2, 102.7, 97.5, 36.7, 29.2, 28.8, 27.4, –0.7; EI MS *m/z* 673.9 (M^+, 2), 73.04 ($[TMS]^+$, 100); EI HRMS *m/z* calcd. for $C_{22}H_{34}Si_2{}^{79}Br_2{}^{81}Br_2$ (M^+) 673.8891, found 673.8895.

5,15-Bis(dibromomethylene)cyclopentadeca-1,3-diyne

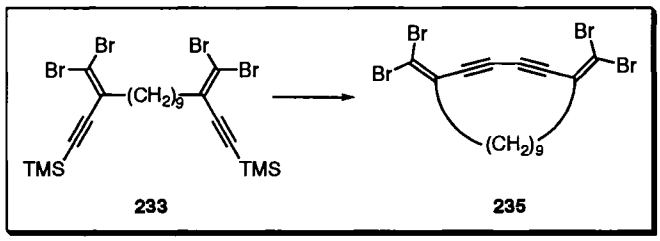

Tetrabromide **233** (0.64 g, 0.93 mmol) was subjected to desilylation and oxidative homocoupling according to general procedure D using K_2CO_3 (0.10 g, 0.70 mmol) in MeOH/THF (20 mL, 1:1 v/v), CuI (0.88 g, 4.7 mmol) and TMEDA (1.4 mL, 9.3 mmol) in CH_2Cl_2 (2000 mL). Purification by column chromatography (silica gel, hexanes) afforded **235** (0.257 g, 50 %) as a white powder: R_f = 0.61 (hexanes); mp 136-139 °C; IR

($CHCl_3$ cast) 2930, 2855, 1533, 1460, 831 cm^{-1}; ^1H NMR (500 MHz, $CDCl_3$) δ 2.38 (*pseudo*-t, virtual J = 6.5 Hz, 4H), 1.66 (*pseudo*-p, virtual J = 6.5 Hz, 4H), 1.43–1.37 (m, 10H); ^{13}C NMR (125 MHz, $CDCl_3$,) δ 130.2, 99.5, 84.1, 82.0, 35.5, 28.4, 27.9, 27.8, 26.1; Anal. calcd. for $C_{17}H_{18}Br_4$: C, 37.68; H, 3.35; found: C, 37.31; H, 3.51; EI HRMS *m/z* calcd. for $C_{17}H_{18}{}^{79}Br_2{}^{81}Br_2$ (M^+) 541.8101, found 541.8105.

5,14-Bis(dibromomethylene)cyclotetradeca-1,3-diyne

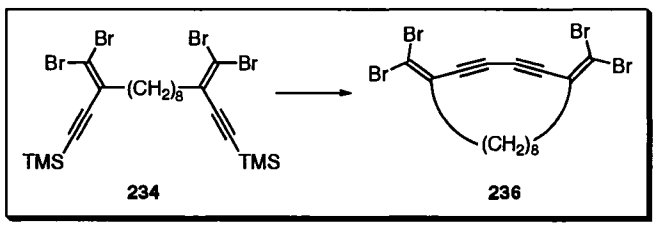

Tetrabromide **234** (1.29 g, 1.92 mmol) was subjected to desilylation and oxidative homocoupling according to general procedure D using K_2CO_3 (0.10 g, 0.70 mmol) in MeOH/THF (20 mL, 1:1 v/v), CuI (1.82 g, 9.75 mmol) and TMEDA (2.91 mL, 19.2 mmol) in CH_2Cl_2 (2000 mL). Purification by column chromatography (silica gel, hexanes) afforded **236** (0.53 g, 53%) as a white powder: R_f = 0.61 (hexanes); mp 158-162°C; IR (microscope) 2927, 2853, 2680, 1700, 1495, 828 cm^{-1}; ^1H NMR (500 MHz, $CDCl_3$) δ 2.44–2.42 (m, 4H), 1.67–1.61 (m, 4H), 1.54–1.48 (m, 4H), 1.42–1.36 (m, 4H); ^{13}C NMR (125 MHz, $CDCl_3$) δ 130.3, 98.6, 86.5, 82.5, 35.4, 27.9, 27.3, 26.8; EI HRMS *m/z* calcd. for $C_{16}H_{16}{}^{79}Br_2{}^{81}Br_2$ (M^+) 527.7944 found 527.7948.

5. References

(1) Schwartz, H. *Angew. Chem. Int. Ed.* **1993**, *32*, 1412-1415.

(2) Faust, R. *Angew. Chem. Int. Ed.* **1998**, *37*, 2825-2828.

(3) Tobe, Y.; Fujii, T.; Matsumoto, H.; Tsumuraya, K.; Noguchi, D.; Nakagawa, N.; Sonada, M.; Naemura, K.; Achiba, Y.; Wakabayashi, T. *J. Am. Chem. Soc.* **2000**, *122*, 1762-1775.

(4) Haley, M. M.; Langsdorf, B. L. *Chem. Commun.* **1997**, 1121-1122.

(5) Kawase, T.; Darabi, H. R.; Oda, M. *Angew. Chem. Int. Ed.* **1996**, *22*, 2664-2666.

(6) Umeda, R.; Morinaka, T.; Sonada, M.; Tobe, Y. *J. Org. Chem.* **2005**, *70*, 6133-6136.

(7) Youngs, W. J.; Tessier, C. A.; Bradshaw. J. D. *Chem. Rev.* **1999**, *99*, 3153-3180.

(8) Blomquist, A. T.; Liu, L. H. *J. Am. Chem. Soc.* **1953**, *75*, 2153-2154.

(9) Sondheimer, F.; Amiel, Y.; Wolovsky, R. *J. Am. Chem. Soc.* **1957**, *79*, 6263-6267.

(10) Scott, L. T.; DeCicco, J. *Tetrahedron Lett.* **1976**, *31*, 2663-2666.

(11) Sondheimer, F.; Wolovsky, R. *J. Am. Chem. Soc.* **1962**, *84*, 260-269.

(12) Matsuoka, T.; Negi, T.; Otsubo, T.; Sakata, Y.; Misumi, S. *Bull. Chem. Soc. Jap.* **1972**, *45*, 1825-1833.

(13) Wong, H. N. C.; Sondheimer, F. *Tetrahedron Lett.* **1980**, *21*, 983-986.

(14) Eisler, S.; McDonald, R.; Loppnow, G. R., Tykwinski, R. R. *J. Am. Chem. Soc.* **2000**, *122*, 6917-6928.

(15) Scott, L. T.; DeCicco, G. J.; Hyun, J. L.; Reinhardt, G. *J. Am. Chem. Soc.* **1985**, *107*, 6546 - 6555.

(16) Scott, L. T.; DeCicco, G. J.; Hyun, J. L.; Reinhardt, G. *J. Am. Chem. Soc.* **1983**, *105*, 7760-7761.

(17) Jiao, H.; van Eikena Hommes, N. J. R.; Schleyer, P. R.; de Meijere, A. *J. Org. Chem.* **1996**, *61*, 2826-2828.

(18) de Meijere, A.; Jaekel, F.; Simon, A.; Borrmann, H.; Koehler, J.; Johnels, D.; Scott, L. T. *J. Am. Chem. Soc.* **1991**, *113*, 3935-3941.

(19) Houk, K. N.; Scott, L. T.; Rondan, N. G.; Spellmeyer, D. C.; Reinhardt, G.; Hyun, J. L.; DeCicco, G. J.; Weiss, R.; Chen, M. H. M.; Bass, L. S.; Clardy, J.; Jorgensen, F. S.; Eaton, T. A.; Sarzoki, V.; Petit, C. M.; Ng, L.; Jordan, K. D. *J. Am. Chem. Soc.* **1985**, *107*, 6556-6562.

(20) Rubin, Y.; Parker, T. C.; Pastor, J. S.; Jalisatgi, S.; Boulle, C.; Wilkins, C. L. *Angew. Chem. Int. Ed.* **1998**, *37*, 1226-1229.

(21) Boese, R.; Matzger, A. J.; Vollhardt, K. P. C. *J. Am. Chem. Soc.* **1997**, *119*, 2052-2053.

(22) Haley, M. M.; Bell, M. L.; English, J. J.; Johnson, C. A.; Weakley, T. J. R. *J. Am. Chem. Soc.* **1997**, *119*, 2956-2957.

(23) Hisaki, I.; Sonada, M.; Tobe, Y. *Eur. J. Org. Chem.* **2006**, 833-847.

(24) Wong, H. N. C.; Garrat, P. J.; Sondheimer, F. *J. Am. Chem. Soc.* **1974**, *96*, 5604-5605.

(25) Marseden, J. A.; Palmer, G. J.; Haley, M. M. *Eur. J. Org. Chem.* **2003**, 2355-2369.

(26) Tobe, Y.; Fujii, T.; Naemura, K. *J. Org. Chem.* **1994**, *59*, 1236 - 1237.

(27) Ohkita, M.; Ando, K.; Tsuji, T. *Chem. Commun.* **2001**, 2570 - 2571.

(28) Tobe, Y.; Furukawa, R.; Sonada, M.; Wakabayashy, T. *Angew. Chem. Int. Ed.* **2001**, *40*, 4072-4074.

(29) Diederich, F.; Rubin, Y.; Chapman, O. L.; Goroff, N. S. *Helv. Chim. Acta* **1994**, *77*, 1441-1457.

(30) Hobday, S.; Smith, R.; Belbruno, J. *Modelling Simul. Mater. Sci. Eng.* **1999**, *7*, 397-412.

(31) Rubin, Y.; Kahr, M.; Knobler, C. B.; Diederich, F.; Wilkins, C. L. *J. Am. Chem. Soc.* **1991**, *113*, 495-500.

(32) Tobe, Y.; Umeda, R.; Iwasa, N.; Sonada, M. *Chem. Eur. J.* **2003**, *9*, 5549 - 5559.

(33) Adamson, G. A.; Rees, C. W. *J. Chem. Soc. Perkin Trans* **1996**, *13*, 1533-1543.

(34) Kroto, H. W.; Heath, J. R.; O'Brien, S. C.; Curl, R. F.; Smalley, R. E. *Nature* **1985**, *318*, 162-163.

(35) Faust, R. *Angew. Chem. Int. Ed.* **1998**, *37*, 2825-2828.

(36) Fallis, A. G. *Synlett* **2004**, 2249-2267.

(37) Johnson, J. A.; Deppmeier, B. J.; Driessen, A. J.; Henhre, W. J.; Klunzinger, P. E.; Pham, I. N.; Watanabe, M. Spartan '02 v1.0.6.

(38) Walton, D. R. M.; Waugh, F. *J. Organomet. Chem.* **1972**, *37*, 45-56.

(39) Chernik, E. T.; Eisler, S.; Tykwinski R. R. *Tetrahedron Lett.* **2001**, *42*, 8575-8578.

(40) Corey, E. J.; Fuchs, P. L. *Tetrahedron Lett.* **1972**, *13*, 3769-3772.

(41) Hay, A. S. *J. Org. Chem.* **1962**, *27*, 3320-3321.

(42) Siemsen, P.; Livingston, R. C.; Diederich, F. *Angew. Chem. Int. Ed.* **2000**, *39*, 2632-2657.

(43) Eisler, S.; Tykwinski, R. R. *J. Am. Chem. Soc.* **2000**, *122*, 10736-10737.

(44) Fritsch, P. *Liebigs Ann. Chem.* **1894**, *279*, 319-323.

(45) Buttenberg, W. P. *Liebigs Ann. Chem.* **1894**, *279*, 324-337.

(46) Wiechell, H. *Liebigs Ann. Chem.* **1894**, *279*, 337-344.

(47) Eisler, S.; Cahal, N.; McDonald R.; Tykwinski, R. R. *Chem. Eur. J.* **2003**, *9*, 2542-2550.

(48) Eisler, S. *PhD. Thesis,* University of Alberta**, 2003**.

(49) Neidlein, R.; Winter, M. *Synthesis* **1998**, 1362-1366.

(50) Wiberg, K. B.; Pratt, W. E.; Bailey, W. F. *J. Org. Chem.* **1980**, *45*, 4936-4947.

(51) Gleiter, R.; Kratz, W.; Schafer, W.; Schehlmann, V. *J. Am. Chem. Soc.* **1991**, *113*, 9258-9264.

(52) Balova, I. A.; Remizova, L. A. *Zh. Org. Khim.* **1994**, *30*, 213-215.

(53) Armitage, J. B.; Jones, E. R. H.; Whiting, M. C. *J. Chem. Soc.* **1952**, 2014-2018.

(54) Armitage, J. B.; Cook, C. L.; Jones, E. R. H.; Whiting, M. C. *J. Chem. Soc.* **1952**, 2010-2014.

(55) Armitage, J. B.; Cook, C. L.; Jones, E. R. H.; Whiting, M. C. *J. Chem. Soc.* **1952**, 2005-2010.

(56) Cram, D. J.; Montgomery, C. S.; Knox, G. R.; *J. Am. Chem. Soc.* **1966**, *88*, 515-525.

(57) Heuft, M. A.; Collins, S. K.; Yap, G. P. A.; Fallis, A. G. *Org. Lett.* **2001**, *3*, 2883-2886

(58) Marshall, A. J.; Wang, X. *J. Org. Chem.* **1991**, *56*, 4913-4918.

A. Appendix 1

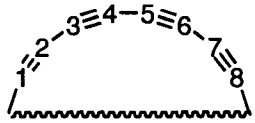

Table A.1. Calculated energy (Kcal/mol) and bond angles (°) for seven minimized structures of compound **202** (n = 12)

Structure	Energy	1-2-3	2-3-4	3-4-5	4-5-6	5-6-7	6-7-8
1	13	166.1	165.8	168.8	168.8	170.8	173.5
2	13	172.3	171.2	170.2	168.7	167.4	166.3
3	12.3	168.3	167.1	167.1	167.8	169.0	171.1
4	12	167.5	167.1	167.6	168.8	170.2	172.3
5	16.4	170.0	168.2	164.4	166.6	166.2	166.3
6	12	167.5	167.1	167.6	168.8	170.2	172.3
7	11	168.3	168.5	169.1	170.1	171.0	172.3

Structure 1

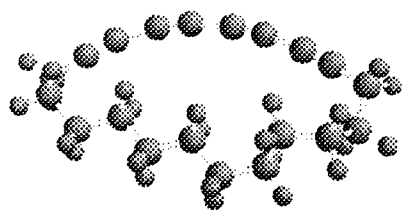

Structure 2

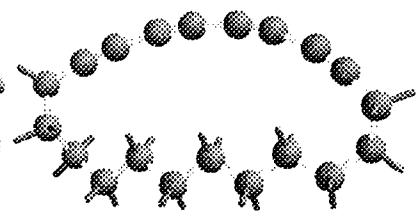

Structure 3

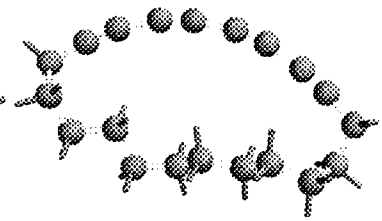

Structure 4

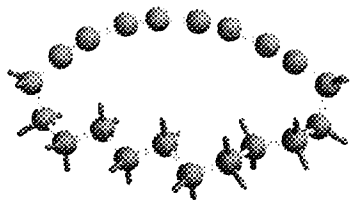

Structure 5

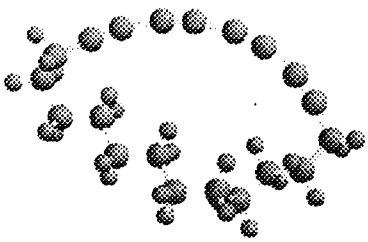

Structure 6

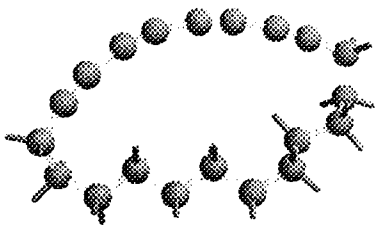

Structure 7

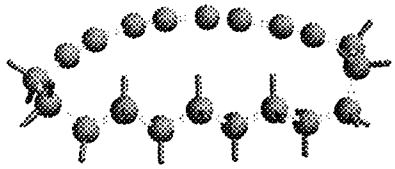

Table A.2. Calculated energy (Kcal/mol) and bond angles (°) for seven minimized structures of compound **203**

Structure	Energy	1-2-3	2-3-4	3-4-5	4-5-6	5-6-7	6-7-8
1	13.7	169.2	167.1	166.1	165.3	165.2	165.8
2	17.4	164.7	164.2	164.8	166.2	167.7	170.2
3	14.4	167.9	166.2	166.0	167.0	168.6	171.4
4	15.4	167.0	167.3	167.6	167.6	167.3	167.0
5	14.2	168.8	168.1	167.9	167.9	168.1	168.8
6	14.4	170.8	168.3	166.8	165.5	165.3	166.3
7	15.7	164.6	163.6	163.8	165.1	166.9	170

Structure 1 Structure 2 Structure 3

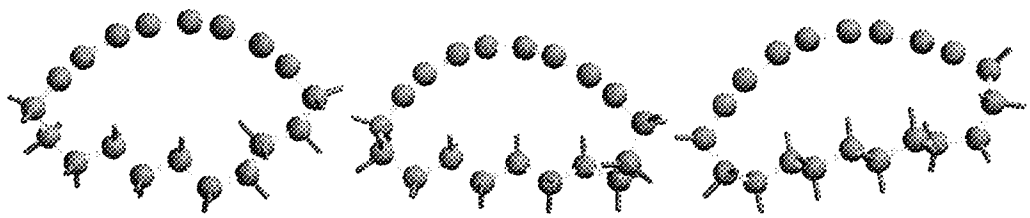

Structure 4 Structure 5 Structure 6

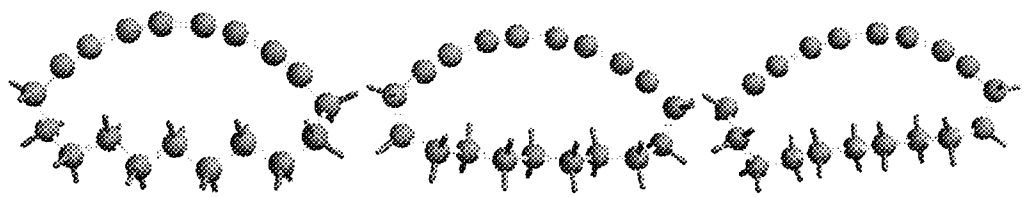

Structure 7

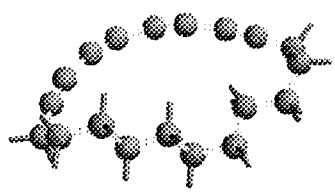

Table A.3. Calculated energy (Kcal/mol) and bond angles (°) for seven minimized structures of compound **204**

Structure	Energy	1-2-3	2-3-4	3-4-5	4-5-6	5-6-7	6-7-8
1	17.9	169.0	165.2	163.5	163.0	163.4	166.9
2	22.9	169.5	165.8	163.2	160.7	159.8	160.5
3	18.5	167.3	165.6	164.9	164.9	165.6	167.3
4	18.4	167.3	165.6	164.9	164.9	165.6	167.3
5	18.5	167.3	165.6	163.2	160.8	165.6	165.6
6	17.6	167.3	165.3	164.1	163.0	162.7	163.3
7	19.0	168.2	164.5	164.2	164.3	165.7	164.8

Structure 1

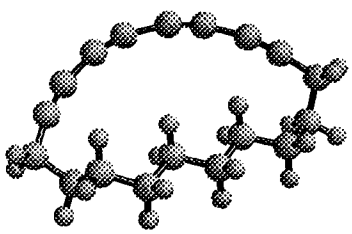

Structure 2

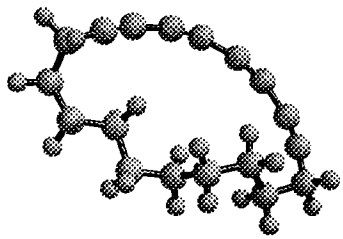

Structure 3

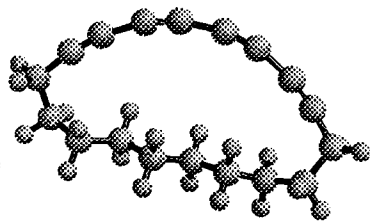

Structure 4

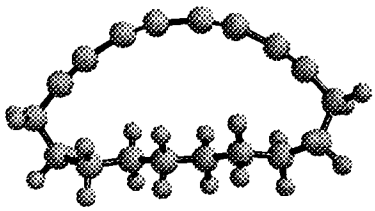

Structure 5

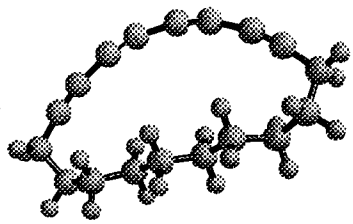

Structure 6

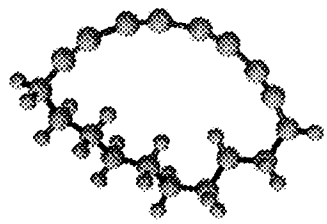

Structure 7

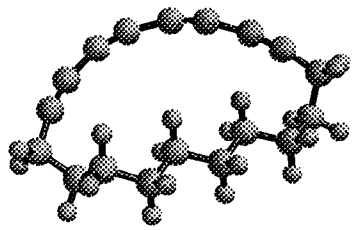

B. Appendix 2

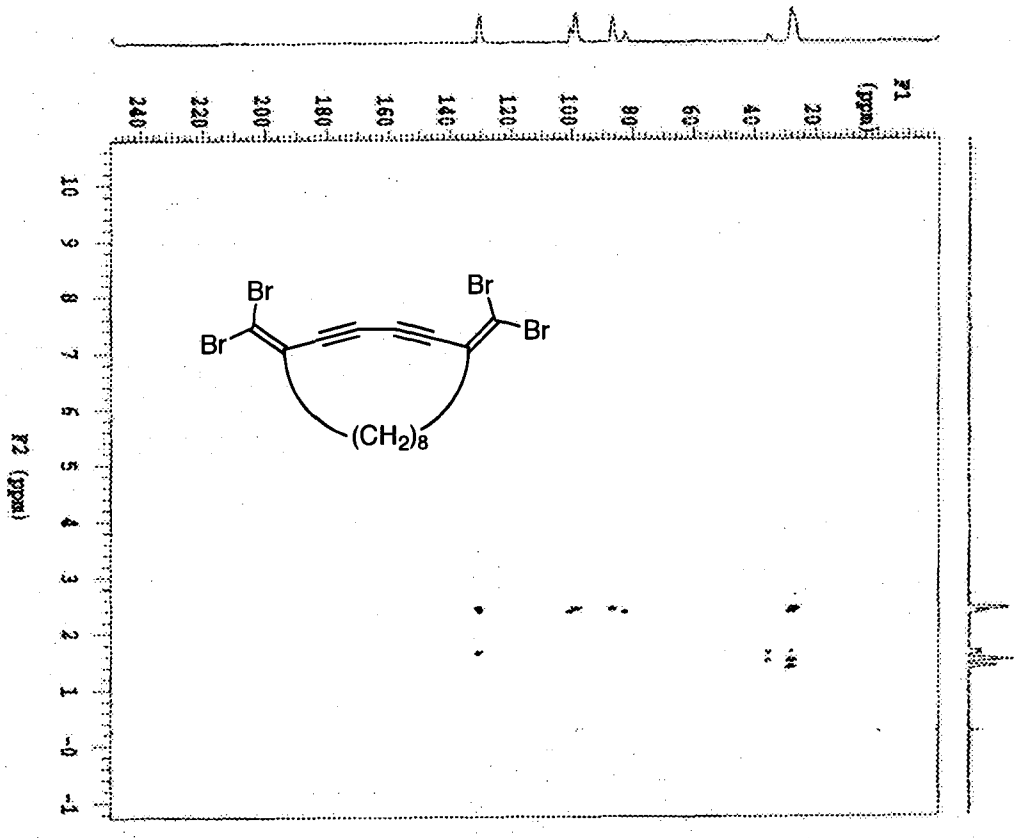

Figure B.1 HMBC spectrum of compound **236** at 125 MHz in $CDCl_3$

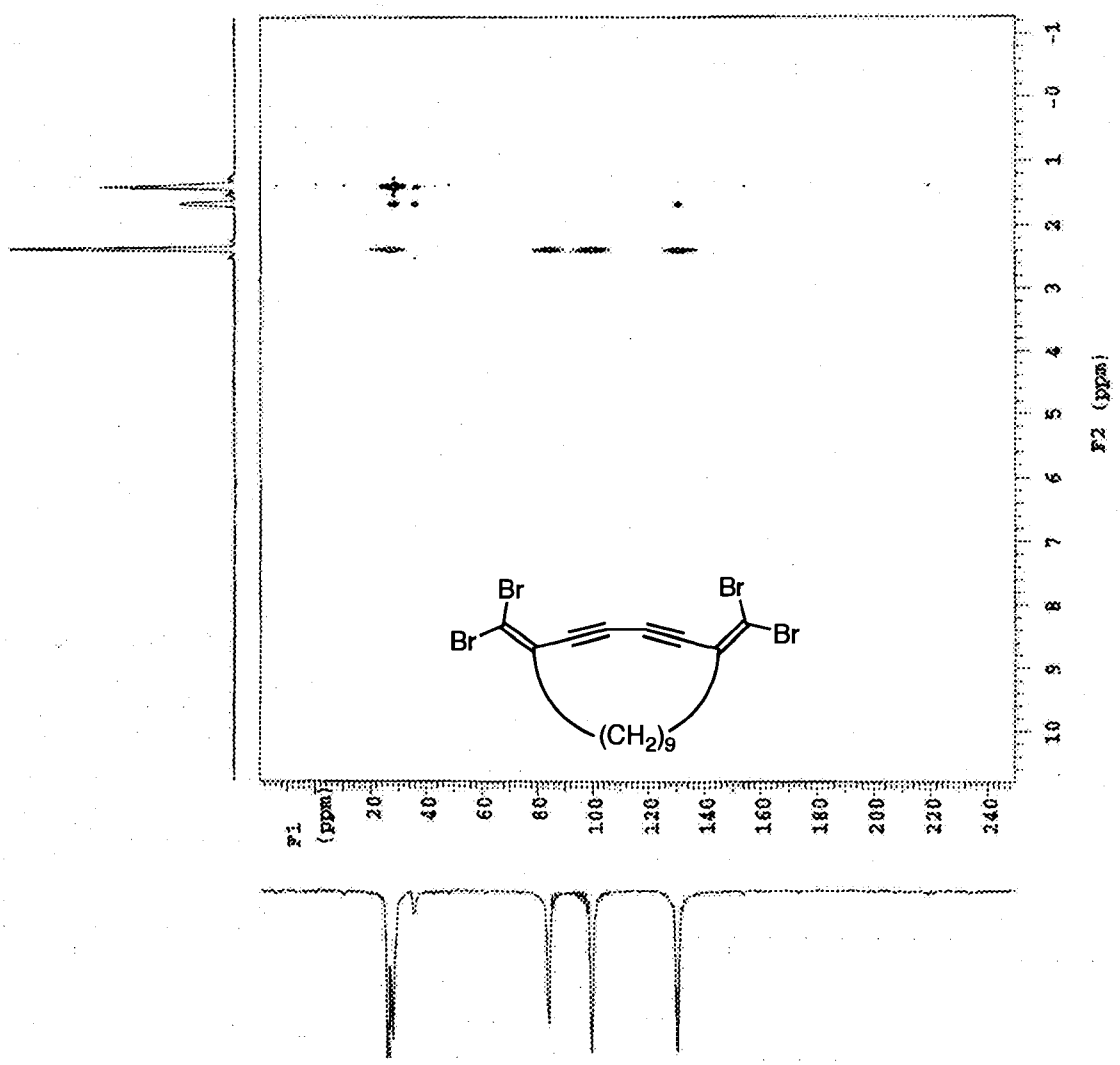

Figure B.2 HMBC spectrum of compound **235** at 125 MHz in $CDCl_3$

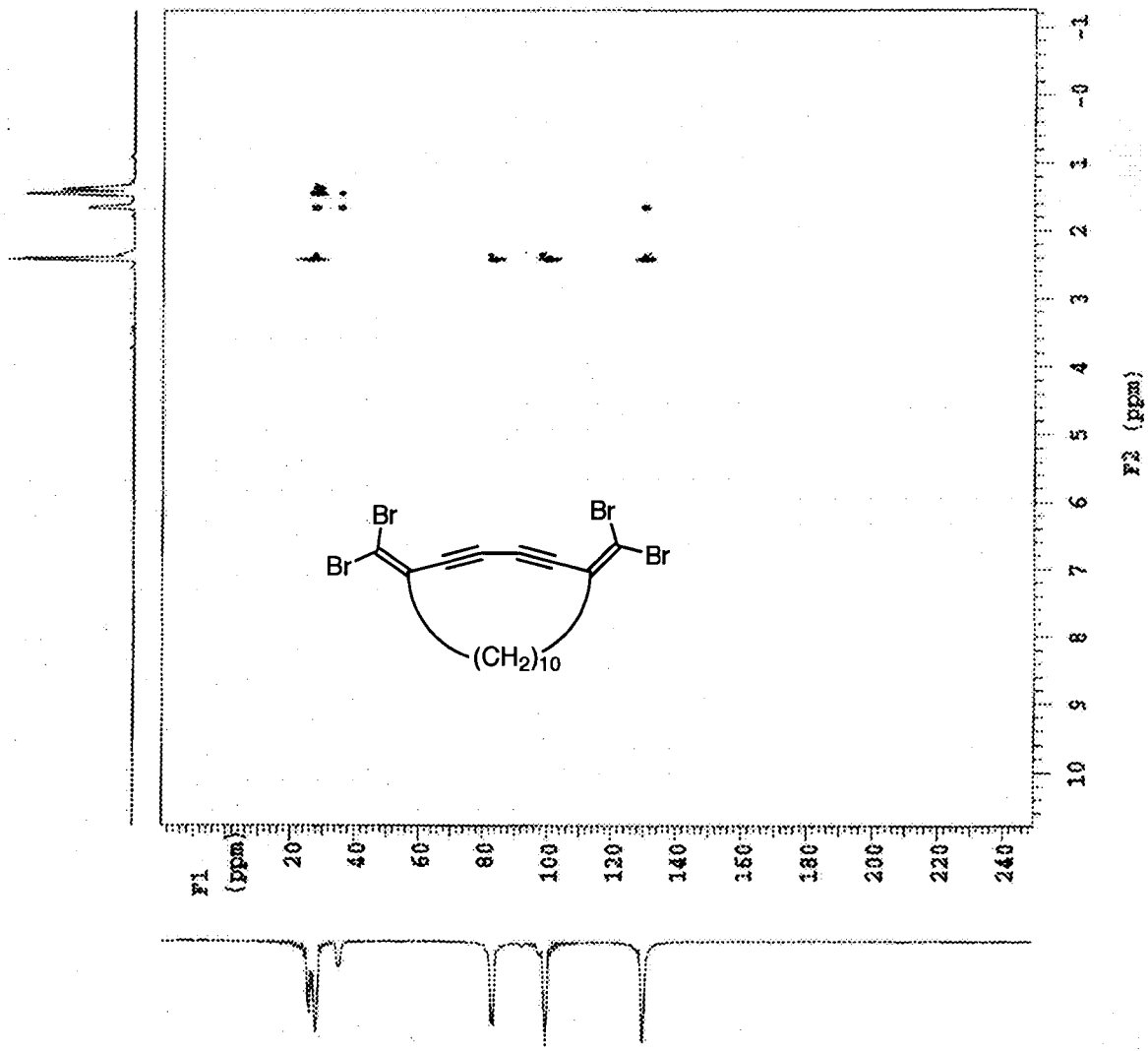

Figure B.3 HMBC spectrum of compound **222** at 125 MHz in $CDCl_3$

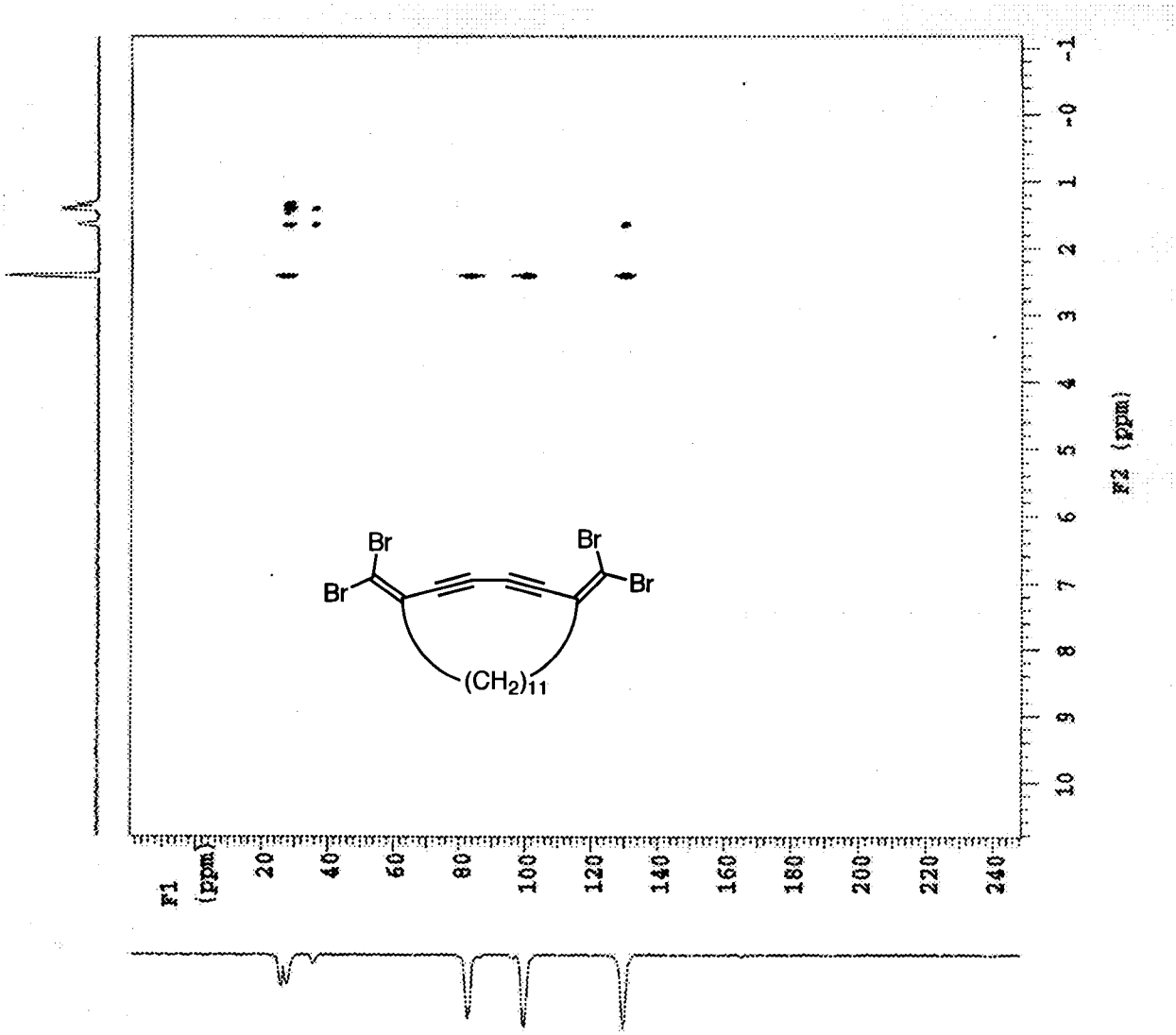

Figure B.4 HMBC spectrum of compound **218** at 125 MHz in $CDCl_3$

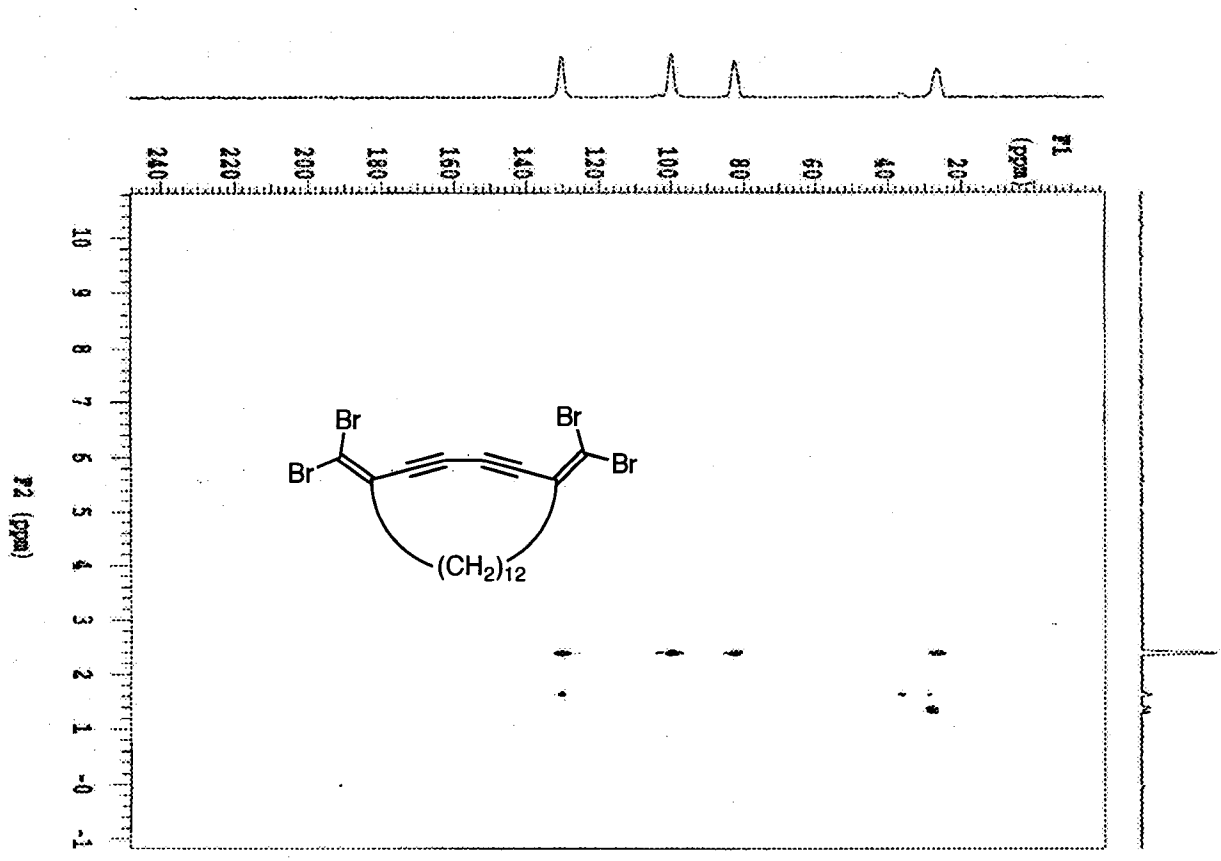

Figure B.5 HMBC spectrum of compound **211** at 125 MHz in $CDCl_3$

C. Appendix 3

STRUCTURE REPORT

XCL Code: RRT0516 **Date:** 24 June 2005

Compound: 5,14-bis(dibromomethylene)cyclotetradeca-1,3-diyne
Formula: $C_{16}H_{16}Br_4$
Supervisor: R. R. Tykwinski **Crystallographer:** M. J.Ferguson

Figure Legends

Figure 1. Perspective view of the 5,14-bis(dibromomethylene)cyclotetradeca-1,3-diyne molecule showing the atom labelling scheme. Non-hydrogen atoms are represented by Gaussian ellipsoids at the 20% probability level. Hydrogen atoms are shown with arbitrarily small thermal parameters.

Figure 2. Alternate view of the molecule

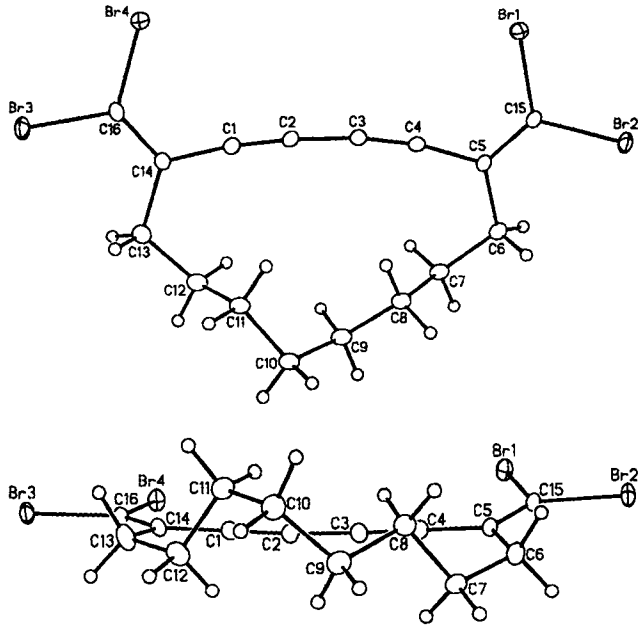

Table 1. Crystallographic Experimental Details
Table 2. Atomic Coordinates and Equivalent Isotropic Displacement Parameters
Table 3. Selected Interatomic Distances
Table 4. Selected Interatomic Angles

Table 1. Crystallographic Experimental Details

A. Crystal Data	
formula	$C_{16}H_{16}Br_4$
formula weight	527.93
crystal dimensions (mm)	0.39 ´ 0.37 ´ 0.18
crystal system	monoclinic
space group	$P2_1/n$ (an alternate setting of $P2_1/c$ [No. 14])
unit cell parameters[a]	
a (Å)	6.3221 (5)
b (Å)	17.9584 (15)

c (Å)	14.9727 (13)
b (deg)	93.3250 (10)
V (Å^3)	1697.1 (2)
Z	4
r_{calcd} (g cm^{-3})	2.066
μ (mm^{-1})	9.474
B. Data Collection and Refinement Conditions	
diffractometer	Bruker PLATFORM/SMART 1000 CCD[b]
radiation (l [Å])	graphite-monochromated Mo Ka (0.71073)
temperature (°C)	–80
scan type	w scans (0.3°) (20 s exposures)
data collection 2q limit (deg)	52.90
total data collected	11975 (-7 ≤ h ≤ 7, -22 ≤ k ≤ 22, -18 ≤ l ≤ 18)
independent reflections	3477 (R_{int} = 0.0351)
number of observed reflections (*NO*)	2886 [$F_o^2 \geq 2s(F_o^2)$]
structure solution method	direct methods (*SHELXS–86*[c])
refinement method	full-matrix least-squares on F^2 (*SHELXL–93*[d])
absorption correction method	multi-scan (*SADABS*)
range of transmission factors	0.2188–0.0614
data/restraints/parameters	3477 [$F_o^2 \geq -3s(F_o^2)$] / 0 / 181
goodness-of-fit (S)[e]	1.074 [$F_o^2 \geq -3s(F_o^2)$]
final R indices[f]	
$R1$ [$F_o^2 \geq 2s(F_o^2)$]	0.0262
$wR2$ [$F_o^2 \geq -3s(F_o^2)$]	0.0667
largest difference peak and hole	0.600 and –0.339 e Å^{-3}

[a]Obtained from least-squares refinement of 6457 reflections with 4.54° < 2q < 52.68°.

[b]Programs for diffractometer operation, data collection, data reduction and absorption correction were those supplied by Bruker.

(continued)

Table 1. Crystallographic Experimental Details (continued)

[c]Sheldrick, G. M. *Acta Crystallogr.* **1990**, *A46*, 467–473.

[d]Sheldrick, G. M. *SHELXL-93*. Program for crystal structure determination. University of Göttingen, Germany, 1993.

[e]$S = [\Sigma w(F_o^2 - F_c^2)^2/(n-p)]^{1/2}$ (n = number of data; p = number of parameters varied; $w = [s^2(F_o^2) + (0.0344P)^2 + 0.3100P]^{-1}$ where $P = [\mathrm{Max}(F_o^2, 0) + 2F_c^2]/3$).

[f]$R1 = \Sigma||F_o| - |F_c||/\Sigma|F_o|$; $wR2 = [\Sigma w(F_o^2 - F_c^2)^2/\Sigma w(F_o^4)]^{1/2}$.

Table 2. Atomic Coordinates and Equivalent Isotropic Displacement Parameters

Atom	x	y	z	U_{eq}, Å^2
Br1	0.18156(5)	0.549353(18)	0.09072(2)	0.03714(10)*

Br2	0.61011(5)	0.560156(19)	0.21006(2)	0.03816(10)*
Br3	-0.34608(5)	0.078918(19)	-0.19441(2)	0.03973(10)*
Br4	-0.37128(5)	0.254528(19)	-0.18125(2)	0.03927(10)*
C1	0.0508(5)	0.23631(17)	-0.0695(2)	0.0300(7)*
C2	0.1406(5)	0.29065(17)	-0.0398(2)	0.0291(7)*
C3	0.2479(5)	0.34812(18)	0.0033(2)	0.0302(7)*
C4	0.3491(5)	0.39198(17)	0.0483(2)	0.0292(7)*
C5	0.4875(4)	0.43385(16)	0.1077(2)	0.0275(6)*
C6	0.6906(5)	0.39688(18)	0.1455(2)	0.0355(8)*
C7	0.7289(5)	0.31697(18)	0.1135(2)	0.0339(7)*
C8	0.5895(5)	0.25765(18)	0.1542(2)	0.0344(7)*
C9	0.6313(5)	0.18053(18)	0.1140(3)	0.0385(8)*
C10	0.4743(5)	0.12003(19)	0.1381(2)	0.0403(8)*
C11	0.2598(5)	0.12268(19)	0.0840(2)	0.0358(7)*
C12	0.2774(6)	0.1024(2)	-0.0136(2)	0.0408(8)*
C13	0.0708(6)	0.09460(19)	-0.0695(3)	0.0435(9)*
C14	-0.0403(5)	0.16719(16)	-0.0990(2)	0.0290(7)*
C15	0.4361(5)	0.50340(17)	0.1306(2)	0.0276(6)*
C16	-0.2220(5)	0.16732(16)	-0.1499(2)	0.0289(7)*

Anisotropically-refined atoms are marked with an asterisk (*). The form of the anisotropic displacement parameter is: $\exp[-2\pi^2(h^2a^{*2}U_{11} + k^2b^{*2}U_{22} + l^2c^{*2}U_{33} + 2klb^*c^*U_{23} + 2hla^*c^*U_{13} + 2hka^*b^*U_{12})]$.

Table 3. Selected Interatomic Distances (Å)

Atom1	Atom2	Distance	Atom1	Atom2	Distance
Br1	C15	1.875(3)	C5	C15	1.340(4)
Br2	C15	1.874(3)	C6	C7	1.536(5)
Br3	C16	1.876(3)	C7	C8	1.531(4)
Br4	C16	1.874(3)	C8	C9	1.539(5)
C1	C2	1.201(4)	C9	C10	1.529(5)
C1	C14	1.428(4)	C10	C11	1.540(4)
C2	C3	1.375(4)	C11	C12	1.515(5)
C3	C4	1.197(4)	C12	C13	1.517(5)
C4	C5	1.426(4)	C13	C14	1.533(4)
C5	C6	1.524(4)	C14	C16	1.341(4)

Table 4. Selected Interatomic Angles (deg)

Atom1	Atom2	Atom3	Angle	Atom1	Atom2	Atom3	Angle
C2	C1	C14	174.0(3)				
C1	C2	C3	173.2(4)				
C2	C3	C4	172.2(3)				
C3	C4	C5	170.7(3)				
C4	C5	C6	118.3(3)				
C4	C5	C15	120.1(3)				
C6	C5	C15	121.5(3)				
C5	C6	C7	115.9(3)				
C6	C7	C8	114.9(3)				
C7	C8	C9	110.8(3)				
C8	C9	C10	114.8(3)				
C9	C10	C11	114.7(3)				
C10	C11	C12	112.8(3)				
C11	C12	C13	116.4(3)				
C12	C13	C14	116.5(3)				
C1	C14	C13	118.7(3)				
C1	C14	C16	119.4(3)				
C13	C14	C16	121.9(3)				
Br1	C15	Br2	115.09(16)				
Br1	C15	C5	123.1(2)				
Br2	C15	C5	121.8(2)				
Br3	C16	Br4	115.10(16)				
Br3	C16	C14	121.8(2)				
Br4	C16	C14	123.1(2)				

STRUCTURE REPORT

XCL Code: RRT0602 **Date:** 10 January 2006

Compound: 5,16-bis(dibromomethylene)cyclohexadeca-1,3-diyne
Formula: $C_{18}H_{20}Br_4$

Supervisor: R. R. Tykwinski **Crystallographer:** M. J. Ferguson

Figure Legends

Figure 1. Perspective view of the 5,16-bis(dibromomethylene)cyclohexadeca-1,3-diyne molecule showing the atom labelling scheme. Non-hydrogen atoms are represented by Gaussian ellipsoids at the 20% probability level. Hydrogen atoms are shown with arbitrarily small thermal parameters. Only the major part (70%) of the disordered decamethylene segment is shown.

Figure 2. Alternate view showing the disordered decamethylene group. Major (70%) form is indicated by the solid bonds; minor (30%) form is indicated by the open bonds.

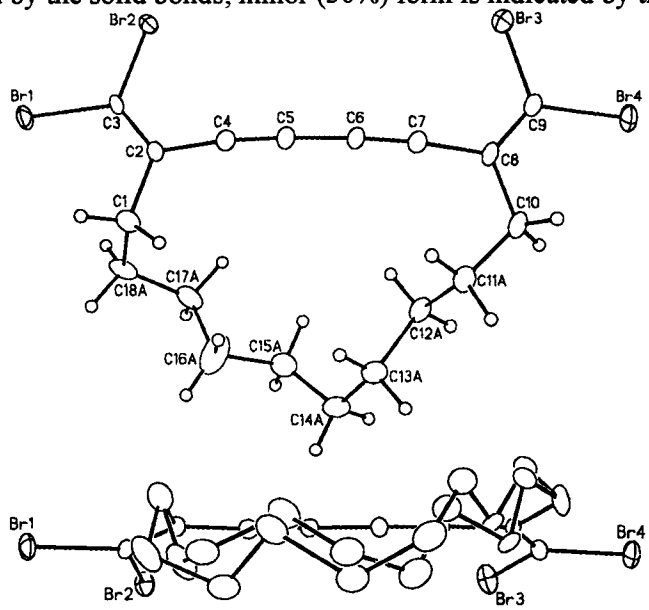

List of Tables

Table 1. Crystallographic Experimental Details

A. Crystal Data	
formula	$C_{18}H_{20}Br_4$
formula weight	555.98
crystal dimensions (mm)	0.42 ´ 0.15 ´ 0.12
crystal system	monoclinic
space group	$P2_1/c$ (No. 14)
unit cell parameters[a]	
a (Å)	12.7748 (9)
b (Å)	6.6476 (5)
c (Å)	23.0944 (17)
b (deg)	101.6580 (10)
V (Å^3)	1920.8 (2)
Z	4
r_{calcd} (g cm^{-3})	1.923

μ (mm^{-1})	8.376
B. Data Collection and Refinement Conditions	
diffractometer	Bruker PLATFORM/SMART 1000 CCD[b]
radiation (l [Å])	graphite-monochromated Mo Ka (0.71073)
temperature (°C)	–80
scan type	w scans (0.3°) (20 s exposures)
data collection $2q$ limit (deg)	52.84
total data collected	14178 ($-15 \le h \le 15$, $-8 \le k \le 8$, $-28 \le l \le 28$)
independent reflections	3938 (R_{int} = 0.0443)
number of observed reflections (*NO*)	3064 [$F_o^2 \ge 2s(F_o^2)$]
structure solution method	direct methods (*SHELXS–86*[c])
refinement method	full-matrix least-squares on F^2 (*SHELXL–93*[d])
absorption correction method	multi-scan (*SADABS*)
range of transmission factors	0.4331–0.1268
data/restraints/parameters	3938 [$F_o^2 \ge -3s(F_o^2)$] / 9[e] / 224
extinction coefficient (x)[f]	0.0070(5)
goodness-of-fit (S)[g]	1.177 [$F_o^2 \ge -3s(F_o^2)$]
final R indices[h]	
R_1 [$F_o^2 \ge 2s(F_o^2)$]	0.0357
wR_2 [$F_o^2 \ge -3s(F_o^2)$]	0.1092
largest difference peak and hole	0.826 and –0.564 e $Å^{-3}$

(continued)

Table 1. Crystallographic Experimental Details (continued)

[a]Obtained from least-squares refinement of 5956 reflections with $4.34° < 2q < 52.36°$.

[b]Programs for diffractometer operation, data collection, data reduction and absorption correction were those supplied by Bruker.

[c]Sheldrick, G. M. *Acta Crystallogr.* **1990**, *A46*, 467–473.

[d]Sheldrick, G. M. *SHELXL-93*. Program for crystal structure determination. University of Göttingen, Germany, 1993.

[e]The C–C distances in the minor component of disordered decamethylene group (C11B to C18B) were restrained to be 1.510 (2) Å.

[f]$F_c^* = kF_c[1 + x\{0.001F_c^2l^3/\sin(2q)\}]^{-1/4}$ where k is the overall scale factor.

[g]$S = [\Sigma w(F_o^2 - F_c^2)^2/(n-p)]^{1/2}$ (n = number of data; p = number of parameters varied; $w = [s^2(F_o^2) + (0.0583P)^2 + 0.0447P]^{-1}$ where $P = [\mathrm{Max}(F_o^2, 0) + 2F_c^2]/3$).

[h]$R_1 = \Sigma||F_o| - |F_c||/\Sigma|F_o|$; $wR_2 = [\Sigma w(F_o^2 - F_c^2)^2/\Sigma w(F_o^4)]^{1/2}$.

Table 2. Atomic Coordinates and Equivalent Isotropic Displacement Parameters

Atom	x	y	z	U_{eq}, $Å^2$

Br1	0.38478(4)	-0.48222(7)	0.54228(2)	0.04759(17)*
Br2	0.13893(4)	-0.57656(7)	0.50738(2)	0.04446(17)*
Br3	-0.34586(5)	-0.10521(8)	0.35841(3)	0.0628(2)*
Br4	-0.42603(4)	0.28090(9)	0.28351(2)	0.05623(19)*
C1	0.3206(4)	-0.0605(7)	0.4807(3)	0.0539(13)*
C2	0.2306(3)	-0.2063(6)	0.48304(18)	0.0322(9)*
C3	0.2475(3)	-0.3897(6)	0.50671(17)	0.0298(9)*
C4	0.1262(4)	-0.1400(6)	0.45676(18)	0.0355(10)*
C5	0.0435(4)	-0.0643(6)	0.43354(18)	0.0352(10)*
C6	-0.0495(4)	0.0269(6)	0.40488(19)	0.0353(10)*
C7	-0.1271(4)	0.1121(6)	0.37834(19)	0.0372(10)*
C8	-0.2122(4)	0.2229(6)	0.34334(18)	0.0361(10)*
C9	-0.3107(4)	0.1468(7)	0.33119(19)	0.0385(10)*
C10	-0.1879(4)	0.4285(7)	0.3203(3)	0.0594(15)*
C11A	-0.0752(11)	0.510(6)	0.3401(15)	0.0474(18)*[a]
C12A	0.0071(8)	0.418(2)	0.3087(3)	0.0430(18)*[a]
C13A	0.1160(7)	0.5338(12)	0.3261(4)	0.0526(19)*[a]
C14A	0.2030(7)	0.4668(13)	0.2938(4)	0.060(2)*[a]
C15A	0.2463(8)	0.2587(13)	0.3096(4)	0.0584(19)*[a]
C16A	0.324(2)	0.225(3)	0.3709(6)	0.094(3)*[a]
C17A	0.3220(6)	-0.0075(12)	0.3739(4)	0.0551(18)*[a]
C18A	0.3830(6)	-0.0896(13)	0.4325(5)	0.064(3)*[a]
C11B	-0.072(3)	0.492(16)	0.333(4)	0.0474(18)*[b]
C12B	-0.0083(18)	0.411(6)	0.2895(9)	0.0430(18)*[b]
C13B	0.1044(14)	0.437(3)	0.3242(9)	0.0526(19)*[b]
C14B	0.1779(12)	0.341(3)	0.2886(8)	0.060(2)*[b]
C15B	0.2963(12)	0.355(3)	0.3138(8)	0.0584(19)*[b]
C16B	0.312(6)	0.267(9)	0.3753(15)	0.094(3)*[b]
C17B	0.3867(14)	0.089(2)	0.3881(8)	0.0551(18)*[b]
C18B	0.3347(16)	-0.075(3)	0.4174(4)	0.064(3)*[b]

Anisotropically-refined atoms are marked with an asterisk (*). The form of the anisotropic displacement parameter is: $\exp[-2\pi^2(h^2a^{*2}U_{11} + k^2b^{*2}U_{22} + l^2c^{*2}U_{33} + 2klb^*c^*U_{23} + 2hla^*c^*U_{13} + 2hka^*b^*U_{12})]$. [a]Refined with an occupancy factor of 0.70. [b]Refined with an occupancy factor of 0.30.

Table 3. Selected Interatomic Distances (Å)

Atom1	Atom2	Distance	Atom1	Atom2	Distance
Br1	C3	1.883(4)	C1	C18B	1.511(2)[a]
Br2	C3	1.865(4)	C2	C3	1.336(6)
Br3	C9	1.876(5)	C2	C4	1.420(6)
Br4	C9	1.877(4)	C4	C5	1.194(6)
C1	C2	1.513(6)	C5	C6	1.378(6)
C1	C18A	1.507(10)	C6	C7	1.198(6)